Natural Ventilation Models and Production Management in an Experimental High Tunnel

A Dissertation Presented for the
Doctor of Philosophy
Degree
The University of Tennessee, Knoxville

Muzi Zheng
August 2017

Dedication

This dissertation is dedicated to my family, especially my mother and father Fei Li and Jiaming Zheng, who has always been there for me through ups and downs, laughter and tears. I would also like to dedicate this writing to my fiancé for his unconditional support and endless encouragement, and I am truly thankful for having you in my life. You guys mean everything in the world to me, and you are the reason I keep my smile all the time whether for my life or studies.

Acknowledgements

I wish to show my sincere gratitude to all those people who have offered me help throughout my Ph.D study. I would like to give my greatest appreciation to Prof. Brian Leib who is my research mentor and provides valuable support to my research. Without his guidance and help, this project would have not been successfully completed.

I would also like to give my greatest appreciation to my committee members: Dr. Ayers Paul, Dr. David Butler, and Dr. Douglas Hayes for being my committee members, who gave me valuable advice for my research and dissertation writing. I am very grateful to be blessed with such wonderful mentors. I would like to show my appreciation to my colleagues and friends, Amir Haghverdi, Tim Grant, Duncan Muchoki, Phue Vanchiasong, I am very lucky to have worked with these wonderful people.

This project is financially supported by Ag Research & Extension Innovation Grants (2011) and Conservation Innovation Grants, NRCS, USDA (2013-2016).

Abstract

High tunnels (HTs) help producers to be more profitable through crop protection and extension of growing season. Proper ventilation and heat managements inside HTs are crucial for adjusting inner microclimates and future obtaining marketable crop production. This study first analyzed daytime ventilation rates that responds to the changes of external weather conditions in a Gothic-type HT located in eastern Tennessee. A mathematical energy balance model and instrumental measurement serve as validation data were developed with a good agreement for ventilation rates (R^2>0.70). The coupling of energy balance model and air-flux calculation based on external weather parameters can be considered a valuable method to predict the interior microclimate condition and also can be used to estimate door opening levels. Also, this study using an advanced artificial neural network (ANN) discovers a better structure of HT ventilation models, and input sensitivity revealed that relative humidity and wind direction had the least significant impact on the prediction of inside air temperature. The result shows that ANN is more strongly effective than the previous theoretical model in the estimation of HT ventilation rates and opening levels.

Moreover, A three-year experiment assessed the beneficial effects of independent and combined practices on temperature changes inside the HTs, and further examined the impact of temperature changes on crop production. Specific practices included surface mulches, row covers, cover crops, and irrigation water types. Statistical differences were analyzed in a randomized complete block design for total marketable yields of spring pepper and fall lettuce, as well as the changes in soil and air temperature. Black

polyethylene mulch is highly recommended for pepper and lettuce production in HTs. Unfortunately, the benefit of cover crop to improve soil health was not found in this study, although there was a positive soil temperature rise surrounding plant root-zones caused by cover crops. Moreover, row covers continuously added protection from freezing during the cold nights resulting in a higher crop production. Stored rainwater was warmer than the city water except in the cold period, and rainwater irrigation is tended to increase the overall production of pepper but lettuce yielded better by using city water.

Table of Contents

List of Tables

List of Figures

Chapter 1
Introduction and Literature Review

Much of the United States is experiencing increased interest in local fruit and vegetable procurement and high tunnels are part of the movement toward local food production (Hinrichs, 2003). High tunnels (HTs) are simple, plastic-covered, greenhouse-like structures without additional heat sources inside that capture and store heat for season extension (Figure 1). The growing season in open fields is limited to spring, summer and fall in most of the continental USA, but season extension can be implemented under protected agriculture using greenhouses and high tunnels (Jensen & Malter, 1995). These protected structures typically target organic farming and allow producers to harvest year-round produce while they also offer many other advantages relative to open fields (Stanghellini & Kempkes, 2003): 1) protecting and buffering crops from variable weather events (e.g. hail, snow or strong wind); 2) producing lower incidence of crop diseases exacerbated by rainfall; 3) increasing water use efficiency; and 4) improving crop growth conditions. All of the benefits allow producers to take advantages of market seasonality with a higher level of income (Blomgren & Frisch, 2007), and improve their crop quality as compared with open field production. HTs also have low overall startup costs, fewer energy requirements, and demand less electrical equipment operation and maintenance than standard greenhouses (Kittas & Karamanis, 2005). Greenhouses typically use glass or an air-inflated double plastic film layer and have fully automatic ventilation or heating/cooling systems, and Wang et al. (1999) found that the electrical system accounts for approximately 30-50% of the total production cost in a large greenhouse. Therefore, HT production can be more profitable because fuel consumption can be replaced with renewable solar energy as the primary heat resource.

Even though the topography of Tennessee is quite varied from the lowlands of the Mississippi Valley to the mountain peaks in the east, most of the state is characterized by warm, humid summers and mild winters. This climate is warm enough in mid-winter to allow HTs to function well for cool-season crops while also significantly extending growing seasons for warm-season crops, which allows harvesting during what are traditionally the off-season periods when prices are higher.

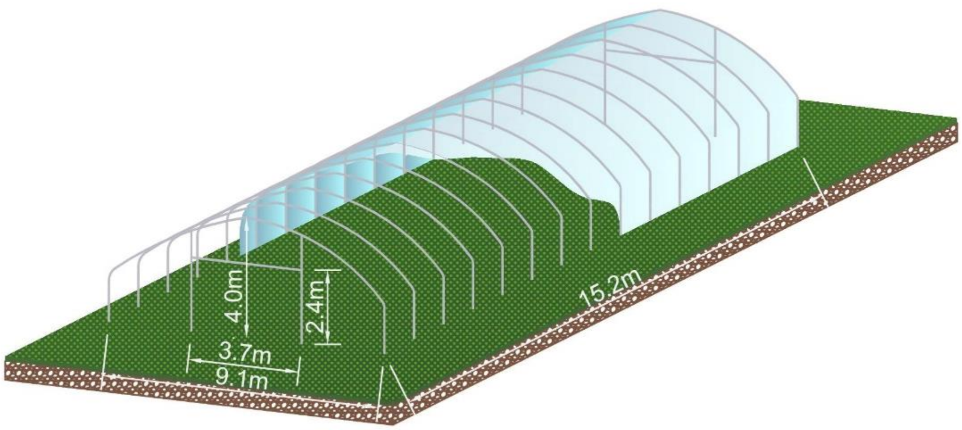

Figure 1. Isometric view of a high tunnel with the covering cut away for clarity.

A HT is considered a solar collector that allows the short-wavelength solar radiation to penetrate but traps the long-wavelength thermal radiation to warm the air and soil temperature (Abdel-Ghany, 2011; Jain & Tiwari, 2002; Kendirli, 2006). The total amount of solar radiation captured by the HT is absorbed as thermal energy by the crop and other components including the ground surface. Part of the solar energy may be transferred by the latent heat through plant transpiration, and the rest contributes to sensible heat warming of the interior air (Baxevanou et al., 2010). Significant variation of air temperature and humidity inside the HT mainly occurs when compared to outside because of the exterior climatic conditions when no auxiliary heating or fan system is utilized inside (Tong & Christopher, 2009). Increasingly producers using HTs desire to lengthen the growing season further than outdoors; but, the trapped heat and humidity inside HTs are difficult to control, especially in subtropical regions. Accordingly, energy effective ventilation management becomes important for HT operators due to the essential function of controlling the interior climatic environment to obtain marketable and sustainable production yield and quality. Ventilation rate through the HT is considered a key process that directly affects the transport of sensible and latent heat to and from the interior air, helping to control the interior soil temperature, humidity and also the evapotranspiration rate in HTs. Compared to forced ventilation, natural ventilation can effectively reduce energy inputs and cost in the production system. Crucial factors affecting natural ventilation include captured solar radiation, the temperature difference between interior and exterior, as well as the inlet and outlet vent openings, heat absorption from internal thermal mass and cooling effects from the exterior wind.

Most studies forced steady-state flow regimes while suppressing unsteady phenomena for designated time periods (Norton & Sun, 2007), even though the experimental conditions do not simulate the real inner microclimate scenario. Various techniques have been offered to measure ventilation flux rates in a more or less direct way: most of the studies estimated ventilation flux based on derivations of energy, mass and momentum balance models along with pressure-difference measurements between the inside and the outside of the structure (Chalabi & Bailey, 1989; Demrati & Boulard, 2001b; Kindelan, 1980; Wang & Deltour, 1996). Teitel and Tanny (1999) used energy and mass conservation to investigate the transient response of air temperature and humidity inside a greenhouse. Dayan et al. (2004) also applied related mathematical models to study the ventilation rate in a greenhouse used for commercial rose cultivation. Since the middle of the 1950s, tracer gas techniques have been commonly used to directly measure the ventilation rate for both glass and plastic greenhouses (Businger, 1963; Kittas & Bartzanas, 2007), with different media such as carbon dioxide (CO_2), methane (CH_4) or nitrous oxide (NO_2) (Bot, 1983; Fernandez & Bailey, 1992; Jain & Tiwari, 2002; Kittas & Draoui, 1995; Kittas & Bartzanas, 2007; Nederhoff et al., 1983). However, tracer gas techniques cannot be applied without electrical fans or electricity in HTs. Since the exterior air velocity affects the heat and mass transfers within the HTs, it is of interest to determine the air-flux patterns in and around the HT which cannot be provided from tracer gas techniques nor energy and mass balances. Therefore, more recently, sophisticated direct measurements were undertaken for quantification of ventilation flux produced by naturally ventilated greenhouses, using uni- or multi-directional sonic anemometers (Wang & Boulard, 1999). Sonic anemometry is considered the only technique accurate enough to determine the instantaneous air velocity vectors and total air-fluxes through the HT, in order to estimate the mean values of interior temperature and humidity, and the technique also works well for the turbulent wind effects (López & Valera, 2011).

Some physical-based ventilation models provide insights into energy and airflow distribution associated with heat and mass exchanges; but, typically the models require intense computation to improve the accuracy of predictive estimation (Körner & Van Straten, 2008). Advanced techniques such as computational fluid dynamic (CFD) and artificial neural network (ANN) modelling have been used to develop models for optimizing crop environments. The CFD technique is used by many researchers to develop a two- or three-dimensional models for air exchange measurements in greenhouses with some results showing that wind direction had significant impacts on the ventilation rate and temperature distribution (Boulard et al., 1999; Campen & Bot, 2003; Khaoua et al., 2006; Majdoubi et al., 2009). This tool has been adopted to describe the flow of fluids for air temperature distribution by the Navier-Stokes equations with good accuracy; but, drawbacks of CFD include the need for special knowledge and experience in grid generation, turbulence modeling, and various types of boundary conditions; and it's also costly and needs considerable computational time. Ruano et al. (2006) indicated that CFD technique would take days for a medium size building to simulate indoor temperature. Moreover, this technique is difficult to use because there are too many physical data inputs required which are often poorly defined, resulting in ambiguity and uncertainty for simulating, predicting and interpreting the output (Lu & Viljanen, 2009).

ANNs have been used as an alternative to study non-linear problems in various scientific fields during the last 20 years, including engineering, medicine, and economics (Kalogirou, 2001). This technique is a powerful tool to offer faster computation than a CFD technique based on a large number of interrelated experimental data, which is easy to apply, and even conducts assessment and prediction. In addition, ANN is widely accepted by the users due to its ability to recognize useful inputs and remove irrelevant values, without explicit evaluation of transfer coefficients or mathematical formulation of how output depends on inputs. It also exhibits fault-tolerance and noise immunity, namely, it is an alternative technique to model incomplete and inherently noisy data, and nonlinear equations. Thus, ANN can not only analyze experimental behaviors, but also leverage the massively interconnected input data for future predictions, which makes this technique suitable for solving complicated scientific problems in climate science such as climate change, or mathematical relationships between climate science-related parameters (Ferreira & Faria, 2002).

In addition to ventilation management, several other factors limit HT sustainability and profitability. First, the HT structure blocks rainwater; thus, groundwater or local water resources are required for crop irrigation. However, many areas around the world face water supply shortages, partially due to rapid population growth and climate change (Coombes & Barry, 2007; Mendez et al., 2011). As an alternative to irrigation systems that consume existing water and energy resources, rainwater can be collected, stored and used inside the HTs through a rainwater harvesting system (RHS). Because many plants are sensitive to soil salinity, the practice of using rainwater is preferable over other artificial water resources.

Another limitation to organic production in HTs is their low insulating ability. In cold climates, the thin plastic cover on HTs does not offer enough insulation to keep favorable temperature for maximum crop growth inside. This is true especially at night since HTs allow the inside temperature to drop close to the outside temperature even though daytime temperatures inside are elevated early and late in the season. However, surface mulching and row covers are expected to increase soil and canopy temperatures without requiring energy from electricity or fuel. First, surface polyethylene mulches are commonly used to provide more sustainable and optimal soil conditions in the open fields. This practice is not only for alleviating soil crusting, controlling weeds and inhibiting pests, but also to significantly influence the microclimates around the plants by modifying the radiation budget of the surface and improving water conservation (Liakatas & Clark, 1986). Mulch colors are considered to have significant impact on the microclimates around plant-root areas because soil temperature under the mulches largely depends on the radiative heat transfer properties (reflectivity, absorptivity or transmittance) of a particular mulch material to capture solar radiation (Schales & Sheldrake, 1963). In addition, biodegradable mulch can be applied to the ground surface as an alternative thermal protection to polyethylene plastic mulch for HTs (Kapanen et al., 2008). Like polyethylene mulch, biodegradable films are also effective in raising soil temperatures, preventing evaporative loss of soil moisture, and suppressing weeds compared to bare ground, thereby contributing to faster crop growth rate and better yield performance (Greer & Dole, 2003; Miles et al., 2012). Despite the similarity, biodegradable mulches deteriorate faster than that of polyethylene ones during the growing season (Ngouajio et al., 2008; Waterer, 2010). Second, floating row covers, by creating a thin insulating layer above and around a crop, are another means of protection from wind and frost, thereby increasing canopy and soil temperature on cold nights. Many studies showed that under field conditions, soil mulch in combination with row covers significantly improved early and total yields of horticultural crops by increasing soil moisture, canopy and soil temperature, thus creating a favorable microclimate for crop growth (Ibarra-Jiménez & Quezada-Martin, 2004). However, the use of row covers may damage plant tissue outdoors due to shear if they flap in the wind which is less likely to occur inside a high tunnel.

An additional limitation for using HTs is that increased cropping and higher soil temperatures can limit the accumulation and decomposition of organic soil matter, thereby negatively impacting soil water and nutrient holding capacity (Kirschbaum, 1995). One important solution is to supplement soil organic matter with organic forms of nitrogen; but, the collection, processing and transportation of the supplements to HTs require energy usage and costs. Pre-planting a cover crop inside HTs is an energy efficient way to promote soil fertility, along with the added benefit of enhanced specialty crop performance. While certain cover crops have the ability to fix nitrogen, there can be a positive impact on crop yield by either incorporating crop residue into the soil or depositing it on the ground surface. However, the effects of cover crop residues incorporated into the soil and then covered by different colored plastic mulches are still limited under HT systems.

Therefore, Chapter 2 investigated HT-dependent air flux in response to exterior climatic conditions, using a typical ventilation system limited to a cooler springtime period when only the end doors are used. In this chapter, human decisions on the size of ventilation openings around solar noon, and the measured exterior weather conditions and the resulting inside microclimate were used to model ventilation adjustments. Chapter 3 provides a unique investigation on HTs' ventilation using advanced artificial neural networks (ANNs) compared with both mathematical calculations and instrumental measurements which were developed in Chapter 2. In addition to the ventilation studies, Chapter 4 used various agricultural practices incorporated in different combinations to modify the microclimate inside the HTs along with better monitoring practices offering producers data to help better manage their operations. Specific practices included mulching (polyethylene and biodegradable film and vegetative), row cover, cover crops, and irrigation water types (rainwater and city water). The primary objective of this chapter is to assess the beneficial effects of independent or combined practices based on energy conservation (temperature) as well as the effects on crop yield in HT systems.

Chapter 2
Modeling Energy Balance and Airflow Characteristics in a Naturally Ventilated High Tunnel

Abstract.

High tunnels (HTs) are used worldwide for greater crop sustainability and profitability; but producers are finding it difficult to control the trapped heat inside HTs. Clearly, proper ventilation management is crucial for obtaining marketable yield and fruit quality, but the ability to predict HT ventilation based solely on external climate parameters is limited. This project analyzes daytime ventilation rates in a Gothic-type HT located in eastern Tennessee. A numerical energy balance model was developed to calculate air flux and then these estimated values of air flux were compared with measured values from sonic and hot wire anemometers. Uniquely, this study takes into account the sensible and latent thermal heat exchanges between interior and exterior conditions, the radiative and convective transfer mechanisms, and the effects of external wind conditions on incoming air-flux. Moreover, relationships between external weather conditions and the internal microclimate were developed so that air flux, inside temperature or door adjustment level can be predicted from the energy balance model using only external weather data. The energy balance model revealed that the HT plastic surface reflected nearly 20% of solar radiation, that 1% of solar energy was stored in air (considered negligible), and 5% of the solar energy was stored in the soil, while the majority of available solar radiation, 74%, was removed through the process of HT natural ventilation. There was a good agreement between the predictive energy balance model and the direct air flux calculation for ventilation rate (R^2>0.70). At the windward end of HT, the airflow entering the door prevails mostly perpendicular to the plane of HT's door opening, which indicated that the fluctuation of outside wind direction had little effect on the airflow patterns through the door. As a significant indicator of Energy Balance model usefulness, the predicted

interior air temperature was validated as being similar to the measured values. Thus, the results showed strong evidence that the coupling of energy balance model and air-flux calculation based on external weather parameters can be considered a valuable method to predict the interior microclimate condition and also can be used to estimate door opening levels.

Introduction

High tunnels (HTs) are simple, plastic-covered, greenhouse-like structures without electrical heat sources inside (Figure 1). They have become widely used for crop production as a mean of protecting crops from potentially damaging weather conditions, such as frost events, temperature fluctuations, and excessive precipitation. HTs also have low overall startup costs, fewer energy requirements, and demand less electrical equipment operation and maintenance than standard greenhouses (Kittas et al., 2005). Greenhouses typically use glass or an air-inflated double plastic film layer and have fully automatic ventilation or heating/cooling systems, but Wang et al. (1999) found that the electrical system accounts for approximately 30-50% of the total production cost in a large greenhouse. Therefore, HT production can be more profitable because fuel consumption can be replaced with renewable solar energy as the primary heat resource. Even though the topography of Tennessee is quite varied from the lowlands of the Mississippi Valley to the mountain peaks in the east, most of the state is characterized by warm, humid summers and mild winters. This climate is warm enough in mid-winter to allow HTs to function well for cool-season crops while also significantly extending growing seasons for warm-season crops, which allows harvesting during what are traditionally the off-season periods when prices are higher. Asian and European farms have used HTs for decades, but this kind of growing system is still relatively new in North America. There are two primary structures for single-bay HTs: Quonset and Gothic arch. Gothic type HTs have become more popular because the steep and pitched roof can readily shed snow, and the Gothic arch angle helps shed interior condensed water and prevent water drip on the crops below. These structures are manually ventilated by rolling up curtains along both sides and opening the sliding doors at both ends of the HT.

A HT is considered a solar collector that allows the short-wavelength solar radiation to penetrate but traps the long-wavelength thermal radiation to warm the air and soil temperature (Abdel-Ghany, 2011; Jain & Tiwari, 2002; Kendirli, 2006). The total amount of solar radiation captured by the HT is absorbed as thermal energy by the crop and other components including the ground surface. Part of the solar energy may be transferred by the latent heat through plant transpiration, and the rest contributes to sensible heat warming of the interior air (Olsen & Gounder, 2001). Significant variation of air temperature and humidity inside the HT mainly occurs when compared to outside because of the exterior climatic conditions when no auxiliary heating or fan system is utilized inside (Tong & Christopher, 2009). Increasingly producers using HTs desire to lengthen the growing season further than outdoors; but, the trapped heat and humidity inside HTs are difficult to control, especially in subtropical regions. Accordingly, energy effective ventilation management becomes important for HT operators due to the essential function of controlling the interior climatic environment to obtain marketable and sustainable yield and quality. Ventilation rate through the HT is considered a key process that directly affects the transport of sensible and latent heat to and from the interior air, helping to control the interior soil temperature, humidity and also the evapotranspiration rate in HTs. Moreover, ventilation operation depends on the season: in winter, ventilation management is needed to exchange the surplus of moisture and retain heat for the crop. While in summer, proper ventilation is mostly applied to cool down the inside air temperature and to evacuate water vapor (Baptista et al., 1999). Compared to forced ventilation, natural ventilation can effectively reduce energy inputs and cost in the production system. Crucial factors affecting natural ventilation include captured solar radiation, the temperature difference between interior and exterior, as well as the inlet and outlet vent openings, heat absorption from internal thermal mass and cooling effects from the exterior wind. HTs have different opening configurations, various building orientations, and locations, with different wind flow obstacles that may affect natural ventilation. Since the ventilated opening like sliding doors and side curtains are not usually automatically controlled, producers have some difficulty manually adjusting their vents to maintain optimum thermal properties for plant growth.

Solar energy efficiency in greenhouses has received considerable attention since the 1990s. Boulard and Baille (1995) studied ventilation rate in a multiple-span greenhouse with different roof or side vents and other researchers also determined ventilation performance based on various vent configurations. Pimpini et al. (1987) analyzed side opening (roll-up type and pivoting door type) and roof openings on combined structures at certain opening levels, and obtained the same results as Arin and Ankara (2001) who showed that the minimum ventilation rate occurred from roof openings alone and the maximum value was achieved by the combination of roof and side vents. Most studies forced steady-state flow regimes while suppressing unsteady phenomena for designated time periods (Siwek & Kalisz, 2007), even though the experimental conditions do not simulate the real inner microclimate scenario. Various techniques have been offered to measure ventilation flux rates in a more or less direct way. Most of the studies estimated ventilation flux based on derivations of energy, mass and momentum balance models along with pressure-difference measurements between the inside and the outside of the structure (Chalabi & Bailey, 1989; Demrati & Boulard, 2001b; Kindelan, 1980; Wang & Deltour, 1996). Kindangen (1996) used the energy and mass conservation to investigate the transient response of air temperature and humidity inside a greenhouse. Since the middle of the 1950s, tracer gas techniques have been commonly used to directly measure the ventilation rate for both glass and plastic greenhouses (Arin & Ankara, 2001; Kittas & Bartzanas, 2007), with different media such as carbon dioxide (CO_2), methane (CH_4) or nitrous oxide (NO_2) (Bot, 1983; Fernandez & Bailey, 1992; Jain & Tiwari, 2002; Kittas & Draoui, 1995; Kittas & Bartzanas, 2007; Nederhoff et al., 1983). Rezaeian et al. (2010) used a trace gas technique to measure air exchange rate in a greenhouse tunnel equipped with continuous side openings, and results showed that the air exchange rate significantly depends on wind speed and total vent area. Fernandez and Bailey (1992) indicated that a tracer gas technique provides better accuracy than the energy balance derivations at low ventilation flux conditions, and used this technique to measure and analyze the air exchange in a Canary type greenhouse (Boulard & Wang, 2000). However, tracer gas technique cannot be applied without electrical fans or electricity in HTs. Thus, an energy balance model is considered a general way to understand each interior microclimate component. Since the exterior air velocity affects the heat and mass transfers within the HTs, it is of interest to determine the air-flux patterns in and around the HT which cannot be provided from tracer gas techniques nor energy and mass balances. Therefore, more recently, sophisticated direct measurements were undertaken for quantification of ventilation flux produced by naturally ventilated greenhouses, using uni- or multi-directional sonic anemometers (Wang & Boular, 1999). Yonaba & Anctil (2010) used a three-dimensional sonic anemometer to investigate the air flux and sensible heat exchange in a naturally ventilated twin-span greenhouse with continuous roof openings, indicating that 58% and 42% of the total energy exchange between interior and exterior were caused by the mean and turbulent sensible heat exchange through the vents. Sonic anemometry is considered the only technique accurate enough to know the instantaneous air velocity vectors and total air-fluxes through the HT, in order to determine the mean values of interior temperature and humidity, and the technique also works well for the turbulent wind effects (López & Valera, 2011).

Objectives

Natural ventilation adjustments of an HT are important decisions made by producers that take into consideration exterior weather conditions and the desired interior microclimate. Most studies investigated ventilated greenhouse and tunnel performance to develop optimum vent arrangements (Nääs et al., 1998; Verlinde & Gabriëls, 1998), but studies are limited concerning the interactions between HT inner microclimates and incoming air-flux purely based on the exterior weather conditions. This study investigated HT-dependent air flux in response to exterior climatic conditions, using a typical ventilation system limited to a cooler springtime period when only the end doors are used, which is a very critical time for improving existing practice in naturally ventilated HTs. Therefore, this study used human decisions on the size of ventilation openings around solar noon, and the measured exterior weather conditions and the resulting inside microclimate were used to model ventilation adjustments. Detailed objectives are as follows:

(a) Use a hot-wire anemometer to map air-flux patterns at the windward sliding-door opening, for better assessing boundary layer effects on total air-flux calculation of two-dimensional sonic anemometer measurements;

(b) Improve understanding of the physics of the natural ventilation process in a Gothic type HT by energy balance techniques, to establish a detailed theoretical model to predict ventilation rate;

(c) Determine natural ventilation flux by using two-dimensional sonic anemometry measurement as a validation of the energy balance technique;

(d) Couple an energy balance model and air-flux measurements to predict the ventilation adjustment levels for optimal HT cooling management using exterior weather parameters.

Material and Methods

The Gothic Type High Tunnel

The experimental HT is a commercial gothic type tunnel constructed with a peaked roof and vertical side walls, covered with 200μm thick single layer polyethylene sheets, orientated N-S, and located at the University of Tennessee's Organic Crop Unit in Knoxville (lat 35.88° N, long 83.93° W, elev 252 m). Dimensions of this 139 m^2 HT are approximately 9 m in width and 15 m in length. It is equipped with two types of natural ventilation: 1) sliding doors that cover an opening that is 2.4 m tall and can be adjusted from 0 to 3.7 m wide, with one door at the northern end and another one at the southern end, and 2) side curtains that can be opened along the whole length of the structure by rolling up the lateral film. However, the study was only conducted with the sliding doors used for ventilation and the side curtains in the closed position because the side curtains are generally opened during warm weather when maximum ventilation is required. During cooler times of the year, the side curtain and sliding doors need to be closed at night to retain heat, and only the doors are opened during the day because minimal ventilation is required. There are two similar HTs constructed at both sides of this experimental HT, and the windward end is usually with respect to the prevailing southern wind.

Climatic Measurements

Weather parameters were systematically measured and recorded to 1) characterize the heat transfer between the interior and exterior climate, 2) investigate the boundary effects for incoming air flux, and 3) calculate the ventilation rate (Table 1). Table 1 provides all the needed sensor parameters: type, location, measurement range and accuracy. The outside meteorological station was located 10m away from the HT and positioned 4m above the ground (Figure 2A). Solar radiation was measured by a pyranometer (*LI-COR LI200R*) on a horizontal surface. Wind speed and direction were measured through a windset (*R.M.Young 03001*). Relative humidity and the air temperature were measured using a sensor (*Vaisala HMP60*) installed in a ventilated radiation shield. Also, an inside climatic station located at 1.5 m above the ground in the middle of the experimental HT (Figure 2A), used the same sensors described for the outside weather station. There is a thermistor placed at the inside weather station for the air temperature measurement, which was painted white for shielding purpose. The HT area was separated equally into 24 plots from six rows with four blocks. An array of 12 thermistors (*PS104J2*) (0.3m above the ground surface) measured canopy temperature and soil temperature was monitored by 24 thermistors inserted 10 cm into the ground, one per plot. All sensors, both inside and outside, were measured every 15 s and recorded every 60 mins by a CR1000 data logger (Campbell Scientific Inc.) via a cellular internet.

Table 1. Variables Measured during the Experiments.

Measured Parameters	Sensors	Range and Accuracy	Location
Solar radiation Q_{solar} (Wm^{-2})	LI200R Pyranometer (LI-COR, Inc.)[a]	400 to 1100nm with ±1%	Inside and outside weather station
Air temperature T_i (K) and Relative humidity H_R (%)	HMP60 Probe (Vaisala, Inc.)[c]	-40 to 60°C with ±0.5°C 0 to 100% with ±3%	Inside and outside weather station
Outside wind speed U (ms^{-1}) and wind direction (°)	Met One 034B Windset (Campbell Scientific, Inc.)[b]	0 to 75ms^{-1} with 0.1ms^{-1} 0 to 360° with ±1.1%	Outside weather station
Incoming wind speed u_{sonic} (ms^{-1}) and wind direction (°)	DS-2 sonic anemometer[*f]	0-30ms^{-1} with 3% 0 to 360° with ±3º	0.8m and 1.7m above the ground with 0.3m inside the door
Instant incoming wind speed $u_{hot\text{-}wire}$ ($m\ s^{-1}$)	Hot-wire anemometer[g]	±0.3 ms^{-1}	Each grid center of the south door opening
Middle wind speed u ($m\ s^{-1}$) and wind direction (°)	DS-2 sonic anemometer[**f]	0-30ms^{-1} with 3% 0 to 360° with ±3º	1.2m above the ground at the inside weather station
Air temperature (°C)	Thermistor (PS104J2)[† e]	±0.1°C with 0.026°C	Inside and outside weather station
Soil temperature (°C)	Thermistor (PS104J2)[†e]	±0.1°C with 0.026°C	10cm below the inside soil surface

[*]means that the sensors are developed by Decagon Company and [†] means the thermistors are made in our lab which are non-linear sensors following a polynomial response to temperature that is defined by the Steinhart-Hart equation, also the superscript letters (abcdef) represent the specific sensor shown in Figure 2.

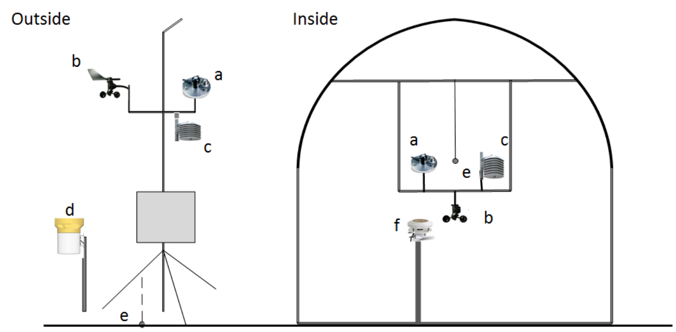

(A)

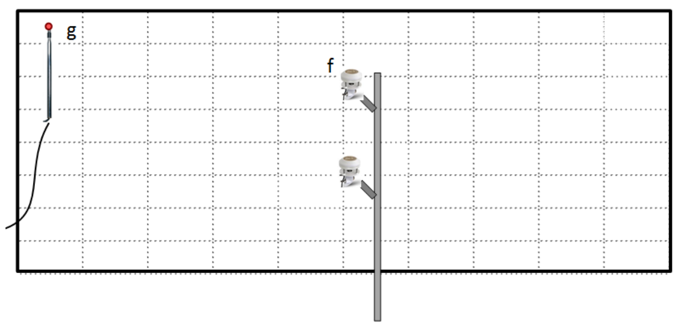

(B)

Figure 2. (A) Inside and outside weather stations and (B) air velocity measurements at the windward door opening with the measurement grids made of fishing line (cross-section view). Sensor systems include (a) LI200R pyranometer; (b) Met One 034B windset; (c) HMP60 probe (e) thermistor (f) DS-2 sonic anemometer; (g) hot-wire anemometer. Portable hot-wire anemometer (g) was applied in each grid and the DS-2 sonic anemometers (f) were placed at the middle part of the windward sliding-door opening.

Wind speed and direction through HT door openings were measured using DS-2 ultrasonic anemometers (Figure 2B). At each door opening, two DS-2 sonic anemometers were aligned along a vertical support at 0.8 m and 1.7 m above the ground, located 0.3 m away from the center point of the door inside the HT. There was another DS-2 anemometer located at the center of the HT, placed at 1.2 m above the ground. The vent openings were adjusted manually at each day and kept at the same level throughout the day. The resulting inside temperature was used to estimate the door opening of future days based on similar outside whether conditions, and wind speed and direction were recorded continuously with a frequency of 5 Hz and 5-minute acquisition periods. Moreover, in order to test if the two measured locations of 2D sonic anemometers could represent the average air-flux pattern through each door opening of the HT, a portable hot-wire anemometer (Extech 407123) was used to map the air-flux distribution through the HT's door opening. Most of the time the wind blew from south to north, and thus these measurements were only applied at the south end-door opening. A grid was made by using fishing lines between PVC pipes which were attached all around the south door opening (each grid is 0.3 m by 0.3 m) and grid centers were used as the location for wind speed measurements by the hot-wire anemometer. Three airflow readings for each grid were taken in approximately 5 minutes, and further the three occurrences were averaged as an air-velocity value of each grid; repeated measurements over the total 80 grids were developed to create a whole airflow map through the sliding-door opening. This kind of hot-wire anemometer is a one-dimensional device, which means the sensors are placed in the air current having the air flow meet the sensor head in the direction of the indentation on the sensor head. The telescoping probe antenna on the hot-wire anemometer allowed convenient access to the grid center in order to minimize the error of blocking the airflow.

The HT was used to grow tomato and sweet bell pepper that were transplanted on March 25, 2015, and laid out in six rows running N-S. The plants were irrigated with a drip system. Data for this study was gathered during the first month of early spring right after transplanting as such the crop grown in this tunnel was still small with a canopy that covered 15-20% of the soil surface. Thus, the effects of crop size and the further changes of leaf transpiration were considered negligible in the modeling effort. DS-2 sonic measurements were performed every single day of April 2015, and the hot-wire measurements were applied in 14 random days. The simulation for this study was conducted around solar noon from 10:00 am to 16:00 pm EST to maximize the solar radiation entering as well as the energy exchange through the high tunnel. The specific time of each hot-wire anemometer measurement was usually selected during noon when fewer wind gusts occurred. Additionally, each term of the mathematical energy balance model was measured every 15 s, averaged online and logged on a 1-hr basis while each term of DS-2 sonic anemometer measurement was averaged over 30 mins. Consequently, the estimated ventilation flux ($m^3\ s^{-1}$) corresponds also to a 1-hour average value over the solar noon period. Tecplot 360 (Tecplot Inc.) was applied for the incoming air-flux visualization at the south sliding-door opening from hot-wire anemometer measurements. Regression analysis with the standard error was applied to estimate the relationships among different variables.

Energy Balances Estimation

The HT is considered a controlled volume enclosed by the plastic covers above and a thin layer of the ground surface below. Many studies present simplified models about energy and mass balance regarding “sources” and “sinks” (Demrati et al., 2001a) to show the effect of the numerous factors and processes in determining a greenhouse’s inner microclimate with factors such as the convection thermal exchanges between the inner air and plastic cover and the ground being excluded. The energy balance of an HT dictates that the energy input equals the sum of the energy losses during a given period. A simplified version of HT energy balance was performed to learn more about the microclimate variables, in order to estimate interior temperature and determine natural ventilation adjustment levels. The factors considered are as follows: the energy removed by the process of thermal losses through the cover (Q_{cover}), used in photosynthesis (Q_{pho}), stored energy (Q_{stored}) and ventilation flux (Q_{vent}) are equal to the solar energy absorbed in the HT ($Q_{solar,i}$). Q_{pho} can be ignored accounting for only about 0.5-1% of the total solar radiation input (Abdel-Ghany & Al-Helal, 2011), and the plants were quite small during the data collection period when Q_{pho} would be even smaller. Energy lost by ventilation includes two components, sensible heat (Q_{sen}) and latent heat (Q_{lat}). Microclimates in the middle of the HT are assumed to represent the whole HT environment. Therefore the energy balance can be formulated by Equation 1 (Kittas & Katsoulas, 2001):

$$Q_{solar,i} = Q_{\mathrm{cover}} + Q_{stored} + Q_{vent} \tag{1}$$

The amount of sensible heat loss represents the energy needed to maintain interior-air temperature at optimal levels while removed latent heat is related to the decrease of interior-air humidity (Kittas et al., 2001), thus the sensible heat loss Q_{sen} and the latent heat loss Q_{lat} in W m^{-2} are shown by Equations 2 and 3 (Campen & Bot, 2003):

$$Q_{sen} = \frac{\rho C_p G}{A_g}(T_i - T_o) \tag{2}$$

$$Q_{lat} = \frac{\rho \lambda G}{A_g}(x_i - x_0) \tag{3}$$

where, ρ = specific mass of air (1.14-3.3 kg m^{-3});

C_p = volumetric specific heat of air (J kg^{-1} K^{-1});

G = air exchange through the vent (m^3 s^{-1});

A_g = high tunnel ground area (m^2);

T_i, T_o = inside and outside air temperature, respectively (K);

λ = latent heat of evaporation of water (J kg^{-1});

χ_i, χ_o = absolute humidity of air inside and outside HT (kg kg^{-1}).

The absolute humidity is a density, mass of water vapor per unit volume of air, and can be mathematically determined by mean air temperature and relative humidity measurements (ASHRAE, 1997), shown in Equation 4.

$$\chi_{i,o} = \frac{6.11(H_{R,i,o})(10^{(\frac{7.5(T_{i,o}-273.15)}{T_{i,o}-35.45})})}{461.5(T_{i,o})} \tag{4}$$

where χ_i , χ_o = absolute humidity inside and outside HT (kg m^{-3});

$H_{R,i,o}$ = relative humidity inside and outside the HT (%);

$T_{i,o}$ = air temperature inside or outside the HT (K).

The solar energy collected in the HT (W m^{-2}) depends on the external solar radiation ($Q_{solar,o}$) and the transmissivity of the plastic roof and side walls (α), expressed by Equation 5. In this research, it was directly measured by installing a sensor inside the HT:

$$Q_{solar,i} = \alpha Q_{solar,o} \tag{5}$$

The thermal loss through the unit area of the cover is represented by Equation 6:

$$Q_{cover} = \frac{UA_c}{A_g}(T_i - T_O) \tag{6}$$

where A_c = the area of HT plastic cover (m^2), U is a non-constant parameter representing the global heat loss coefficient of the cover. This coefficient could be determined based on the difference of environmental conditions inside and outside of the HT, such as the effect of convective and radiative resistances on the plastic cover surface. The parameter U strongly depends on the external wind speed and the relation is expressed by Equation 7 (Demrati et al., 2001a):

$$U = a + bu \tag{7}$$

where u = outside wind speed (m s^{-1});

a, b = constants with values of 6 and 0.5 (for single cover high tunnel).

The stored energy (W m^{-2}) inside the HT includes the sensible and latent heat transfer into the plastic cover, inner air, crop, and soil. The general relations are given by the following Equation 8:

$$Q_{stored} = Q_{stored}^{Cover} + Q_{stored}^{Air} + Q_{stored}^{crop} + Q_{stored}^{soil} \tag{8}$$

Since the plastic cover is very thin just around 200μm, the interior and exterior temperature of the cover surface can be considered approximately the same (Majdoubi et al., 2009). Therefore, cover energy storage can be negligible in this calculation. The crop was at the initial growth stage which meant the canopy storage was also excluded. The soil was assumed to be a homogeneous layer in which the thermal storage inside the soil could be applied in a small time interval as a quasi-steady state condition. Thus, the stored sensible ($Q_{stored/s}$) and latent energy ($Q_{stored/L}$) inside the air and soil were determined from Equation 9 and 10, respectively. These equations were used to perform the rate of change of stored energy of the masses enclosed inside the HT during a certain period (1hr):

$$Q_{stored/s} = \frac{M_i C_{pi}(T_B - T_E)}{A_g(t_E - t_B)} \tag{9}$$

$$Q_{stored/L} = \frac{M_i \lambda \, (x_B - x_E)}{A_g(t_E - t_B)} \tag{10}$$

where M = mass per unit HT area (kg m^{-2});

T_B, T_E = temperature of the components at the beginning and the end of the experiment (K);

t_B, t_E = start and end time of the experiments (s);

The index i = one of the components (air or soil).

Volumetric Air-flux Estimation by DS-2 Sonic Anemometric Measurement

The vent openings in HTs can cause rapid and turbulent airflow. Kittas and Bartzanas (2007) indicated that the airflow inside a greenhouse started as a large air flux through the windward vent, which was characterized by a stronger flow rate at the crop level, with a re-circulation loop of slower air velocity situated on the top area. Also in Boulard and Wang (2000), the air flux was a strong current crossing the tunnel from windward to leeward opening, and the wind speed reduced in the upward direction perpendicular to the main current inside the tunnel. The ventilation flux can be deduced by multiplying the mean air speed and the opening section in m^2 perpendicular to the ventilation flux (Wang and Boulard, 1999). However, it is evident that homogeneous air velocity conditions do not adequately represent the real conditions through the HT openings. Therefore, it is of interest to determine air-flux patterns and air turbulent characteristics through each door opening. Two main driving forces determine air movement in natural ventilated HTs: thermal buoyancy and wind forces, which are dependent on the ratio between wind velocity and the root square of the inside and outside temperature difference. If the wind velocity is low, buoyancy forces are more significant which is contributed to a rise in air temperature and relative humidity inside the HT, forming an air loop around the plastic roof area, which in turn accelerates the rate of heat and water vapor transfer through the plastic and sliding-door openings. However, wind forces prevail if the wind velocity is greater than 2 m s^{-1}. Ventilation rate was linearly depending on wind speed regardless of the greenhouse type (Kacira & Sase, 2004), but some other studies indicated that ventilation rate increased at a reduced rate with increasing wind speed, thus the ventilation rate is not always directly proportional to the wind speed (Kittas et al., 1995; Yonaba and Anctil, 2010). The average value of wind speed when using a two-dimensional sonic anemometer is expressed as the sum of mean value $\bar{u}$ and a fluctuating value $u'(t)$, followed by Equation 11 (Cebeci T, 2004):

$$u(t) = \bar{u} + u'(t) \tag{11}$$

The air velocity variance value during a period Δt is estimated by Equation 12:

$$\sigma^2 = \overline{u'^2} = \frac{1}{\Delta t}\int_t^{t+\Delta t} (u - \bar{u})^2 dt \tag{12}$$

The accuracy of the airflow calculation depends on the stability of the wind conditions, such as wind intensity and direction. The mean and turbulent volumetric air-flux rate (m^3 s^{-1}) though each HT opening was determined by multiplying the average value of wind speed u which was measured by using DS-2 sonic anemometers and the perpendicular opening surface S_{vj}, expressed by Equations 13 (Boulard et al., 1998):

$$G_j = \sum_{j=1}^{n} S_{Vj} u \tag{13}$$

Results and Discussion

Boundary Layer Effects

Drag effect occurs as a result of viscous shearing that takes place around the outside of a body, like the friction drag on the ground surface and the layer of fluid air above it that is called skin friction drag. The velocity of the wind increases with height, and the wind power law is usually defined to describe skin drag as Equation 14 (Gupta & Moss, 1993):

$$u_{ref} = u \times (\frac{h_{ref}}{h})^{1/\alpha} \quad (14)$$

where u = wind speed (m s^{-1}) at height h in meter;

u_{ref} = known wind speed (m s^{-1}) at a referenced height h_{ref};

α = empirically derived coefficient which is approximately 0.143.

A boundary layer effect – form drag – occurs at each HT opening, which can reduce the wind speed passing through the door opening at the edges. Each HT opening usually experiences both skin friction drag and form drag, which can have significant effects on the ventilation rate depending on the wind incidence angle and external ground roughness, thus strongly influencing the incoming air-flux pattern. A portable hot-wire anemometer was used to measure air velocity through the south sliding-door opening, which could act as either the windward or leeward section depending on the exterior wind direction. The measured values from each grid center were processed to develop wind speed profiles, calculating the computed contours of air velocity occurring when the sliding-door opening area was adjusted to various positions under varying wind conditions (Figure 3).

Figure 3. Computed contours of the air velocity through the HT southern door acting as a windward (a) or leeward (b) opening. X and Y axes represent the width and the height of the sling-door opening (unit: meters); each contour exhibits an actual door opening size with a fixed opening height (2.4m) and different adjusted width levels. The specific width in Figure 3 (a) is 1.2, 1.2, 1.5, 1.8, 2.1, 2.1, 3.4, 2.4, 3.4, while in figure 3(b) it is 0.9, 1.5, 1.8, 2.7, 2.1 (unit: meters). The legend at the right corner shows the gradient of air velocity values measured by hot-wire anemometer (unit: ms^{-1}): generally redder color expresses greater air velocity, while the bluer color express slower air velocity; Dashed arrows in each contour represent the wind directions measured by the upper and lower sonic anemometers, while the solid arrow represents the outside wind direction. Looking at the front horizontally, the arrows indicate where the wind was coming from, and the various arrow directions indicate the incident angle of incoming air flux. For example, the arrow pointing upper-left means the wind was coming from southeasterly direction, while arrow pointing down-right means the wind was coming from northwesterly direction. The numbers close to the solid arrow represent the outside wind speed, while the one close to the dashed arrow represents the average air velocity of the two sonic anemometer readings (unit: m s-1).

(a)

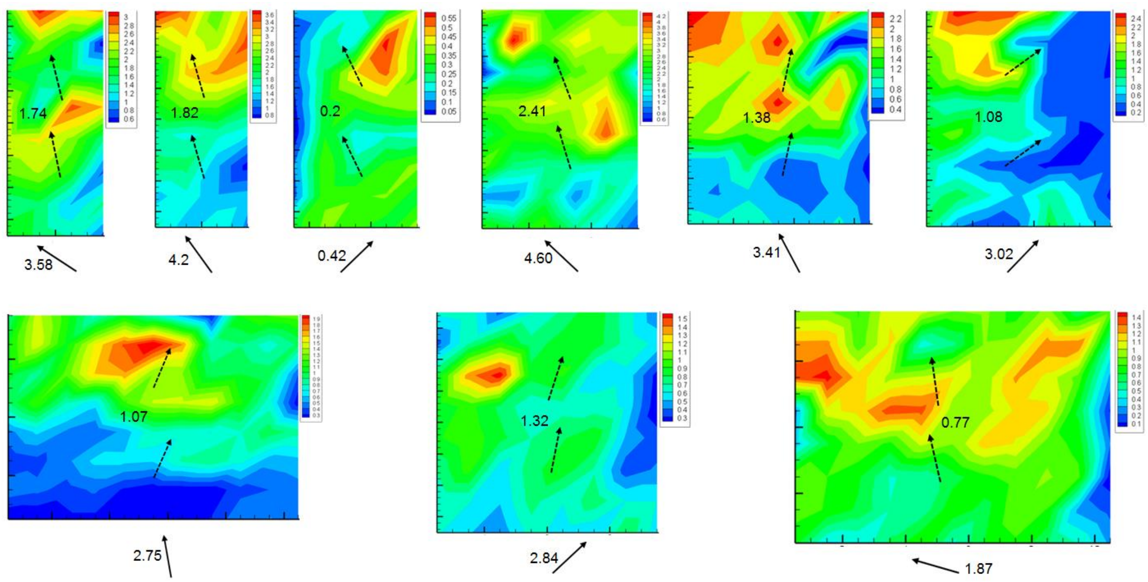

(b)

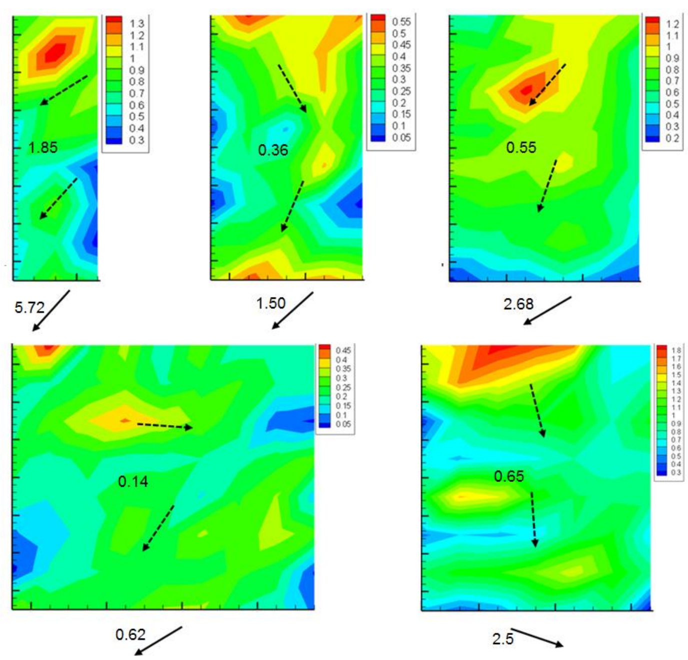

Figure 3 continued.

If the outside wind blew from south to north, the southern windward opening was markedly characterized by a slower air current near the ground and the opening edges, whereas faster velocity consistently occurred near the upper part of the door opening, which confirmed previous understanding of boundary layer drag effects (Figure 3a). The incoming wind was bent or straightened in the perpendicular direction through the middle part of sliding-door openings based on the direction readings of sonic anemometers; therefore, outside wind direction had little effect on incoming wind direction through the door opening. If the southern door acted as a leeward opening with a much slower air stream flowing out, the variation of wind profiles was more stable and less turbulent (Figure 3b). The air velocity inside the HT decreased as the cross-sectional area increased after entering the door opening; the slower-velocity air flowed out through the leeward side where the air flux was distributed more uniformly, but still exhibited the similar characteristics as the windward case, showing the boundary layer effects over and around the opening area. Since the incoming air flux was predominantly parallel to the HT axis, both sliding doors acted simultaneously as inlet and outlet, meaning the air entered the HT through the windward end (mostly at the southern opening) and exited through the leeward end (mostly at the northern opening). Figure 4 shows that average air velocity near the windward end was approximately two times greater than the leeward end, and significantly reduced at the middle part of the cross-sectional HT. Also, a vertical air velocity difference between the upper and lower locations of two DS-2 sonic anemometers was performed at each sliding-door opening showing a faster air current occurs at the upper part of windward opening, while the wind speeds were similar between the upper and lower part of leeward opening. This observation agrees with the previous flow visualization profiles in Figure 3. The leakage would be one reason to cause the air velocity drop from the windward to leeward end. Also based on the theory of momentum, strong air-flux from the windward end diverted upwards and sideways along with the bigger opening section at the middle of the HT, and thus forms a reduced air velocity. Furthermore, air velocity may tend to increase a little bit more when the air passing through the constricted opening of the leeward end.

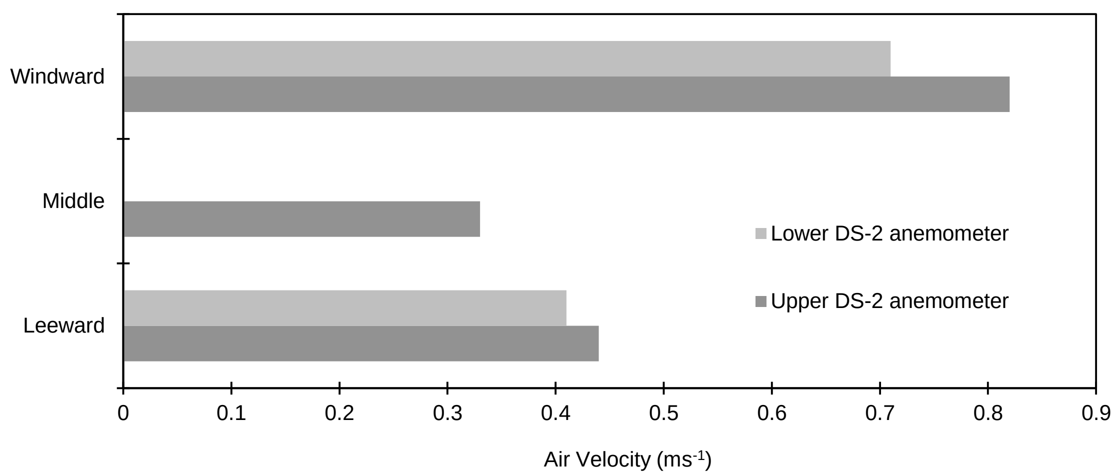

Figure 4. Average air velocity at the middle section, the windward and leeward ends of the high tunnel (an example of April 9, 2015, with 3.7 m opening width).

Since drag force is related to air velocity distribution, it was difficult to predict by a purely theoretical method. Thus, an empirical drag coefficient was provided based on the experimental data. The portable hot-wire anemometer was used to measure the instant incoming air velocity without blocking air-flux due to the small size probe (≈ 8mm diameter). The data measured was assumed to be the actual and instant incoming wind speed normal to the door opening, because the incoming wind was showed to be bent or straightened in the perpendicular direction through the middle part of sliding-door openings based on the direction readings of sonic anemometrical measurements. From the total 25 events, 70% of hot-wire anemometrical measurements at the windward section were selected after removing the outliers (significant standard deviation larger than 0.5m s^{-1} for air velocity). Without considering wind direction from the sonic anemometer, the average air velocity of hot-wire measurements through the total opening area was calculated and compared with the mean sonic anemometrical values during the corresponding period, resulting in a high correlation with an R-square of 0.94 (Figure 5, a). The air velocity measured by the hot-wire anemometer ($WS_{hot\text{-}wire}$) was related to the sonic anemometer according to Equation 15,

$$WS_{hot\text{-}wire} = 0.95WS_{sonic} + 0.051 \tag{15}$$

Equation 15 shows that average air velocity measured by the hot-wire anemometer was less than that of the sonic anemometers when the air velocity was greater than 1 m s^{-1}, and the coefficient less than 1.0 is probably due to the boundary layer effect. Moreover, an air-flux empirical equation was also developed to predict the total air flux through the windward section of HT openings. For the total air-flux estimation through the southern opening, summing up individual values of air-flux measured by the real-time and instant hot-wire anemometers from each 0.3m by 0.3m grid of the southern opening was more realistic to the true incoming air flux than that sonic anemometry calculation of average wind velocity multiplied by the opening area. However, the hot-wire anemometer measurements are unidirectional normal to the sliding-door opening, thus the omnidirectional air-flux values of sonic anemometers can be corrected using the vectors and triangle geometry, which is representation of the relationship between the component vectors of the wind. Wind direction measured by sonic anemometers was converted to an incident angle interval from 0º to 90º relative to the opening edge and the equation $v = WS\frac{\tan\theta}{\sqrt{1+\tan\theta}}$ was applied to calculate the wind speed vector perpendicular to the door opening where θ is the wind incident angle. Thus, the incoming sonic air flux through the door can be corrected for incidence angle and compared with the outputs from the hot-wire method. The total hot-wire air flux ($G_{hotwire}$) was compared to the sonic anemometrical values (G_{sonic}) with and without the correction of wind direction (Figure 5, b), and the relationships exhibit strong similarity with coefficients of 0.83 and 0.87 and intercept of 0.6 and 0.7, respectively (Equations 16 & 17). After the correction for wind direction, the regression slope is steeper with a slightly larger intercept compared to values without the correction for wind direction, which may be due to the weak influence of wind direction on the boundary layer effects. Air flux measured by the hot-wire anemometer was smaller than the sonic anemometers method when the air flux was greater than 5.38 $m^3 s^{-1}$, and the boundary layer effect increased with outside wind speed. The general rising tendency indicates that the stronger outside wind can result in higher boundary forces around the opening edges. Since each hot-wire measurement was applied at the instant of occurrence, while the sonic anemometer automatically averaged the air velocity for the air-flux calculation during a 30-minute period. The measurement differences may cause error due to turbulent wind characteristics and boundary layer effects. Wind direction measured from sonic anemometers can be used to partially explain the differences, and thus the relationship between the hot-wire and sonic anemometer readings serves to some extent as a correction for the boundary layer effect shown in Equation 17.

$$G_{hotwire} = 0.83G_{sonic} + 0.60 \quad (without\ the\ correction\ of\ wind\ direction) \tag{16}$$

$$G_{hotwire} = 0.87G_{sonic} + 0.70 \quad (with\ the\ correction\ of\ wind\ direction) \tag{17}$$

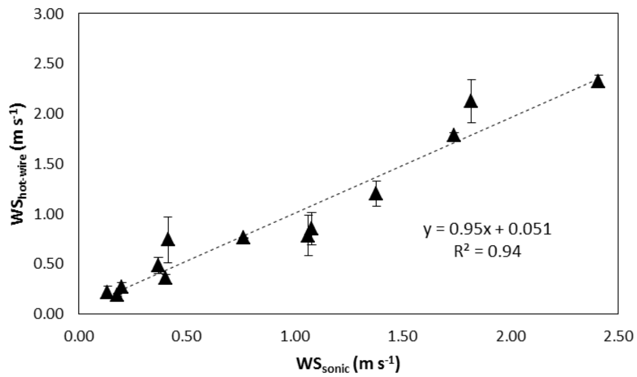

(a)

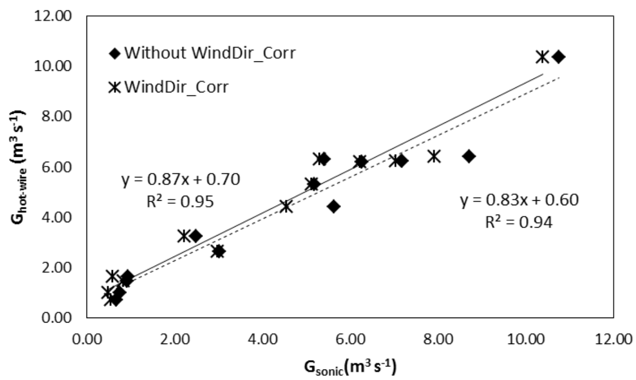

(b)

Figure 5. Comparison of average wind speed (a) and air-flux (b) between hot-wire and sonic anemometrical measurements at the southern windward opening.

The Influences of Outside Weather Conditions on HT Microclimate

Ventilation rate was simulated as the function of the following major parameters: inside-outside air temperature difference, humidity difference, intercepted solar radiation, and outside wind speed. This study assumed that the effective volume of the HT was the same as the physical volume after taking into account the initial stage crops (young tomatoes). Solar radiation as the main energy resource provided the photosynthesis energy for plant growth and thermal radiation to increase the temperature of the HT microclimate. Solar radiation was measured by inside and outside weather stations and used in the energy balance model; the transmission of solar energy depends on the reflective characteristic of the plastic cover. The cover used in this case was a 200µm-thick single layer polyethylene sheet and resulted in a strong relationship between the solar radiation values inside and outside with an R-square of 0.97 and` intercept of 0.006 kW m^{-2} (Figure 6). Based on 180 observations, an average of 17% of the solar radiation was reflected by the plastic cover. Moreover, at higher levels of solar radiation (>0.5kW m^{-2}), greater variability in solar transmission occurred compared with the lower solar radiation. The average level of solar radiation transmission through HT covers was strongly influenced by the optical properties of the cover material, and other studies have shown that solar incident angle may also affect the transmissivity level of solar radiation for certain geometric HT (Kasirajan & Ngouajio, 2012; Tong & Li, 2006). Although this study observed the solar radiation performance only during the time (10:00 am to 16:00 pm) for which the incident angle of the solar radiation may not be very different, but the incident angle of the solar radiation is still considered a potential reason for increased variability in the difference between inside and outside solar radiation.

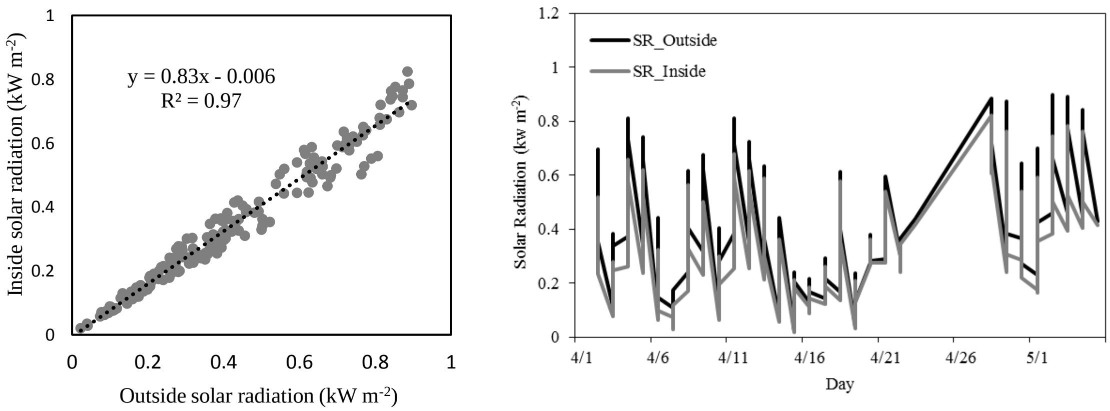

Figure 6. The comparison of inside and outside solar radiation in 2015 spring (daily data). The daily data was averaged by hourly values between 10:00 to 16:00.

The overall consistency of solar transmission can be a prerequisite to simulate other climatic variables accurately. This study measured the climate characteristics both inside and outside the HT (Table 2). The level of solar radiation outside the HT varied from 0.02 kW m^{-2} up to 0.9 kW m^{-2}, with a mean value of 0.43 kW m^{-2} and standard deviation of 0.23 kW m^{-2}. Inside, the mean value was 0.35 kW m^{-2}, with the standard deviation of 0.2 kW m^{-2}. Moreover, the local average temperature was around 17℃, while air temperature inside the HTs was raised from 2℃ to 16℃ depending on cloud cover, wind speed/direction, and how far the tunnel doors were opened. Ventilation adjustment was a significant factor impacting the variation of the inside climate by affecting how quickly inside air was exchanged. Soil temperature at 10cm was lower and varied less than the air temperature as soil temperature ranged from 17℃ to 25℃, but the air temperature was between 15℃ to 35℃ (Figure 7). The prevailing outside wind speed was as high as 7 ms^{-1} and as low as 0.05 ms^{-1}, but most measurements were distributed around 1-4 ms^{-1}, which significantly impacted the ventilation rate. The predominant wind blew from south to north, so this study analyzed air-flux characteristics though the HT mainly at the southern windward sliding-door opening. Also, evapotranspiration inside the HT could cause higher relative humidity than outside, but the result shows that inside relative humidity was lower than outside by around 5%-20% for 94% of the measurements. The likely reason is that during the day, inside air can hold more moisture as it warms, and also the effect of evapotranspiration was limited since the crop canopy was very small. Also high ventilation rates can accelerate the exchange between inside and outside humidity.

Table 2. Experimental measurements performed inside and outside of the high tunnel between 10:00 to 16:00 during April 2015

Parameters	Range	Mean	Stdev
Inside solar radiation $Q_{solar,i}$ (kW m^{-2})	[0.02, 0.82]	0.35	0.20
Outside solar radiation $Q_{solar,o}$ (kW m^{-2})	[0.02, 0.90]	0.43	0.23
Inside air temperature T_i (°C)	[14.5, 37.3]	25.5	2.6
Outside air temperature T_o (°C)	[9.5, 28.9]	17.5	3.4
Inisde soil temperature $T_{i,s}$ (°C)	[16.6, 25.2]	20.8	2.7
Outside wind speed u (m s^{-1})	[0.05, 7.16]	2.40	1.60
RH difference between inside and outside* (%)	[-42.9, 32.7]	21.1	12.4

*Positive values represent that outside relative humidity was larger than inside while negative values represent that the inside air gets drier than outside of the high tunnel.

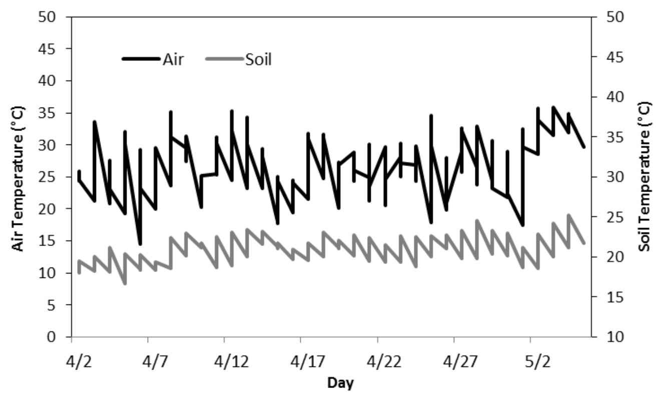

Figure 7. The comparison of inside soil and air temperature in 2015 spring (daily data). The daily data was averaged by hourly values between 10:00 to 16:00.

Energy Balance Model (EB) and Direct Air-flux Calculation (AF)

The energy balance model was used to calculate the ventilation rate of the HT based on inside and outside climatic conditions. Necessary parameters that went into this model included: captured solar radiation (SR_{inside}) as the input resource, sensible and latent thermal loss through the surrounding plastic cover as related to inside and outside temperature difference (ΔT_{air}) and absolute humidity difference ($\Delta\chi$), and the stored thermal energy inside the ground as related to soil temperature difference (ΔT_{air}) before and after a specific period. Coefficients used in this model depend either on the actual structure of HT (A_c, A_g, V) or on the textbook standard values (ρ, λ, $C_{p,i}$, $C_{p,s}$,$C_{p,s}$) (Table 3). The ventilation rate calculated by the energy balance model was up to 12 $m^3 s^{-1}$, with a mean value of 2.43 $m^3 s^{-1}$ and standard deviation of 2.66 which depending on the sky cloudiness, wind speed, external temperature, and the dimension of the sliding-door opening area of each occurrence.

Table 3. Coefficients used in energy balance calculation

Coefficients	Value
Constant *a*	1.44
Constant *b*	0.12
The area of HT plastic cover A_c (m^2)	191.1
HT ground area A_g (m^2)	156.1
HT volume V (m^3)	475.7
Specific mass of soil ρ (kg m^{-3})	1.3
Latent heat of evaporation of water λ (kJ kg^{-1})	2264.7
Volumetric specific heat of air $C_{p,i}$ (J kg^{-1} C^{-1})	1.005
Volumetric specific heat of soil $C_{p,s}$ (wet)(J kg^{-1} C^{-1})	1.48
Volumetric specific heat of soil $C_{p,s}$ (dry)(J kg^{-1} C^{-1})	0.8

The energy balance calculations were based on theoretical (physically-based) equations with inside-to-outside climatic parameters used to predict ventilation rate or air flux through the HT. In order to validate the ventilation rate calculated by the energy balance, direct experimental measurements using the DS-2 sonic anemometers were applied. The total ventilation rate depends on the incoming air flux as measured by multiplying the air velocity and adjustable door opening area. Since the boundary effects were characterized by an empirical relationship (Equation 17), the air flux was calculated from sonic anemometer measurements corrected for boundary effects. Furthermore, some studies have shown that wind incidence angle affected ventilation rate, so the correction of wind speed with respect to sonic or entry wind incident angle was also investigated to determine whether wind direction is a necessary factor affecting ventilation rate for this type of HT. The entering air flux should be equal to the exiting air flux, so inlet air flux was assumed to be the total ventilation rate through the HT. The actual incoming air velocity though the opening was corrected by the boundary layer effects (Equation 17). The linear regression relationships between ventilation rate obtained by the energy balance simulation (EB) and the anemometer measurement (AF) were calculated without and with a wind incident angle correction; the regression slope was 0.99 with an intercept of 1.35 m^3 s^{-1} when not considering incident angle, while the slope and intercept were reduced with a lower correlation after correcting for inlet wind incident angle (Figure 8). This slight difference indicates that the wind direction did not exhibit a significant effect on the ventilation rate of the sonic anemometric method when compared to the energy balance model. The calculated ventilation rate was between 0 to 14 m^3 s^{-1}. The regression relation indicates that the values of ventilation rate from EB were less than that of AF over most of the range of the data (≈1.35 m^3 s^{-1}), which probably means that leakage through the side curtain interface with the structure and corner detachment of the plastic need to be considered in this case. Field observation shows that the big leakages are located around the corners of windward end, which can be accounted for a part of thermal loss through the plastic covering (Q_{cover}). Based on the Equation 1, EB model deduced that the term Q_{ven} is to be lower due to the greater Q_{cover} from the solar energy resource (Q_{solar}). While the higher differences of air temperature (T_i-T_o) and absolute humidity (χ_i-χ_o) between the inside and outside can be elevated because a part of incoming wind going out from the windward leakages and thus less cool incoming air travels the length of the HT. Therefore, G calculated from the equation 2 and 3 of EB model is to be decreased because of the lower Q_{ven}, as well as the higher (T_i-T_o) and (χ_i-χ_o) under the leakage situation, compared to that of AF when its ventilation rate was measured at the inlet without considering any leakages. In addition, outside wind direction had a limited effect on inlet wind direction as the wind was bent to in a direction parallel to the length of the HT such that most of the inlet incident angles only varied from 70º to 90º with respect to the door opening (Figure 9). Baytorum (1986) and Fernandez and Bailey (1992) also indicated that outside wind direction does not have a significant effect on ventilation rate. It should be noted that the HTs on each side of the monitored HT could be helping to straighten the wind in a direction parallel to the HT length. Therefore, the ventilated rate calculated from sonic anemometer with boundary effects only was considered the best method for verifying the energy balance model. The measured and simulated method of obtaining G is calculated as:

$$G_{AF} = 0.99G_{EB} + 1.35 \ \ (R^2 = 0.76) \quad (18)$$

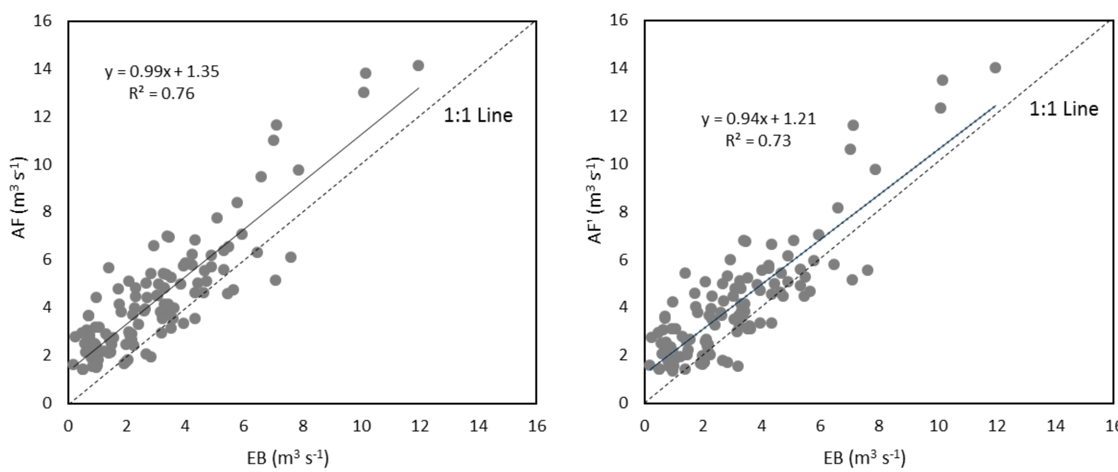

(a) (b)

Figure 8. Ventilation rate comparison between energy balance simulation and sonic anemometer measurement without wind incident correction (a) and with wind angle correction (b).

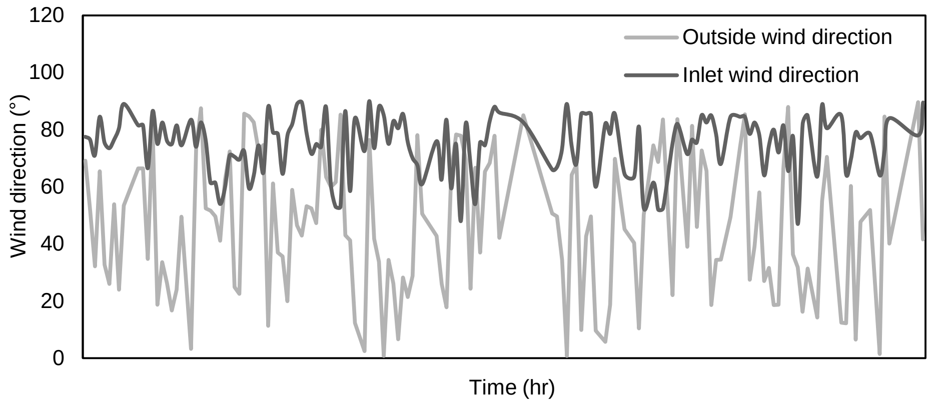

Figure 9. The wind incident angles relatives to the outside wind direction. X-axis represents the hourly time between 10:00 to 16:00 from the dates of April 2, 2015 to May 5, 2015.

Derived Models Based on External Climate and Model Validation

The final applied goal of this study was to use the energy balance model to estimate the adjustments of the natural ventilation system in HTs. Since outside weather forecasts are available all over the world, the possibility of using only external weather data as inputs to the EB model was investigated. In order to facilitate this new derivation of the EB model, processes that were formerly derived from internal measurements were either related to external weather data or to the overall impact on the energy balance (Table 4). Outside solar radiation was used to predict inside solar radiation based on 83% transmission. Moreover, the stored thermal energy of the inside air and soil was related to a specific proportion of the total solar energy resource; stored energy in the air was considered negligible at around 1% of the total solar resource. Soil acted mostly as an energy sink during solar noon, storing approximately 5% of the incoming solar radiation. The soil thermistor sensors were placed 10 cm below the soil surface, which was assumed to be the average soil temperature of 0-20 cm of the soil. However, in reality, the actual thermal storage inside the soil could be greater if the solar radiation was strong enough to heat the ground deeper than that 0-20cm of soil. In addition, inlet air velocity at the southern door opening can be predicted based on external wind speed by an exponential equation (Figure 10). The outside wind was first corrected for friction drag using the wind power law (Equation 17). According to Figure 10 when the outside wind was larger than 2 m s^{-1}, the inlet air velocity increased exponentially.

Table 4. Inputs, output and their relations for new formulations of the energy balance calculation

Output	Input	Relations
Inside solar radiation $Q_{solar,o}$ Stored thermal energy inside Air $Q_{stored,air}$ Stored thermal energy inside Soil $Q_{stored,soil}$	Outside solar radiation $Q_{solar,i}$	$Q_{solar,i}$ = 0.83 $Q_{solar,o}$ - 0.006 $Q_{stored,air}$ = 1% $Q_{solar,o}$ $Q_{stored,soil}$ = 5% $Q_{solar,o}$
Outside wind speed of drag effect u	Wind speed at the outside weather station u_{ref}	$u_{ref} = u \times (\frac{10}{h})^{1/0.143}$
Incoming wind speed u_i at the southern door	Outside wind speed u	$u_i = 0.365\ e^{0.4181u}$
Ventilation rate of hot-wire measurement $G_{hot\text{-}wire}$ (with boundary effects without incident angle)	Ventilation rate of air-flux calculation G_{sonic}	$G_{hotwire} = 0.87G_{sonic} + 0.70$

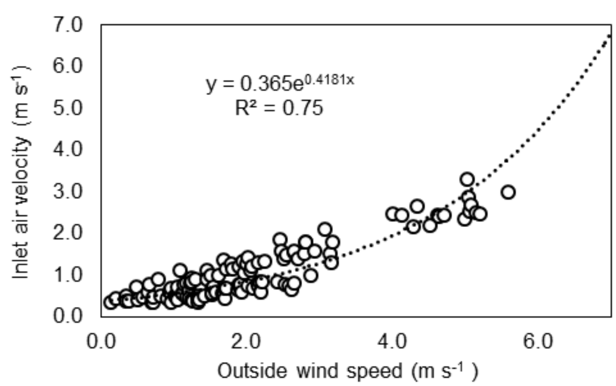

Figure 10. Inlet air velocity and outside wind speed (hourly data)

As an input of the energy balance model, absolute humidity was used by converting from relative humidity and air temperature (Equation 4) plus it was really difficult to predict the inside relative humidity based on outside corresponding weather values. But the changes in humidity closely depend on the rise in temperature as air enters the HT. In this study, absolute humidity was changed as the temperature changed, providing the correlation of 0.70, which means that the increase in absolute humidity is related to the increase in inside temperature as it enters the HT. Thus, a sensitivity analysis was undertaken for the purposes of simulation by using the percentage change method. Based on the regression relations between the temperature difference and humidity difference, the results showed that when the difference of air temperature between inside and outside increased by 10%, the absolute humidity difference correspondingly changed approximately 17.1%, an elasticity level of 1.71 (Equation 19). This high elasticity factor means that the absolute humidity difference responds more than proportionally to the air temperature difference.

$$f = \frac{\cup_{temp}}{\varphi_{ah}} \frac{d\varphi_{ah}}{d\cup_{temp}} = \frac{\%\cup_{ah}}{\%\cup_{temp}} \qquad (19)$$

where f = elasticity level;

$\% \, U_{ah}$ = percentage change of absolute humidity difference;

$\% \, \Phi_{temp}$ = percentage change of air temperature difference.

After converting the energy balance model to use only external weather parameters (EBn), the new simulation was compared to measured values of air flux based on outside wind speed (AFn), revealing a close agreement between AF based on external wind speed and the new energy balance with an R^2 of 0.82, slope of 0.80 and offset of 2.28 (mean absolute error MAE=1.8 m^3s^{-1}) (Figure 11). The estimated ventilation rate was mostly distributed below 10 m^3 s^{-1} in this particular small HT, but the ventilation rate calculated by the AFn method was higher than that of the EBn simulation, On the other hand, the effectiveness of ventilation aims to keep the inside temperature in the desired range by exhausting excess heat through the natural ventilation, as it is related to the door opening. As such ventilation opening is the only component that a producer can adjust to obtain beneficial temperature increases inside the HT. Therefore, the EBn model was solved to predict inside air temperature and then compared with measured air temperature (Figure 12). The regression between measured and predicted inside temperature resulted in a slope of 0.97 with an intercept value of 1.74 and R-square of 0.82 (mean absolute error MAE=1.1°C). The predicted air temperature was lower than the measured values, and the difference was less than 3°C if the goal which was to keep the inside air at a desired temperature around 20 to 30°C. Inside air temperature may have been higher because the leakage out of the HT did not allow the inlet air flux to be maintained at the outlet. Finally, the estimation of sliding-door opening levels from the EBn and AFn models was compared to the measured values (Figure 13). Each specific range represents a 0.6m width of door opening. For example, range 1 and range 2 directly account for 0.3 to 0.6 m and 0.9 to 1.2 m openings, respectively. Due to previous errors in predicting inside weather parameters from EBn and AFn, there is an error in ventilation range prediction. However, the changes of measured and calculated values had similar trends, and the difference is generally found to be within a single range.

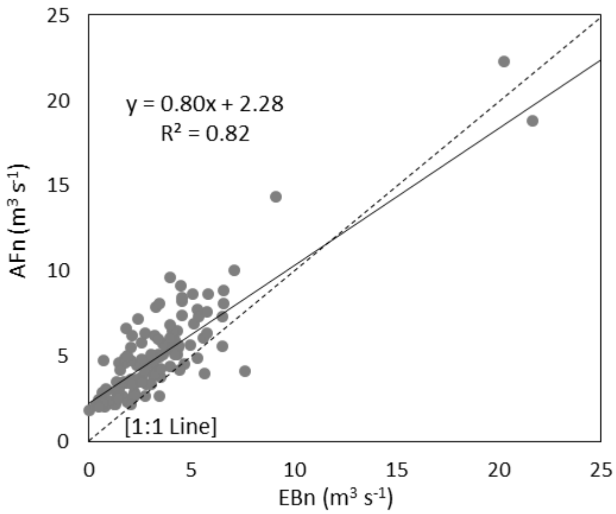

Figure 11. Ventilation rate comparison between new energy balance and new sonic calculation

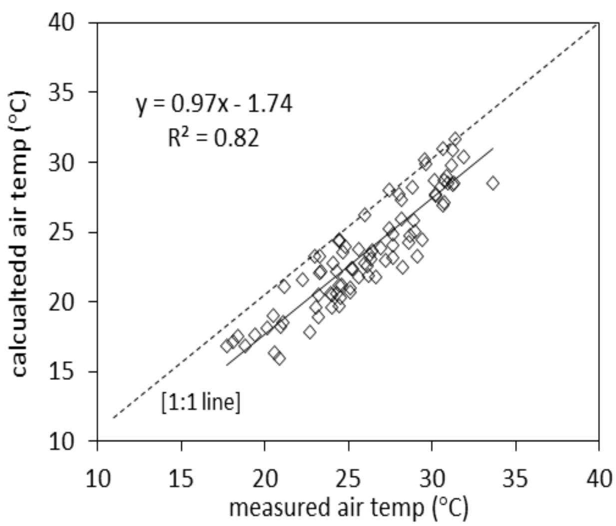

Figure 12. Predicted inside air temperature compared with the measured values

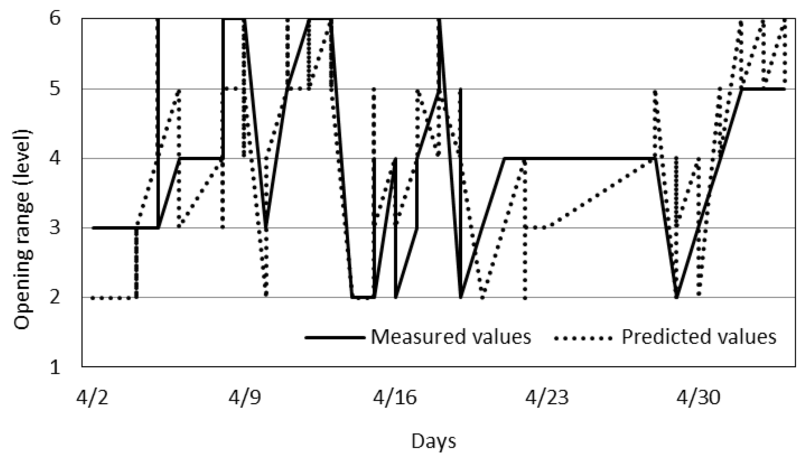

Figure 13. Predicted ventilated range compared with the measured values (daily data)

Conclusion

This study developed an energy balance method simulating the heat exchange mechanisms between the inside and outside of a HT in order to estimate the ventilation rate. The simulated ventilation rate was then compared to measured air velocity multiplied by the cross-sectional area to determine the incoming air-flux using both a 2D sonic anemometer and a hot-wire anemometer. The period studied was in April of 2015 when only the end doors were opened to cool the HTs during the mid-day. Boundary layer effects occurring at each HT opening reduced the wind speed passing through the door opening at the edges, which can have a significant effect on ventilation rates. Result shows that the ventilation rate calculated by the energy balance model was up to 12 m^3s^{-1}, and there was a relatively close agreement between the ventilation rate estimated by the energy balance model and the air-flux calculations based on air velocity measurements. Moreover, an additional EBn model was derived to estimate either the ventilation rate (air flux) or the inside temperature from outside weather data by using simplified relationships between inside and outside conditions.

This research was applied to a very common type of gothic HT with basic ventilation systems and revealed that natural ventilation in HTs can be predicted from readily available weather forecast to determine the appropriate door opening. Although the result only concerns one specific experimental case, other HTs with similar size and ventilation system may also be successfully modeled. For a bigger HT either longer or wider, it seems that the energy balance approach (EB) would stay the same, but the incoming air flux may experience a greater resistance traveling along the building, just as a longer pipe has more resistance to water flow. Therefore, a larger door opening is to be required in order to keep the same ventilation rate as a smaller tunnel. Also, it would be good to have a real time temperature warning system in the HT in conjunction with the modeling because a producer cannot pay attention to a temperature sensor all day long just waiting to change the doors whenever needed. The producers will benefit from a future prediction of where the doors will need to be with a warning system if temperatures get outside of a desired range. In reality, a small producer with many other jobs may only set the door opening in the morning and then adjust it around lunchtime. Now automation of the door open with temperature sensors is a different story but perhaps outside the scope of this research to predict the cost, and also many HTs do not have electrical power in them to start with. Therefore, the ability to better predict ventilation adjustments can improve the crop growth environment and save the cost of making additional ventilation adjustments throughout the day whether or not a human operator has the ability to adjust to all pertinent factors without quantifying them. Since a large part of HT cost is related to the design of the openings, the ability to model higher ventilation effectiveness is essential. More investigation about how an energy balance model can be applied in high tunnels to assist producers improving effective ventilation should be continued in future research.

Chapter 3
Neural Models to Predict Temperature and Natural Ventilation in a High Tunnel

Abstract.

As a response to the rising demand of local food, high tunnels (HTs) can help small producers be more profitable through crop protection and extension of growing season. Proper ventilation that responds to the changes of outside weather conditions can remove the excess temperature and humidity inside and lead to better solar energy utilization, while maintaining a favorable growth environment. Instead of depending on complex mathematical routines which may result in oversimplified prediction; this study provides a unique investigation on HTs' inside air temperature as well as ventilation performance using an advanced artificial neural network (ANN). Mathematical calculation and instrumental measurement were developed in Chapter 2 serve as validation data. Results show that the average air temperature from an array of 15 thermistors inside the HT was predicted more accurately in terms of mean square error (MSE=1.7°C^2) and mean absolute error (MAE=1.0°C) than using the prediction of single inside temperature at the center of HT (MSE=17.7°C^2, MAE=3.3°C). Also, relative humidity and wind direction had the least significant impact on the prediction of inside air temperature, and only four inputs of outside weather data were found to have a significant impact on ANN prediction of inside temperature: outside air temperature, vent opening level, solar radiation and wind speed. Moreover, ANN optimal structure was determined as neurons 29, 25, and 13 in a single hidden layer, as well as neurons 30 in two hidden layers for the prediction of HT inside air temperature, ventilation rate by measurement, vent opening levels and ventilation rate by modeling, respectively. Based on the accuracy of predictions and adaptability, ANN is more strongly effective in predicting HT ventilation rates and opening levels compared to the theoretically based modeling of Chapter 2.

Introduction

Much of the United States is experiencing increased interest in procuring local fruits and vegetables (Hinrichs, 2003). The growing season in open fields is limited to spring, summer and fall in most of the continental USA; but, season extension can be implemented under protected agriculture using greenhouses and high tunnels (Jensen & Malter, 1995). These protected structures are typically used for organic farming and allow producers to harvest year-round produce, and offer many other advantages relative to open fields (Stanghellini and Kempkes, 2003): 1) protecting and buffering of crops from variable weather events (e.g. hail, snow or strong wind); 2) producing lower incidence of crop diseases exacerbated by rainfall; 3) increasing water use efficiency; and 4) improving crop growth conditions. The benefits allow producers to take advantage of seasonality in crop markets with a higher level of income (Blomgren & Frisch, 2007), and improve crop quality as compared with open field production. In contrast, traditional greenhouses consume high energy levels and negative environmental impacts that need to be considered. The fossil fuel and electricity required for heating and cooling loads in greenhouses are a large production input (Vine, 2008); for example, energy accounted for 60-80% of total production cost in Turkey (Ozgener & Hepbasli, 2006). Therefore, producers have given primary attention to the reduction of energy cost and greenhouse gas emissions by reducing or avoiding the use of electrical and fossil fuel resources. Accordingly, a concept of a “net-zero” energy building is being investigated through design strategies that reduce heating and cooling loads in order to enhance energy efficiency by the uses of renewable resource (Stevanović, 2013). In agriculture, the same principal is being adopted for high tunnels (HTs), which are quickly expanding in usage of North America. Unlike greenhouses, HTs do not have any electrical or fossil fuel inputs to maintain the growth environment, and thus provide lower energy consumption, capital investment, and maintenance. HTs are typically made of steel hoops covered by plastic film. Renewable solar energy, the main energy source inside HTs, is transformed into thermal heat during the day which directly warms the air and is stored in soil for nighttime warming. However to create a micro-climate that maximizes crop productivity, natural ventilation must be properly managed.

HT infrastructure expenses vary based on its size and materials. A basic structure costs approximately \$20-30 per square meter; thus, a 200 m^2 tunnel totals approximately \$7500 including an additional 25% cost factor for end-wall lumber, site preparation and water lines (not counting the cost of labor). Since additional high-valued organic crops (e.g. pepper, tomato, strawberry, and lettuce) can be produced during an extended growing season, the added value can compensate for the increased cost of the HT when compared to open field production. In addition, as a low-risk structure, many small- and medium-scale producers, and decentralized urban farms that sell products directly to high-end markets (e.g. local retail and restaurants) are starting to use HTs for increasing their harvests in the off-season months (early spring and late fall). Consumers are willing to pay 31 to 58 percent higher price for fruits and vegetables that enter the market early, particularly when these products were grown locally via HTs (Conner et al., 2009; Sanders, 2006). There are also many support programs from government agencies providing financial assistances to HT producers. The largest program is from the Natural Resource Conservation Service’s Environmental Quality Incentives Program (EQIP) of the United States Department of Agriculture (USDA). The Seasonal High Tunnel Initiative of EQIP was established in 2009, and it has already provided assistance for over 13,000 HTs in all 50 states as well as Puerto Rico and the Pacific Basin, totaling approximately $61 million of cost-share assistance (Huff, 2015).

HT location is important to ensure that the incoming solar energy is sufficient for the thermal requirements of the crop. Compared with the harsher winters of the northern and eastern states in U.S., western and southern parts are more suitable for HT utilization due to the warmer average temperature and higher solar radiation levels (Huff, 2015). Studies have already indicated that HTs can significantly increase the productivity of many crops, such as lettuce, tomato, berries, muskmelon and peppers (Demchak, 2009; Kadir and Carey, 2006; Waterer, 2003). In producing high value crops in a HT with a passive ventilation system, temperature and humidity management is challenging. The conversion of solar to thermal energy in HTs is essential to warm inner air and soil temperature; but, dangerously high temperature and humidity can occur without prompt and effective ventilation, thus resulting in low yield and poor fruit quality. The ability to successfully manage ventilation in a HT is a primary obstacle for producers of any scale or level of experience. Thus, without any heating or cooling mechanical systems to consistently control inside HT conditions, producers must maintain a beneficial growth environment while responding to varying weather conditions by using passive ventilation systems. Typically, incoming air movement is necessary to prevent the buildup of temperature and humidity; but, strong and gusty wind can create excessive ventilation and generate a rapid temperature drop which can lead to shorter stems and smaller fruits in HTs (Wien, 2009). Therefore, the ventilation rate controlled by the degree of vent opening is the key factor to modify inside microclimate, but the calculation of ventilation rates is very complex depending on many erratic weather behaviors such as solar radiation levels, wind performance, air temperature, and humidity changes.

Some theoretical ventilation models provide insights into energy and airflow distribution associated with heat and mass exchanges; but, typically the models require intense computation to improve the accuracy of predictive estimation (Körner & Van Straten, 2008). Advanced techniques such as computational fluid dynamic (CFD) and artificial neural network (ANN) modelling have been used to develop models for optimizing crop environments. The CFD technique is used by many researchers to develop two- or three-dimensional models for air exchange measurements in greenhouses with some results showing that wind direction had significant impacts on the ventilation rate and temperature distribution (Boulard et al., 1999; Campen & Bot, 2003; Khaoua et al., 2006; Majdoubi et al., 2009). CFD has been adopted to describe the flow of fluids for air temperature distribution by the Navier-Stokes Equations with good accuracy; but, drawbacks of CFD include the need for special knowledge and experience in grid generation, selection of calculation algorithms, turbulence modeling, and various types of boundary conditions; and it is also costly due to its need for considerable computational time. Ruano et al. (2006) indicated that CFD technique would require many days for a medium size building to simulate indoor temperature. In addition, this technique is difficult to use because there are many physical data inputs required that are often poorly defined, resulting in ambiguity and uncertainty for simulating, predicting and interpreting the output (Lu & Viljanen, 2009). ANNs have been used as an alternative to study non-linear problems in various scientific fields during the last 20 years, including engineering, medicine, and economics (Kalogirou, 2001). This technique is a powerful tool to offer faster computation than a CFD technique based on a large number of interrelated experimental data, which is easy to apply, and even conducts assessment and prediction.

A biological neural network has the natural propensity to store experiential knowledge through a learning process by the inter-neuron connection strengths (synaptic weights), and then make the information available to use (Haykin & Lippmann, 1994). Thus, the computational ANN is a type of intelligent black-box based on human brain functions in engineering analysis and prediction using a large number of highly interconnected processing elements (neurons) to approximate or estimate specific functions. A standard multiplayer feedforward ANN is typically organized in layers that involve an input layer, some hidden layers, and an output layer. The inputs are 'weighted' by a coefficient w_i and then transferred to a hidden layer to activate with a transfer function. The activation functions generate signals which are multiplied by weight w_j and sent to the output layer. At the output layer, all the information are summed and used for activation functions to finally generate an output (Yonaba and Anctil, 2010). Therefore, by studying previously recorded information, ANNs learn the relationship between input variables without concern for excess data which are minimally significant, in order to produce the desired output. Once the ANN processes the relationships between the inputs and outputs, it is said to be trained. After being fully trained, the network will allow another untrained new dataset input to make predictions based on its previous experience. Therefore, ANN is widely accepted by users due to its ability to recognize useful inputs and remove irrelevant values, without explicit evaluation of transfer coefficients or mathematical formulation of relationships between outputs and inputs. It also exhibits fault-tolerance and noise immunity; namely, it is an alternative technique to model incomplete and inherently noisy data, and nonlinear equations. Thus, ANN can not only analyze experimental behaviors, but also leverage the massively interconnected input data for future predictions, which makes this technique suitable for solving complicated scientific problems in climate science such as climate change, or mathematical relationships between climate science-related parameters (Ferreira & Faria, 2002). ANN was successfully applied to investigate interior air motion based on the opening size and location in a naturally ventilated building as reported by Kindangen (1996). This technique offered reliable results in the cases where many parameters were taken into account. Kalogirou and Eftekhari et al. (1999) also predicted the indoor temperature and combined velocity inside a naturally ventilated and lightweight test room by using a multi-layer feed-forward ANN. Later, this technique with the back-propagation learning algorithm was applied in a passive solar building, and the observed energy consumption was predicted with a satisfactory coefficient of multiple determination (R^2=0.9991) (Kalogirou & Bojic, 2000). Greenhouse studies using ANN are also being broadly applied for indoor temperature investigation and the forecasts of thermal and energy demand (Ferreira and Feria, 2002; Ruano et al., 2006; Thomas & Soleimani-Mohseni, 2007; Zhang et al., 2005). Overall, most of the ANN studies focused on greenhouses instead of HTs. Analytical and mathematical models (e.g. energy and mass balance) can be applied but may cause oversimplification of the system. Therefore, this study provides a unique investigation on HTs' ventilation using advanced ANNs compared with both mathematical calculations and instrument measurements which were developed in Chapter 2. Therefore, the objectives of this chapter are as follows:

1) Use ANN to determine which outdoor weather parameters are significantly related to a HT's inner microclimate and which inputs are insignificant and therefore can be neglected in subsequent analyses;
2) Investigate the prediction suitability of the ANN technique in terms of ventilation rate and vent opening levels as validated by inside air temperature based on outdoor weather parameters.

Method and Materials

The Gothic Type High Tunnel and Climatic Measurements

The experimental HT was located at the University of Tennessee's Organic Crop Unit in Knoxville (lat 35.88° N, long 83.93° W, elev 252 m), covered with a 200 um thick single layer polyethylene sheet, and orientated N-S. This 139 m^2 HT is approximately 9 m in width and 15 m in length with two types of natural ventilation: sliding-doors and side-curtains. However, the study was only conducted with the sliding-doors used for ventilation and the side-curtains in the closed position because the side curtains are only generally opened during warm weather when maximum ventilation is required. The dimensions of each sliding-door are 3.7 m in width and 2.4 m tall, with one door at the northern end and another one at the southern end. There were two similar HTs constructed at both sides of this experimental HT, and the windward end was usually with respect to the prevailing southern wind. There were two meteorological weather stations located inside and outside of the experimental HT. The outside one was 10 m away and positioned 4 m above the ground. Solar radiation was measured by a pyranometer (*LI-COR LI200R*) on a horizontal surface. Wind speed and direction were measured through a windset (*R.M.Young 03001*). Relative humidity and air temperature were measured using a sensor (*Vaisala HMP60*) installed in a ventilated radiation shield. Also, an inside climatic station located at 1.5 m above the ground in the middle of the experimental HT, interfaced with the same sensors described for the outside weather station. A thermistor was placed at the inside weather station for the air temperature measurement, which was painted white for shielding purposes. An array of 15 shielded thermistors also measured the inside air temperature to show how well the ventilation decisions were optimizing air temperature across the entire HT. The initial sliding-door opening was adjusted by looking at the weather forecast for the day and then making door adjustments based on inside air temperature feedback when inside temperature varied by ±2.7°C from optimum during the day (pepper 24°C and lettuce 18°C). All the thermistor units (PS104J2) were assembled in our lab. These non-linear sensors followed a polynomial response to temperature that is defined by the Steinhart-Hart equation, and the range and accuracy is ±0.1°C with 0.026°C. The natural wind behavior causes random air movement into the HTs that created special and temporal temperature fluctuation. In order to avoid data being interrupted by non-steady natural wind, wind speed with other measurements were averaged over a constant time where the noise was less likely to affect the measured wind data. Therefore, both inside and outside sensors were measured every 15 s and average reading was recorded every 60 mins by a CR1000 datalogger (Campbell Scientific Inc.) via a cellular internet connection. Also, the hourly weather data for this study was selected from 10:00 to 16:00 EST to reflect the time when solar radiation and the energy exchange through the HT was greatest in every day of early spring (April through early May of 2015). During this period, the plants were quite small, and thus the canopy effects were ignored.

Physical Model of Energy Balance and Artificial Neural Networks (ANNs)

A theoretically based energy balance model was developed in Chapter 2. Air temperature and ventilation rate were simulated and predicted based on energy balance equations (EB) with the consideration of conduction, convection, radiation and mass transfer between inside and outside of the experimental HT. Solar radiation is the main resource providing thermal energy inside the HT, and conduction through the plastic covers of HT is related to the difference between inside-to-outside temperature. In the modeling of convection phenomena for each passive ventilation event, natural air-flux exchanges are considered as sensible and latent heat transfer between inside and outside of a HT. The ventilation rates calculated by the EB model were then compared with direct experimental measurements of total air-flux per time unit (AF) which depended on the inlet wind velocity and the size of the adjustable-door-opening area with a correction of boundary layer effects using DS-2 sonic and hot-wire anemometers. Based on the relations between inside and outside weather data provided in Chapter 2, the new energy balance model (EBn) and total air-flux (AFn) purely using outside weather data were derived to estimate the ventilate rates with a validation of inside air temperature. Results in Chapter 2 showed that EBn model was able to predict inside air temperature, and there was a relative close agreement between measured and predicted values (R-square of 0.82 with regression slope of 0.97 and offset of 1.74). However, there is an inevitable error in the prediction of sliding-door opening levels from the theoretical EBn and AFn models when compared to the measured values. Thus, instead of using mathematical parameters and the calculated relations between inside and outside weather conditions to predict HT ventilation performance, the artificial neural network (ANN) using empirical data is an alternative computational method to overcome the complexity of the theoretical models. Table 5 includes the input and output parameters (hourly data) for the analysis of ANN model.

Table 5. ANNs Parameter Identification

ANNs	Parameter	Description
Input	S_o	Solar radiation (W m^{-2})
	T_o	Outside air temperature (°C)
	RH_o	Outside relative humidity (%)
	U_o	Outside wind speed (m s^{-1})
	V_o	Outside wind direction (°)
	$L^{\dagger}$	Sliding-door opening (m)
Output	$T_i^{\dagger}$	Inside air temperature (°C)
	G^*	Natural ventilation rate (m s^{-1})

† represents that sliding-door opening (L) and inside air temperature (T_i) were exchange for the predication of HT ventilation adjustment levels.

* means the ventilation rates achieved from the mathematical calculation of energy balance (EBn) and instrumental measurement (AFn) which is developed in the Chapter 1.

Inside air temperature was considered to be a significant output to validate the sliding-door opening levels of HT ventilation in order to retain a desired crop environment. Two methods of representing inside air temperature were used in the ANN analysis as output values: one was measured from a single thermistor recording at the middle of the experimental HT (Air_sig); and another one was averaged from an array of 15 thermistors all over the HT (Air_ave). Ventilation rates were originally developed from the mathematical calculation of an energy balance (EBn) and experimental measurement (AFn) which were previously described in Chapter 2. Time was not applied in this model as an input variable since this system was required to learn the behavior of the system based only on the outside weather conditions and not the time from the start of a trial. Also, ANN can be applied to identify significant model inputs and remove irrelevant variables from the original data set based on the accuracy of each outcome (T_i and G). Once the irrelevant inputs were removed, sliding-door opening levels (L) were applied as a final output dependent of the significant outdoor parameters and inside air temperature.

ANN analyses were taken from 189 datasets from April 2 to May 5 in early spring of 2015 when only the side doors were being adjusted resulting in high temperature increases and drier air inside the HT as compared to outside. Also, the hourly data in each day was conducted around solar noon from 10:00 am to 16:00 pm EST to maximize the solar radiation entering as well as the energy exchange through the high tunnel. This network using the Matlab package (2014) was first trained with the real meteorological data which was normalized to fit in the interval [0, 1] before training and de-normalizing the output at the end. A three-layer feedforward neural network was used as the fundamental structure. After the identification of network inputs and outputs, selecting the element number in the hidden layer becomes another crucial parameter for the accurate performance of a neural network. ANN datasets were randomly separated into three non-overlapping groups for the training, validation and testing sets with default proportion 7:1.5:1.5. This network used a 'tangent sigmoid' transfer function instead of logis and purelin since it can detect different features better with higher accuracy in a patterned process (Rezaeian et al., 2010; Yonaba and Anctil, 2010). Levenberg–Marquardt (LM) was used for the variants of the algorithm. Figure 14 shows the ANN detailed procedures for data processing. First, the training process calculated the model's weights and thresholds, in order to "fit" the ANN model. Then the predicted outputs were compared to their actual output values, and a back-propagation algorithm adjusted the weights until the error between predicted and actual outputs were reduced to an appropriate level. The number of hidden units had a crucial impact on the ANN performance; thus, it was necessary to adjust the hidden units and repeat the training and validation processes till the ANN offered the best results. With the example of the logistic-sigmoid activation, the error term was developed as equation (18) and equation (19) for a node in an outlier node and a hidden layer, respectively.

$$\delta_{pi} = (t_{pi} - \alpha_{pi})\alpha_{pi}(1 - \alpha_{pi}) \tag{18}$$

$$\delta_{pi} = \alpha_{pi}(1 - \alpha_{pi}) \sum_k \delta_{pk} w_{kj}) \tag{19}$$

$$\Delta w_{ij} = \varepsilon(\delta_{pi}\alpha_{pj}) + m w_{ij}(old) \tag{20}$$

where, α_{pi} = the activation for each node;

t = the network output (target);

ε = learning rate;

m = momentum factor;

w_{ij} (old) = previous training iteration;

subscript k = a summation over all nodes in the downstream layer;

j = the weight position in each node.

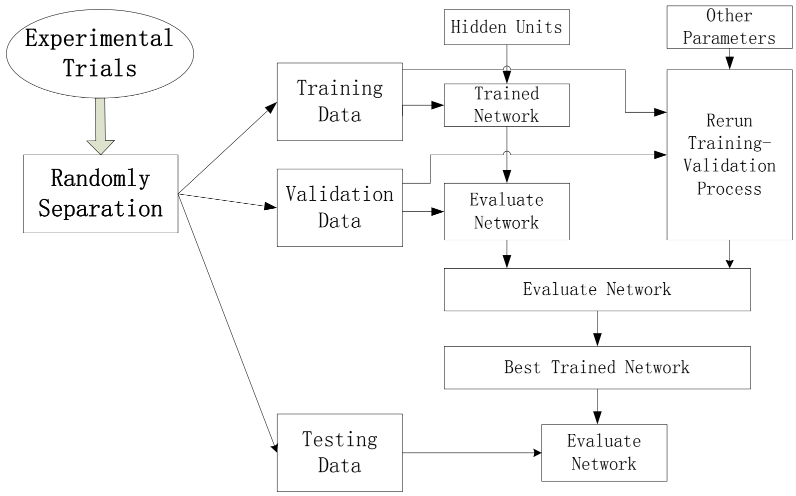

Figure 14. Schematic depicting the artificial neural network (ANN) data processing.

And then α and δ for each node were applied to compute an incremental change to each weight term through equation (20) (Kalogirou & Bojic, 2000). In the end, test data evaluated the best-trained network (Trost, Wong, Pfeiffer, & Zheng, 2012). Moreover, some researchers pay great attention on the training stage, with less concern on validation stage. Thus, there are three criteria for accuracy estimation: R (regression reliability), as well as MSE (the mean of square errors) and MAE (the mean of absolute errors) from equation (21) and (22), respectively.

$$MSE = 1/N\sum_{t=1}^{N}[\hat{y}(t) - y(t)]^2 \quad (21)$$

$$MAE = 1/N\sum_{t=1}^{N}|\hat{y}(t) - y(t)| \quad (22)$$

where,

$\hat{y}$ (t) = predicted output;

y (t) = the measured value.

Results and Discussion

Inside air temperature prediction

The ANN models revealed that the performance in predicting inside air temperature vary according to different hidden layers and neurons. Starting from a single hidden layer with neuron 9, different combinations of hidden layer and neurons were tried. Table 6 shows the optimum models based on the highest regression reliability estimator (R-value) of training, validation, test and overall performances. A single hidden layer with 15 neurons provides the optimum results for Air_sig. Also for the prediction of Air_ave, a single hidden layer with 29 neurons provided relatively better regression than using other neurons, although the R values from neuron 20 to 29 were similar. Specifically, increased neuron numbers in each hidden layer allow the model to get more degrees of freedom and store more complex patterns, thus increasing the general accuracy of ANN performance. Once the model achieved the best results with specific network parameters, more neurons can only produce worse prediction because of overlearning issues. The best ANN structure for the two air temperature models (Air_sig and Air_ave) were chosen using a single hidden layer; but, the R-value of using hidden layers larger than 1 (such as 2) significantly reduced the regression reliability between prediction and measurements under the stages of validation and testing, indicating that the prediction networks are not capable of generalizing further for more accurate data acquisition. Compared to Air_sig, the regression reliability (R) of Air_ave model were not sensitive to different neuron numbers within the single hidden layer, which are all above 0.91 in ANN training, validation and testing stages with just two exceptions of 25 neurons (test R=0.88) and 9 neurons (test R=0.87). Also, R-value and the slope and intercept from the equation (not listed in Table 6) can represent how well the predicted regression fit the 1:1 line (very close in most cases).

Therefore, Air_ave possesses a more linear relation between the values of prediction and measurement than Air_sig, based on its strong regression reliability (R-value) and model stability.

Table 6. Coefficient R of regression reliability for ANN predictions of Air_sig and Air_ave based on different combinations of hidden layer and neuron numbers.

Hidden Layer	Neuron	Air_sig				Air_ave			
		Trianing	Validation	Test	All	Trianing	Validation	Test	All
1	33	0.86	0.9	0.82	0.85	0.93	0.92	0.93	0.94
1	31	0.84	0.86	0.9	0.88	0.92	0.93	0.93	0.92
1	29	0.9	0.86	0.89	0.87	0.95	0.98	0.94	0.95
1	27	0.89	0.92	0.87	0.9	0.95	0.94	0.95	0.95
1	25	0.89	0.9	0.91	0.89	0.91	0.96	0.88	0.91
1	23	0.9	0.87	0.85	0.91	0.96	0.97	0.91	0.95
1	21	0.87	0.94	0.86	0.88	0.94	0.96	0.97	0.95
1	19	0.91	0.88	0.91	0.91	0.93	0.96	0.95	0.94
1	17	0.83	0.83	0.82	0.83	0.94	0.91	0.96	0.94
1	15	0.93	0.93	0.94	0.93	0.94	0.92	0.95	0.94
1	13	0.91	0.88	0.9	0.91	0.93	0.92	0.95	0.93
1	11	0.88	0.93	0.85	0.88	0.92	0.93	0.91	0.92
1	9	0.89	0.92	0.89	0.9	0.92	0.92	0.87	0.93
2	9	0.89	0.94	0.9	0.9	0.93	0.89	0.92	0.92
2	11	0.92	0.79	0.83	0.88	0.93	0.93	0.88	0.93
2	15	0.95	0.84	0.86	0.91	0.94	0.84	0.8	0.92
2	19	0.9	0.89	0.92	0.9	0.92	0.89	0.89	0.91
2	23	0.96	0.83	0.93	0.93	0.93	0.93	0.88	0.91
2	25	0.94	0.88	0.92	0.93	0.93	0.94	0.9	0.91

In order to see how the regression between the output (prediction) and target (measurement) in each model fit the desired 1 to 1 relationship, another two error criteria (MSE and MAE) were also considered. Figure 15 shows that Air_ave has a smaller error (MSE & MAE) than that of Air_sig model. The best output of Air_ave had an MSE of

0.0050 (1.7°C^2 after de-normalization) and MAE of 0.052 (1.0°C after de-normalization), where the errors for Air_ave were 91% (MSE) and 71% (MAE) lower than that of Air_sig prediction (MSE=0.054 in de-normalized 17.7°C^2, and MAE=0.181 in de-normalized 3.3°C^2). Since MAE and MSE are good means to evaluate how well the output and target values fit the 1:1 line. It was confirmed that Air_ave model had the better performance to predict HT inside air temperature when compared to Air_sig. In addition, Figure 16 demonstrates the regression between the measured output and predicted target values obtained in the Air_ave model using a single hidden layer with 29 neurons. The training data had a good regression reliability (R=0.95), and the validation and test stages provided R as 0.98 and 0.94, respectively which are considered satisfactory values. All data appear to be well distributed along the 1:1 line. The training was stopped when it achieved a mean MSE of 9.98x10^{-8} and validation of the network was stopped at mu of 1.00x10^{-9} at 328 epochs.

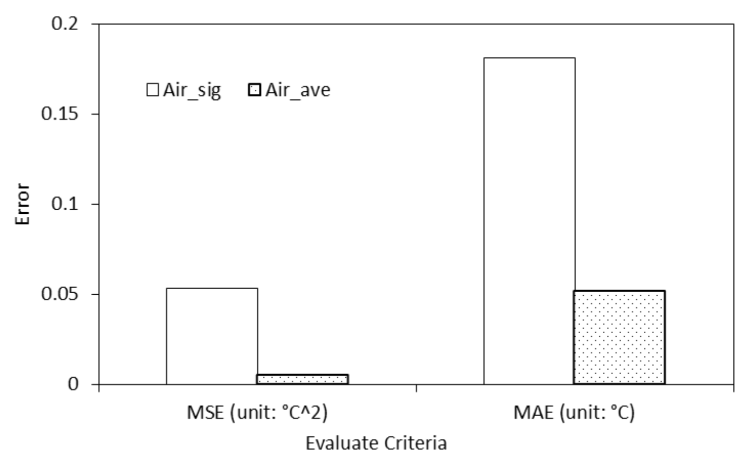

Figure 15. Comparison of ANN evaluated criteria between the best models Air_sig and Air_ave (before de-normalization). *MSE* represents mean square error and *MAE* represents mean absolute error.

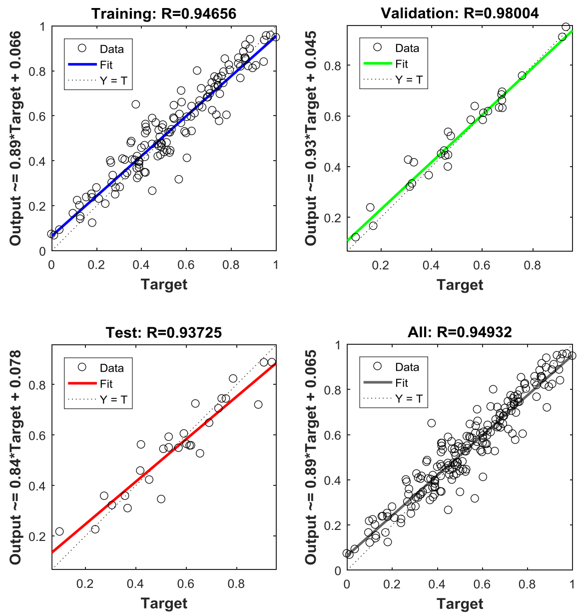

Figure 16. Comparison of the output and predicted targets using the optimal ANN model for Air_ave prediction (a single hidden layer with 29 neurons)

ANN input modification was performed to decrease data requirements, simplify network structure, reduce ANN dimension, and eliminate the interference of unnecessary variables. It is therefore important to examine the weight given to the initial input parameters. The relative importance of different input parameters is provided by the sensitivity of network accuracy when each particular input was removed from the original datasets. Figure 17 expresses that removing either the outside wind direction or relative humidity inputs did not substantially reduce the network predictive power of the Air_ave model, since the R-values of ANN training, validation and test stages were barely affected by removal of these inputs with average regression reliability of 0.95 (R-value). This ANN analysis reveals that outside weather inputs in terms of relative humidity and wind direction had no significant impact on the prediction of indoor air temperatures, which may be explained, in part, by the specific structure and location of the experimental HT. Chapter 2 indicted that 94% of the time, inside relative humidity was lower than outside by around 5% to 20% depending on the different adjustments of sliding-door opening levels, since the warmed air can hold more water vapor during the day. Periodic evaporation from irrigation and plant transpiration can be expected to change the humidity inside, but the situation did not generally occur in this study since the crop was quite small with little irrigation required. Therefore, increased indoor temperature from accumulated long-wavelength solar energy was significantly correlated to the changes of inside RH, but outside RH seems to have little impact on the indoor RH, and air temperature inside the HT. Few studies show that the outside relative humidity has direct influence on HT inside air temperature and this study also indicates that outside relative humidity is one of the least sensitive input variables for the Air_ave prediction (Patil et al., 2008). Moreover, although some research indicates that wind direction was an important factor affecting inside microclimate, wind direction showed no significant impacts on indoor air temperatures according to the ANN model, in agreement with the mathematical modelling results obtained from Chapter 2. A plausible explanation may be related to the location of the experimental HT. The other two HTs on each side could be helping to straighten the wind in a direction parallel to the HT length causing outside wind direction to have limited effect on ventilation rate and inside temperature. On the contrary, ANN performance was more sensitive to the other input parameters because elimination of outside air temperature, vent opening level, solar radiation, and wind speed resulted in a noticeable reduction in the overall coefficient R-value by 0.13 (14%), 0.1 (11%), 0.07 (7%), and 0.04 (4%), respectively.

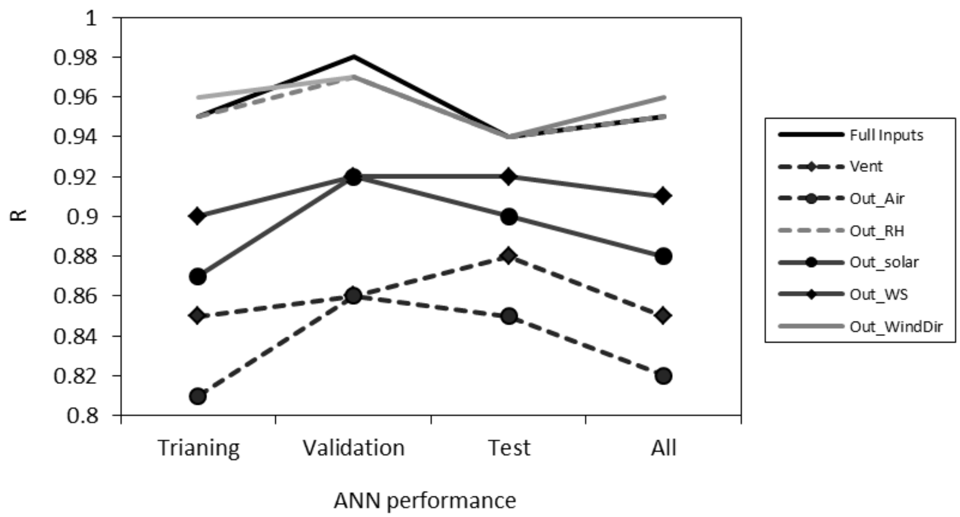

Figure 17. ANN sensitivity analysis for model input modification based on the ANN regression reliability R-values.

As the most sensitive ANN input parameter, the parameter of outside air temperature lost approximately 13% of its regression reliability (R) if omitted from the analysis. This can be explained by the normally strong correlation and close regression relationship between outside and inside air temperatures (Jamaludin & Ahmad, 2014). During daylight hours, air enters the HT at the outside temperature. Therefore, the incoming air is always the starting point for determining inside air temperature which increases during the day due to solar radiation conversion to thermal energy. The degree of temperature increase is then mitigated by ventilation rate of air leaving the HT and conduction through the plastic film, the latter of which is determined by the difference between the outside and inside temperature. The degree of vent opening was stronger determinant of the inside temperature than solar radiation. Removing the extent of vent opening as a parameter of the analysis decreased the regression reliability by 11% while removing solar radiation from the analysis decreased the reliability by only 7%. The reason is partially explained by low variation of solar radiation values in the training datasets (collected between10:00 to 16:00 daily in the early spring of 2015, when a relatively high amount of ventilation was needed to counteract the higher levels of solar radiation. In addition, removing outside wind speed as a parameter from the analysis decreased the regression reliability by only 4% effect, suggesting the extent for which the vent was opened has a stronger effect on the ventilation rate. Therefore, only four inputs were used for the development of ANN predictive models with ranking of input importance as follows: outside air temperature (T_o), vent opening levels (L), solar radiation (S_o), and wind speed (U_o).

Ventilation Prediction

The ventilation rate through the natural ventilated HT was also predicted in ANNs using two theoretical models that were developed from the same dataset in Chapter 2: energy balance (EBn) and wind correction (AFn) models. The EBn model was derived to estimate the ventilation rate based on the outside weather data; while, the experimental values of the AFn model were used to perform a validation of the EBn ventilation rate measured using a DS-2 sonic anemometer corrected by a hot-wire anemometer measurement (Chapter 2). These air-flux models indicated that wind direction did not exhibit a significant effect on the inside micro-climate performance similar to the previous mathematical model in Chapter 2 confirming that wind direction and relative humidity had little impact on predicting inside temperature in the specific HT configuration used in this study. Thus, a new ANN with five inputs (S_o, U_o, T_o, L and inside air temperature, T_i) was developed for the prediction of HT ventilation rates, and the best models were achieved by applying 30 neurons with two hidden layers, and 25 neurons with a single hidden layer for EBn and AFn, respectively. ANN regression results for both EBn and AFn methods of obtaining air-flux are shown in Figure 18. The agreement between output (previous model) and target (predicted from ANN) were acceptable: the R-value of regression lines were 0.91 and 0.97 in the training process for the EBn and AFn models, respectively. Also, the error variance of the ventilation rate indicated that MSE and MAE generated from the AFn model using the ANNs were about 2.9 and 1.6 times lower than values provided by the EBn model, respectively. The stronger accuracy of AFn ventilation rate in the ANN model occurred due to the continuous measurements of incoming air-flux (Chapter 2), which can provide more accurate ventilation predictions than that using theoretical estimation of the EB model. Also, Figure 18 (a) shows that the ANN regression based on the EB model had several zero points for target values while the predicted output has actual numbers (0-0.2 in normalization). This scenario occurs in all phases of ANN training, validation and test processes, leading to the conclusion that the ANN model can learn from the training datasets and predict non-zero ventilation rate while the actual estimation values of theoretically based EB model showing there is no air-flux exchange occurring.

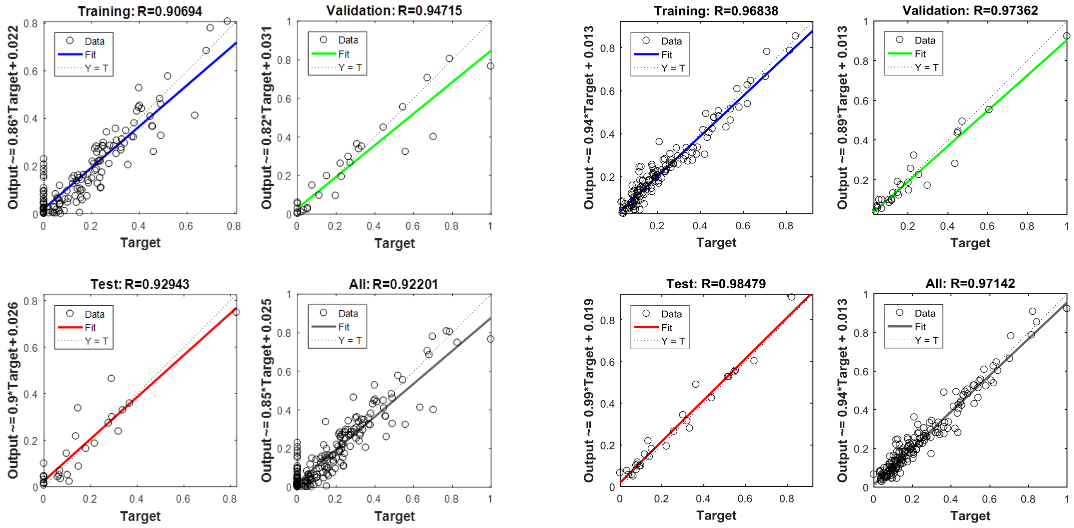

(a) (b)

Figure 18. ANN regression performances of HT ventilation rate between target and predict output for EBn (a) and AFn model (b).

In addition, ANN was employed to make a further model for sliding-door opening level (L), with neuron 13 in a single hidden layer (Figure 19). The linear relation between the predicted and measured values proves that the ANN model had higher agreement than the previous mathematical energy balance model in Chapter 1 based on the criteria of model validation (after de-normalization): MSE=0.1 m^2, MAE= 0.5 m from ANN model with R^2 of 88%, while MSE=2.3 m^2, MAE=1.3 m from the theoretical EBn model with R^2 at 50%. Although the prediction on how much the vents were opened developed in ANN showed has less errors between the predicted and measured values, but it still did not achieve a significant level of accuracy with a slope of 0.89 and intercept of 0.013 before de-normalization (Figure 19). Thus, further development of the ANN model is needed using more training datasets to increase the model's stability and accuracy for its use as a tool for ANN architecture selection.

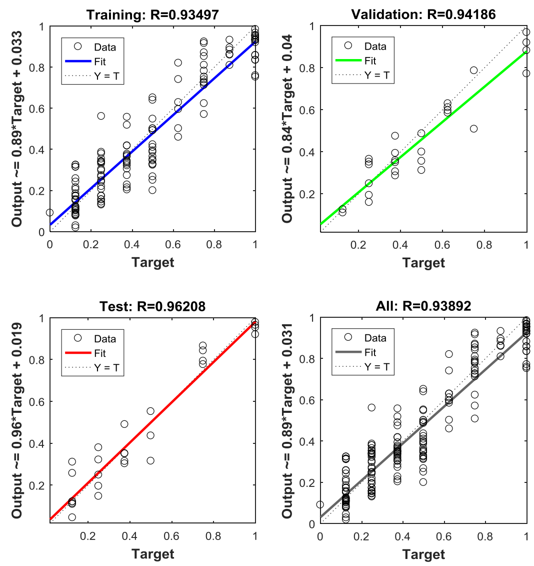

Figure 19. ANN regression performances of HT vent opening levels between targets and predict outputs.

In summary, the analysis results of ANN performance provide a relative strong foundation for using the ANN models to predict HT temperature and ventilation rate under a variety of outside weather conditions. Overall results show that ANN optimal neurons were determined as 29, 25, and 13 in a single hidden layer, as well as neurons 30 in two hidden layers for the prediction of HT inside air temperature, ventilation rate of AFn, vent opening levels and ventilation rate of EBn, respectively. Based on the accuracy of predictions and adaptability, average inside air temperature was predicted best with the highest regression reliability (R-value) along with the lowest values for error criteria MSE and MAE. The accuracy of predictions and adaptability for other models decreased as follows: ventilation rate of AF measurements, ventilation rate of EB estimation, and vent opening levels.

Conclusions

Advanced computational neural networks can discover the best structure of the prediction models, like the number of hidden layer and neurons, and the significances of input parameters. This study with the ANN model has been evaluated for the predictions of inside thermal conditions and ventilation levels. Results show that the ANN model can predicate inside air temperature in a natural ventilated HT as a function of the outside weather variables including solar radiation, air temperature, vent opening levels, relative humidity, wind speed and direction. The average air temperature (Air_ave) from an array of 15 thermistors inside the HT was predicted more accurately in terms of MSE (1.7°C^2) and MAE (1.0°C) than using the prediction of single inside temperature at the center of HT (MSE=17.7C^2, MAE=3.3°C). Moreover, ANN input modification was carried out based on a sensitivity analysis that provided insight into the usefulness of individual variables. Of the six potential inputs (5 outside weather parameters and ventilation opening size), only four were important for performing ANN modeling. Relative humidity and wind direction in this study had the least significant impact on the prediction of inside air temperature; thus, these two inputs can be omitted from the ANN model. The ANN model results agreed with the mathematical model based results reported in Chapter 2. The other four inputs were found to be sufficient for the ANN modeling with their ranked importance as follows: outside air temperature, vent opening level, solar radiation and wind speed with omission for these parameters causing a noticeable reduction in the overall coefficient R-value by 0.13 (14%), 0.1 (11%), 0.07 (7%), and 0.04 (4%), respectively. In addition, the performance of ANN was compared with the theoretical model of ventilation rate from Chapter 2 and result depicts the fact that the ANN outperformed the mathematical model with a higher degree of accuracy. This study indicates that ANN can be a suitable means of modeling natural ventilation in high tunnels.

The greatest advantage is that ANN does not depend on physically based relationships, and it is faster to formulate, better at filtering the required input parameters and ultimately was superior at predicting the required ventilation in this study. It should be emphasized that ANN modeling is transferable to HT structures that differ from the one used in this study because the ANN model does not require transfer of mathematical expressions with coefficients that can vary from structure to structure. As long as the ANN model can learn from the historical dataset about the relationship between HT ventilation levels and outside weather conditions with a validation of inside air temperature, the corresponding vent-opening can be trained and predicted by the neural network. Further work is needed to address more training datasets to increase the model stability and accuracy with better architecture selection. Also, automation of the door opening with an inside temperature sensor powered by solar energy can be addressed in the future research, to gathering more training datasets in ANN models for step ahead prediction of vent-opening. Thus, this ANN model can play an important role in the ventilation design or at least provide an operational guide to producers on how to adjust their vents in advance to obtain an optimum air temperature based on public weather forecasts given 1 or 2 hours in advance.

Chapter 4
Assessing Heat Management Practices in High Tunnels to Improve Organic Production

Abstract.

This study assessed the beneficial effects of independent and combined practices on temperature changes inside the high tunnels (HTs), and further examined the impact of temperature changes on crop production. Specific practices included mulching (polyethylene and biodegradable film and vegetative), row covers, cover crops, and irrigation water types (rainwater and city water). Sweet pepper (‘*Socrates’*) was grown in the springs of 2011, 2013 and 2015, and romaine lettuce (‘*coastal star”*) was grown in the falls of 2011, 2013 and 2014 at the University of Tennessee’s Organic Crop Unit in Knoxville. Statistical differences were analyzed in a randomized complete block design (*RCBD*) for total marketable yield regarding plant weight and fruit numbers, as well as the changes in soil and air temperature. Results show that the employment of black polyethylene mulch (*black*) produced the highest pepper yield by warming the soil, but not excessively, during the day when compared with clear polyethylene mulch. For lettuce production, *black* and *clear* all worked best on plant weight, but the raised soil temperature produced under the plastics might not be beneficial on lettuce production. Moreover, the biodegradable mulch (*biobag* and black *spunbond*) did not generate as much soil warming as black polyethylene, thus total pepper marketable yield was statistically similar to that for the latter mulch treatment; while the white *spunbond* used on lettuce production reduced plant numbers per plot than *black* plastic. Also, row covers continuously provided protection from freezing during the cold nights for both pepper and lettuce crops. But black mulch can act alone without a row cover to have a positive effect on soil temperature and pepper development. Cover crops allowed for greater heat transfer to soil and increased soil temperatures, but lead to reduced overall pepper and

lettuce yield. However, the cover crops with *black* and *clear* mulches saved more lettuce per plots. For spring pepper production, rainwater irrigation not only enhanced water conservation, but also warmed the soil and tended to increase the overall pepper production; while for fall lettuce, the irrigation using city water warmed the soil and provided more nutrients for increased lettuce production than rainwater.

Introduction

Fruit and vegetable producers are becoming increasingly interested in organic farming because organic products can bring 10-30% more income at local markets. Both producers and customers consider organic fruits and vegetables to be more flavorful and healthy at the same time they are more beneficial to the environment than the conventional growing systems (Pérez-López & López-Nicolas, 2007). According to the 2015 Census of Agriculture, certified organic farms utilized approximately 0.97 million ha of croplands in the United States generating $3.5 billion in organic sales, and the certified cropland acreage and total organic sales increased about 50% and 80%, respectively, compared to 2008. Protected agriculture, such as greenhouses and high tunnels, have become an important strategy for organic production as they can significantly extend crop-growing seasons, which allow harvesting during what are traditionally the off-season periods when prices are higher. Organic production under protection may be particularly important to the profits of small-scale growers who market produce directly to customers. Some high-value organic crops such as sweet bell peppers, tomato and lettuce are well adapted to protected agriculture, because high tunnels and greenhouses prevent rainfall from wetting or splashing soil onto fruit and foliage creating cleaner produce with less disease (Lamont et al., 2005). Due to less bacterial rot and sunscald, peppers harvested under protection can have a higher percentage of first and second quality fruit than those grown in open fields (Reid et al., 2010). In the United States, vegetable production under either glass or other protections totaled 182 ha at a cumulative value of over $75 million in 2014; peppers, tomato and lettuce accounted for 7%, 32% and 7% of that total, respectively (USDA, 2014).

Crop yield and profitability for both organic and conventional production can potentially be increased by better heat management in high tunnels (HTs). Typically, greenhouses have fully automatic ventilation and heating/cooling systems; but, fuel or electricity may account for approximately 30-50% of the total production cost (Wang et al., 1999); while the use of HTs can be more profitable and sustainable than greenhouses because renewable solar energy can replace the primary heat source. HTs made from clear plastic films also provide many of the benefits of greenhouses with significantly lower capital and operating cost. First, the plastic covers are capable of affecting the property of spectral light reaching the foliage by absorbing ultraviolet radiation at 340 nm and can reduce the incident and severity of some specific plant diseases, such as gray/white mold by inhibiting sporulation (Gullino & Albajes, 1999). Secondly, HTs have become widely used for organic production by protecting crops from potentially damaging weather conditions such as frost, temperature fluctuations, and excessive precipitation. Surveys performed in Tennessee by Wszelaki et al. (2013) reported that in 2011, hail severely damaged the open field crops, but HTs production was successfully protected. As a result, HTs increased the overall marketable yield of strawberries by over three fold of that grown outdoors. In addition, HTs shift plant growth timing to coincide less with natural pest cycle and provide a barrier to inhibit entry of pests or weed seed. Temperature and humidity inside the HTs can be passively regulated by raising and lowering the side curtains of the HTs without fans and heaters. Another advantage of this system is the ability to create an inhospitable plant-growth environment before planting by the process of soil sanitation. By closing all the vents and withholding irrigation during the hottest periods of summer season, weed growth can be limited and soil-borne plant pathogens can be reduced under the excessively high temperature and dry soil conditions (Katan, 1981). All of the cost-effective and sustainable aspects of HT production are attractive to organic growers. Since 2010, USDA's Natural Resources Conservation Services (NRCS), under the Environmental Quality Incentives Program (EQIP) has provided cost-share funds for nearly 2,500 tunnels in 43 states (NRCS, 2014), and continues to offer financial assistance to help producers install HTs up to 202.34 m^2. The climate of Tennessee allows cool-season crops to be grown in mid-winter with a HT, while also significantly extending the growing seasons for warm-season crops. As such, the Agricultural Enhancement Program of Tennessee provides Tennessee producers cost-share for long-term investments in HT production.

Although HTs are advantageous to organic vegetable production, several factors limit their sustainability. First of all, the HT structure blocks rainfall; thus, groundwater or other local water resources are required to replace rainwater for crop irrigation. However, many areas around the world face water supply shortage due to rapid population growth and climate change (Coombes & Barry, 2007; Mendez et al., 2011). Thus, instead of developing an irrigation system that consumes existing water and energy resources, rainwater can be collected, stored and used inside the HTs as a rainwater harvesting system (*RHS*) (Figure 20). Because many plants are sensitive to soil salinity, the practice of using rainwater can be preferable over other artificial water resources. Also, rainwater is free of pollutants, minerals, and other natural and human-made contaminants. Rainwater irrigation under *RHS* also helps in reducing local flooding in some low-lying areas during rainy seasons, since the roof runoff generated from excess rainfalls can be collected and stored, as opposed to contributing to stormflows. RHS has additional advantages in semi-arid regions where treated water is inadequate and costly; ultimately, RHS improves soil moisture, prolongs the period of moisture available, and enhances horticultural crop productivity. However, there is limited research investigating how *RHS* water affects soil temperature through a HT irrigation system and further impacts crop productivity. This study proposes that rainwater collected and enclosed inside of black polyethylene *RHS* tanks can be warmer than other water resources including groundwater and local treated water, via capturing solar energy. When the warmer rainwater is transferred to the soil through drip irrigation, it in turn modifies the soil temperature in a significant way, especially in cold climates and can further accelerate crop development in HTs.

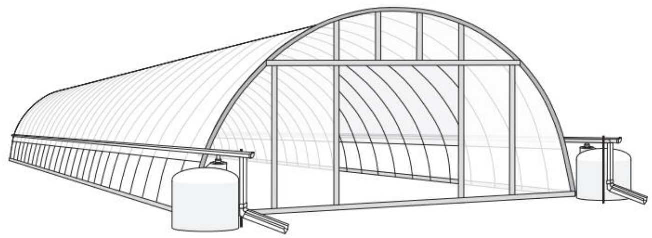

Figure 20. High tunnel with rainwater catchments and poly storage tanks (Shawn Shouse 2012)

Another limitation to production in HTs is their insulating ability. In cold climates, the thin plastic cover of HTs does not offer enough insulation to retain a favorable temperature for maximum crop growth. This is especially true at night since HTs allow the inside temperature to drop close to the outside temperature even though daytime temperatures inside are elevated early and late in the season. However, surface mulching and row covers are approaches that may counteract heat loss in the HT soil that do not require a direct energy input. Polyethylene plastic mulches are commonly used to provide more sustainable and healthier soil conditions in the open fields (Kasirajan & Ngouajio, 2012). This practice is not only for alleviating soil crusting, and controlling weeds, but also to significantly influence the microclimates around the plants by modifying the radiation budget of the surface and improving water conservation (Liakatas and Clark, 1986). Mulch colors are considered to have significant impact on the microclimates around plant-root areas because soil temperature under the mulches largely depends on the thermal properties (reflectivity, absorptivity or transmittance) of a particular mulch material to capture solar radiation (Schales & Sheldrake, 1963). Black is the predominant color used because it absorbs most wavelengths of incoming solar radiation and re-radiates the absorbed energy in the form of thermal radiation (Lamont, 2005). In contrast, clear polyethylene absorbs little but transmits approximately 85-95% of solar energy to the soil surface which can produce a substantial buildup of heat in the soil. Ham and Kluitenberg (1993) reported that black and clear plastics increase the soil temperature 2-3°C and 5-8°C, respectively during the day, compared to bare ground in open fields. In another outdoor experiment of Nimah (2005), the highest soil temperature was obtained under clear polyethylene, then black polyethylene and finally bare ground. Also, in a plastic tunnel, Iqbal and Amjad (2009) reported that peppers mulched with black plastics showed significantly better growth in plant height and leaf area; while clear plastic significantly increased soil temperature and reduced the number of days to first flower compared to black plastic and bare ground. Tomato production in HTs was observed to be increased approximately 25% using clear plastic mulch in the first four harvests, with 2-4°C increase in soil temperature (Arin & Ankara, 2001). From a two-year lettuce experiment in the open field (Siwek et al., 2007), three plastic mulches (*clear*, *white* and *black*) all increased the overall lettuce yields compared to the control (bare ground) with yield difference, at 33%, 40% and 39%, respectively. Moreover, biodegradable mulch can be applied to the ground surface as an alternative thermal protection to polyethylene plastic mulch for HTs (Kapanen et al., 2008). Biodegradable mulches are composed of aliphatic polyesters or starch–polymer blends, and soil microorganisms transform them into CO_2 and CH_4, water and biomass, in order to eliminate film removal and plastic disposal problems (Kasirajan & Mathieu, 2012). Like polyethylene mulching, biodegradable films are also affective at raising soil temperatures and suppressing weeds compared to bare ground, and contribute to crop growth rates and improved yields (Greer

& Dole, 2003; Miles et al., 2012). Despite the similarity, the mechanical resistance of biodegradable mulches are lower than those made of polyethylene, which make them deteriorate faster during the growing season (Ngouajio et al., 2008; Waterer, 2010); however, Sarnacke and Wildes (2008) reported the material cost of biodegradable film is 2-3 times higher than that of standard polyethylene mulches without considering removal expenses. However, the biodegradable mulches can be potentially tilled into the soil after crop harvest. In contrast, polyethylene mulches need to be retrieved (required for organic agriculture), which is a major labor costs. Therefore, biodegradable mulching can help the farmer by reducing labor costs.

In field tests of biodegradable films, overall crop marketable yield varied across climates. Moreno and Moreno (2008) observed that the outdoor use of biodegradable mulches did not significantly affect overall tomato yield and fruit quality in Central Spain. Olsen and Gounder (2001)‘s study in Australia also showed that although polyethylene and biodegradable mulches create a slightly higher soil temperatures than paper mulch, there was no significant difference in pepper production. Miles et al. (2012) reported increased tomato yield using biodegradable mulching compared to bare ground in northwestern Washington, USA.

Floating row covers create a thin insulating layer around the crop, which is another method to provide protection from wind and frost and increase canopy and soil temperature on cold nights. Research on the use of row covers began at the University of Kentucky in the 1950s (Emmert, 1956). Wells and Loy (1985) reported that row covers offered approximately 2-3°C of thermal protection when the ambient air temperature is near-freezing, and this practice is more effective when the soil is warm. Therefore, many studies show that under field conditions, mulching in combination with row covers significantly improved early and total yields of horticultural crops by increasing soil moisture, air and soil temperature, thus creating a favorable microclimate for crop growth (Ibarra-Jiménez & Quezada-Martin, 2004). Since the use of row covers may damage plant tissue outdoors with movement caused by wind, there are limited studies on expanded applications of row covers and HTs. Wells (1998) reported that in a high tunnel, row covers accentuate extension of the fall season due to a significant amount of heat stored in the soil as compared to spring. A layer of light row cover has the capacity to protect pepper and tomato plants from ambient air temperature down to about -3.8°C, which is more than twice the protection afforded by row covers in the spring. In addition, row covers can hinder insect pests from reaching the crop if the row cover edges are secured by soil while the semi-enclosed environment of HTs excludes larger pests. For maximum insulation, there is a need for more studies on the effects of row cover and different colored plastic/biodegradable mulches on HT production.

The last limitation to be examined is related to the increased cropping and higher soil temperatures in high tunnels. Both factors have the potential to limit the accumulation and decomposition of soil organic matter and negatively impact soil water and nutrient holding capacity. One important solution is to supplement soil organic matter with organic amendments; but, organic matter may still need to be collected, processed and transported to HTs requiring energy at each step. Pre-planting a cover crop inside HTs is an energy efficient way to promote soil fertility, along with a potential added benefit of enhanced crop performance. While legume cover crops have the ability to fix nitrogen, there can be a positive impact on crop yield by either incorporating crop residue into the soil or leaving it on the ground surface. The mixture of cover crop residue with surface soil can accelerate the residue's decomposition to provide nitrogen, increase the infiltration rate, and alleviate soil compaction. On the other hand, cover crop residue left on the soil surface may reduce weed germination and establishment due to the modification of solar radiation and light transmittance (Teasdale & Daughtry, 1993). Due to decreased transmitted sunlight, daily maximum soil temperature was reduced correspondingly under vegetative mulch as shown by Liebman and Davis (2000), which may increase the overall yield of summer crops. Also, this vegetative mulching can be expected to work better for early-season weed suppression than full-season weed control (Teasdale, 1996). However, the effects of cover crop residues incorporated into the soil and then covered by different colored plastic mulches are still limited under HT systems.

Overall, various agricultural practices can be incorporated in different combinations to modify the microclimate inside the HTs, and better monitoring practices offer producers data to help them better manage their operations. As an innovative HT system, instead of developing an irrigation system that consumes existing water and energy resources, rainwater was collected, stored, and distributed using gravity or renewable solar power inside HTs. In place of heaters, surface mulches and row covers were utilized to increase soil and air temperature by increasing absorption of solar radiation and reducing nighttime heat loss without electricity or fuel consumption. As an alternative to import organic fertilizer, legume cover crop residue was incorporated to add organic matter and nitrogen for crop enhancement. Because only a few studies investigated the previous mentioned practices, this project focused on small to mid-size HT producers who wanted to increase their profitability with low input sustainable approaches that also improved crop production and quality. Therefore, the primary objective of this study is to assess the beneficial effects of independent or combined practices based on energy conservation (temperature) as well as the effects on crop yield in HT systems. Specific aims were as follows:

(1) Determine HT impacts on inner microclimates such as air and soil temperature, solar radiation, wind speed, and relative humidity when compared to the outdoor conditions;

(2) Determine the effects of soil surface mulches (polyethylene or biodegradable plastic film, or vegetative) alone or combined with floating row covers during cold periods, on changes of soil and air temperatures, and further examine the impact of temperature changes on marketable yield of crops (pepper and lettuce) grown inside HTs;

(3) Investigate the effects of different soil surface mulches combined with each irrigation type (rain and municipal) on the changes of soil temperature, and further examine the impact of soil temperature on marketable yield of crops (pepper and lettuce) grown inside HTs; and

(4) Determine changes in soil temperature by incorporating cover crop residues into the soil and polyethylene mulching as compared to standard mulch practices, and further examine the impact of soil temperature on marketable yield of crops (pepper and lettuce) grown inside HTs.

Part 1. Spring pepper of 2011, 2013 and 2015

Material and Methods

The Gothic type high tunnel

This experimental HT is a commercial gothic building constructed with a peaked roof and vertical side walls. The three structures are covered with 200 *um* thick single layer polyethylene sheeting, orientated N-S, and located at the University of Tennessee's Organic Crop Unit in Knoxville, TN in the United States (lat 35.88° N, long 83.93° W, elev 252 m). These HTs are approximately 9.1 m in width and 15.2 m in length (139 m^2), equipped with two types of natural ventilation: 1) sliding doors that cover an opening 2.45 m tall and can be adjusted from 0 to 3.35 m wide, with one door at the northern end and another one at the southern end; 2) side curtains that can be opened by rolling up the lateral film. However, the side curtains were generally only opened during warm weather when maximum ventilation was required. During cooler times of the year, the side curtain and sliding doors were closed at night to retain heat, and only the doors were opened during the day because minimal ventilation was required. According to the USDA soil survey, soil at the study site is classified as a Dewey silt loam. These soils have around 15 cm of silt loam overlying deep clay subsoil. The slope at the study site is 6-7%, and the soil is somewhat eroded. These three experimental HTs have been managed organically since 2010, but this study of sweet peppers ('*Socrates'*) was conducted just over spring seasons in 2011, 2013 and 2015. All pepper transplants were grown in a greenhouse at the Organic Crop Unit, and the peppers were transplanted on March 24 (2011), March 27 (2013), and March 20 (2015). There were six beds laid out in each HT, and each bed was 12.2 m long by 0.9 m wide with double rows planted in each bed. Transplants were spaced 0.46 m apart within each planting row and the double planting rows were spaced 0.3 cm apart. Each bed was divided into four plots with 12 plants in each plot totaling 48 plants per row.

Spring 2011. This was a pilot project. In each HT, there were six different surface mulches and two sources of irrigation water. The twelve treatments were replicated and randomized in all three HTs following a split-plot design. Figure 21 (a) shows that there were five surface mulches compared with a bare soil control: 1) a compostable black geotextile prepared via spunbond nonwoven technology (*spun*), 2) vegetative mulch from a cover crop (*veg*), 3) black polyethylene (*black*), 4) clear polyethylene (*clear*), 5) biodegradable black "biobag" film (*biobag*). Specifically, biodegradable *biobag* mulch is a commercial film-based mulch formed from starch-copolyester blend (BioAgri , BioBag, Palm Harbor, FL) and spunbond nonwovens technology which can accelerate biodegradation due to the small fiber size (Hayes et al., 2010). The other biodegradable *spun* mulch was prepared from 100% (corn-derived) poly (lactic acid) and 85% poly (lactic acid) / 15% poly (hydroxybutyric acid). For the vegetative mulch treatment, a cover crop (*cereal rye*) was planted in January when sweet peppers were not being produced, and then cut and left as a cover crop residue on the ground as organic surface mulch. Polyethylene *black* and *clear* mulches (Rain-Flo Irrigation, Inc.) were characterized as 0.032mm embossed types. In-season breakdown of the biodegradable mulches was incomplete so that both the polyethylene and biodegradable mulches were manually removed after the pepper harvest. In addition, two types of water for HT irrigation (rainwater & city water) were randomly arranged among the surface mulches. Rainwater was harvested using a system designed to direct water off the roofs, and then gutters directed the water into black polyethylene tanks that are sized to store 55 cm^3 of water per square meter of the HT surface area. Also, rainwater was applied to the vegetable crops by two methods: gravity pressure and solar power. In the first house, the rainwater storage tanks were elevated with cinder blocks to provide low gravity pressure that supplied in-line drip tubing (Rivulis Hydrogol 16 mm-40 mil-1.6 l/h-40 cm); and in the other two houses, a solar powered pump provided irrigation via drip tapes (T-Tape 508-12-450) that operated at a pressure of 10 psi. The gravity and solar system were operated for different lengths of time to apply the same amount of water for each irrigation event. In each HT, only half the house was irrigated using stored rainwater, while the other half used treated city water. Depending on the time of year, if enough rain had not fallen to adequately replenish the tanks, city water was added to the tanks in measured amounts. Partially-composted poultry litter was applied in the late fall of 2010 to supply crop nutrients. Drip tubing/tapes covered with the different surface mulches were laid out one week before peppers were transplanted (March 24, 2011), and mature fruits were harvested for six consecutive weeks starting on June 14 and ending on July 18.

Figure 21. Split-split-plot design for the production of peppers in HTs in 2011, 2013 and 2015. In 2011, mulch treatment laid out through row 1 to row 6, including (1) black biodegradable spunbond (*spun*), (2) vegetative mulch from a cover crop (*veg*), (3) bare ground (*bare*), (4) black polyethylene film (*black*), (5) clear polyethylene film (*clear*), and (6) black biodegradable biobag (*biobag*). In 2013, the mulch distribution followed by (1) black polyethylene film (*black*), (2) vegetative mulch from a cover crop (*veg*), (3) bare ground (*bare*), (4) black polyethylene film with a cover crop (*blackCC*), (5) clear polyethylene film with a cover crop (*clearCC*), and (6) clear polyethylene film (*clear*). In 2015, anothor crop tomato was added. Thus, the mulch treatments for pepper were just laid out in three rows, inclduing (1) black polyethylene film (*black*), (2) bare ground (*bare*), and (3) black polyethylene film with a cover crop (*blackCC*). Also, two different water types for HT irrgation (rainwater and city water) were randomly arranged among the surface mulches through all three spring seasons of 2011, 2013 and 2015. In addition, over the spring 2013 and 2015, a floating row cover was put on half of each HT, covering half a length of the mulch rows at nights as an extra protection. All the treatments regarding water and surface mulch with or without a row cover were also arranged randomly among three HTs at the UT site.

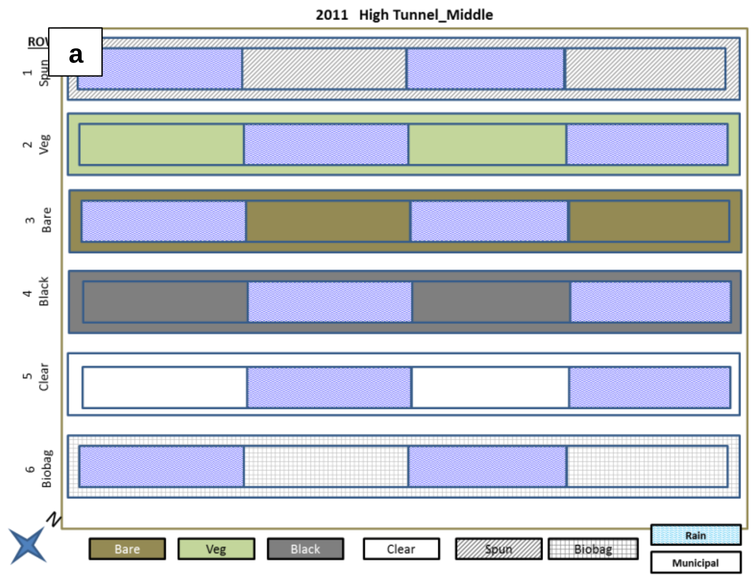

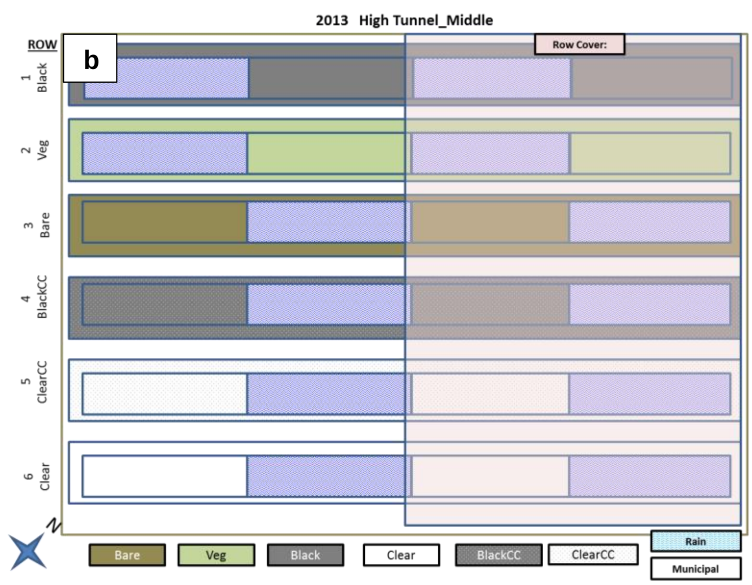

Figure 21 continued.

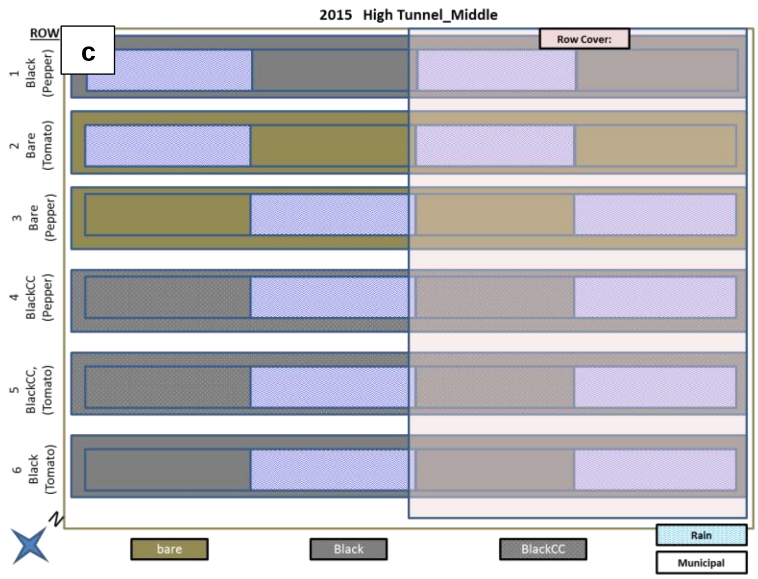

Figure 21 continued.

Spring 2013. Since the project received additional funding via a Conservation Innovation Grant (CIG, USDA-NRCS), the experimental design in 2013 was partially adjusted from 2011 by adding two practices (cover crop and row cover). Thus, the biodegradable mulches *biobag* and *spun* were removed and replaced by polyethylene black and clear films following cover crop incorporation (*blackCC* and *clearCC*). The cover crops were mixed with cereal rye (*Secale cereale*) and bell bean (*Vicia faba*) planted in winter 2012. However, the cover crops failed to either germinate or reach maturity probably due to the unfavorable growth temperature inside the HTs. Thus, external cover crop biomass was imported and tilled into the soil for the treatments using cover crops that were followed by polyethylene mulches (*blackCC* and *clearCC*) while the cover crop treatment without polyethylene mulch (*veg*) was left as crop residue on the ground as a vegetative mulch. The final aspect of the design added, a 7.5 by 9 m row cover placed over half of each HT covering half a length of the mulch rows. Row covers were typically used at nights when the inside minimum temperature dropped more than 5°C below the optimum growth temperature of sweet peppers (18°C). Therefore, Figure 21 (b) shows that there were a total of 24 treatments in the spring of 2013. It included two water resources, five surface mulches (*black*, *veg*, *blackCC*, *clearCC*, *clear*) and a bare ground control, with or without a row cover. All the treatments were replicated and randomized in three HTs following a split-split plot design. No extra fertilizer was added to the cover crop treatments, but organic fertilizer was added to the non-cover crop treatment in this year. Peppers were transplanted in each HT on March 27, 2013 and harvested four consecutive weeks on July 8 and ending on July 26.

Spring 2015. The mulch treatments in 2015 changed from 2013 due to some negative experimental observations and funding for the project coming to an end. Three mulch treatments including *clear*, *clearCC* and *veg* were removed in all three HTs, but tomatoes were added as another crop in half of each house. These adjustments were made because in spring 2013, *clear* and *clearCC* accidently burned many pepper transplants resulting in a poor marketable crop quality and yield, and the *veg* mulch was dropped because it had the least pepper production in the two previous experiments. Therefore, the remaining mulch treatments in spring 2015 just included black polyethylene film (*black*) and black polyethylene film with cover crop incorporation (*blackCC*) compared with a bare ground control (*bare*). Also, it was determined that supplemental nutrients would be needed, so additional 0.93 kg of feather meal (typically 13% nitrogen) was added to each half-row except in the *blackCC* treatment. Therefore, Figure 21 (c) shows a total of 12 treatments for sweet peppers in spring 2015: two sources of water (rainwater & city water), two surface mulches (*black* & *blackCC*) and a bare ground control, with or without a row cover. All the treatments were replicated and randomized in three HTs following a split-split plot design. Peppers were transplanted in each HT on March 20, 2015 and harvested for five consecutive weeks starting on July 2 and ending on July 30.

A summary of the treatment changes over three spring seasons includes the biodegradable mulches *biobag* and *spun* being applied just one time as a part of 2011 pilot project. Vegetative mulch (*veg*) being used twice in 2011 and 2013 but removed from 2015 due to the continuously low crop production. Clear polyethylene (*clear*) being applied twice in 2011 and 2013, but clear polyethylene with cover crops (*clearCC*) only applied once in 2013. Also, black polyethylene with cover crops (*blackCC*) being applied twice in 2013 and 2015, but treatments of black polyethylene mulch (*black*) with bare ground control (*bare*) all repeated three times in 2011, 2013 and 2015.

Climatic monitoring and instrumentation

There were two weather stations located outside and inside of the experimental HT. The outside meteorological station was located 6 m away from the HT and positioned 4.0 m above the ground. Solar radiation was measured by a pyranometer (LI-COR LI200X) on a horizontal surface. Wind speed and direction were measured using a three cup anemometer and wind vane (R.M.Young 03001). Relative humidity and air temperature were measured using a capacitive chip and platinum resistance thermometer, respectively (*Vaisala HMP60*) that was installed in a gill multi-plate radiation shield. Also, an inside climatic station was placed at 1.5 m above the ground at the center of the middle experimental HT. This station used the same sensors described for the outside weather station.

The proof that energy conservation was the cause of temperature modification came from soil, water, and air monitoring. An array of 15 thermistors, potted in solar reflecting white mold, was used to measure air temperatures at 1.2 m above the ground surface. Between crop rows, a total of 12 of these thermistors were placed 30 cm above the ground surface to measure air temperatures at the canopy level. Half these thermistors were under the row cover and half were outside the row cover. The difference between these canopy temperatures determined how much the row cover improved nighttime canopy temperature. Also, soil temperature was monitored in each combination for the water, mulch, and row cover treatments by 24 thermistors inserted 10 cm into the ground. The water temperatures were monitored by placing thermistors at the bottom of polyethylene storage tanks and in the supply line of city water. All sensors, both inside and outside were measured every 15 seconds and the average recorded every hour by a CR1000 datalogger (Campbell Scientific Inc.). Table 7 provides the specifications for the sensors.

Table 7. Environmental Paramters Measured during the Experiments

Measured Parameters	Sensors	Range and Accuracy	Location
Solar radiation Q_{solar} (Wm^{-2})	LI200X Pyranometer (LI-COR.INC)	0 to 3000 Wm^{-2} with ±5%	Inside and outside weather station
Air temperature T_i (K) Relative humidity H_R (%)	HMP60 Probe (Vaisala.INC)	-40 to 60°C with ±0.6% ±3% RH over 0 to 90%, ±5% RH over 90 to 100%	Inside and outside weather station
Wind speed U (ms^{-1}) Wind direction (°)	R.M.Young Wind Sentry (Campbell Sci. Inc)	0 to 50ms^{-1} with ±1% 0 to 360° with ±5°	Outside weather station
Air temperature (°C)	Thermistor (PS104J2)†	±0.1°C with 0.026°C	An array of 15 thermistors all over the inside of middle HT located 1.5 m above the ground
Canopy temperature (°C)	Thermistor (PS104J2)†	±0.1°C with 0.026°C	12 thermistors located 30 cm above the ground between crop rows
Soil temperature (°C)	Thermistor (PS104J2)†	±0.1°C with 0.026°C	24 thermistors located 10.16 cm below the ground
Water temperature (°C)	Thermistor (PS104J2)†	±0.1°C with 0.026°C	Polyethylene storage tank bottom for rainwater and supply line of city water

† means the thermistors are made in our lab which are non-linear sensors following a polynomial response to temperature that is defined by the Steinhart-Hart equation.

Statistical analysis

The experiments in this study applied a randomized complete block design (RCBD) to determine statistical differences, based on a split-split-plot sub-design for overall crop marketable production and temperature changes. Total marketable yield including pepper weight (g/plant) and fruit number (#/plant) per plant was estimated from the first harvest until the end. Also, hourly data of different air/water/soil temperature reading were organized and preprocessed for missing data or other interrupted readings. Daytime and nighttime hours in each day were selected from 10:00 to 16:00 and 21:00 to 8:00, respectively. A pivot table was established in MS Excel to average the hourly data for each day. Division of the data points into two parts of the growing season was done to reflect the change in ventilation within the HT. The first division is the early spring (*ES*) that represents the month of April when the side curtains were closed and only the sliding-end doors were used for ventilation, and the second division is the late spring (*LS*) that represents May to July when the side curtains and sliding-end doors were fully opened for maximum ventilation. Analyses of yield and temperatures were performed by SAS statistical software to determine differences between various treatments, as well as their interaction (SAS Institute Inc., Cary, NC). The temperature model used in SAS was created by blocking on date but also considering the dates as correlated samples on the plots. All of the outliers were eliminated based on SAS diagnosis before analysis to meet the assumptions of normality and homogeneity of variance. Fisher's least significant difference test (*LSD*) at an alpha value of 0.1 was used to compare treatment means for interpretation of results.

Results and Discussion

High tunnel benefits on inside microclimates

The high tunnels create microclimates inside by affecting weather inputs such as: solar radiation, air and soil temperature, wind speed and relative humidity. A total of 1460 solar radiation observations were measured over the span of three springs of 2011, 2013 and 2015. Results showed that there is a strong linear relationship between the inside and outside solar radiation (SR) and that approximately 12% of total SR was reflected by HTs' polyethylene covering (Figure 22). The slight differences of the inside-to-outside SR may be affected by the period of the year, and the aging or dust deposition of the plastics. At higher levels of solar radiation (>0.6 kW m^{-2}), greater variability in solar transmission occurred compared with the lower solar radiation. Also, based on the average values of all three spring seasons, the air temperature differences between inside and outside significantly varied from day to day. During the *ES*, daily maximum air temperature inside the HT was mostly raised from 3°C to 17°C (sometimes even up to 28°C) as compared with the outdoor conditions, depending on cloud cover, ambient wind conditions, and extent that the tunnel sliding doors were opened (Figure 23). After fully opening end-doors and side-curtains in *LS* (starting around May 12), inside air temperatures were consistently increased by approximately 1.5-4.5°C to those outdoors. The transmitted solar radiation was absorbed as thermal energy by the crop and other components including the ground surface resulting in a rise in temperature. Part of the energy can be released by the latent heat through the crop transpiration, and the remainder would contribute to the sensible heat to warm the inside air (Papadakis & Frangoudakis, 1989). In addition, the comparison of shielded outside and shielded inside thermistor readings shows that HT night time air temperatures were as much as 4°C higher than outdoor temperatures. The HTs are considered “heat reservoirs,” which can transfer the stored heat from the soil back to the surroundings at night. However, results show that there were several nights when the minimum air temperature dropped to within 0.3-1.0°C of the ambient outside temperature. This behavior is believed to be caused by the thermal heat loss from the inside air to the colder polyethylene covers. According to Papadakis et al. (2000), the net radiation loss through the cover is intensive during extreme cold nights. Since the rate of long-wave radiative heat loss of the cover is higher than its convective heat gains from the air, the cover temperature becomes lower than both the inside and outside air temperature. Because the inside air loses heat by convection to the colder cover, the inside air temperature sometimes maybe lower than the outside (Baytorun & Abak, 1993; Montero and Munoz, 2005).

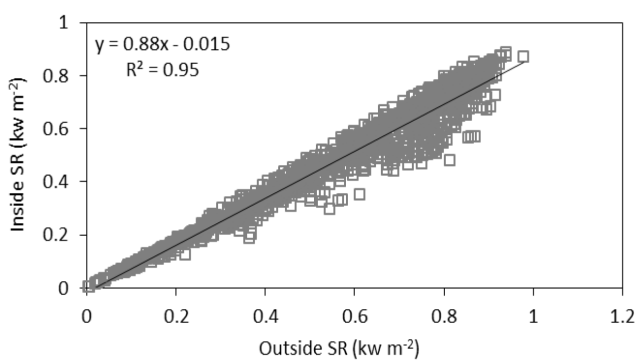

Figure 22. Relationship between inside and outside solar radiation over the average of 2011, 2013 and 2015 spring seasons. Hour-based average data during solar noon period (10:00 am to 16:00 pm EST) and the solid lines represent the linear relationship y = 0.88x - 0.015 (R^2 = 0.95) between inside and outside solar radiations for all three springs.

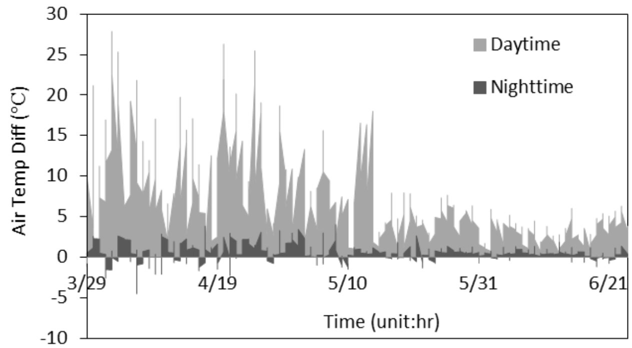

Figure 23. Effects of high tunnels on daytime and nighttime air temperature over the average of 2011, 2013 and 2015 spring seasons. Temperature differences were calculated as inside air temperature minus outside air temperature. Daytime includes 10:00 am to 16:00pm and nighttime includes 21:00pm to 8:00am. Sidewalls and end-doors were fully opening during summer periods when maximum ventilation required which started around the middle May.

The outside soil temperature in 2011 was not recorded; thus the analysis of soil temperatures was calculated over the average of two spring seasons in 2013 and 2015. Because of the "heat reservoir" effect, the average soil temperature inside the HTs during the day was up to 3.5-5°C higher than field temperatures of bare ground during the *ES*. But, over the season, inside-to-outside soil temperature differences were continuously decreased (Figure 24). The results show that the temperature differences at nights were always greater than that during the day; this situation was even more significant in *LS*. Also, there are some rapid changes after mid-June, indicating that the outside soil temperatures being warmer than inside both for daytime and nighttime. Probably during this *LS* period, there was grass grown on the outside ground which may have been trimmed allowing more sun to heat the soil and the conduit protecting the sensor wire. At the same time, inside soil temperatures were also reduced compared to the bare soil outside (after trimmed), which was likely the result of increased leaf shading from the fully mature peppers.

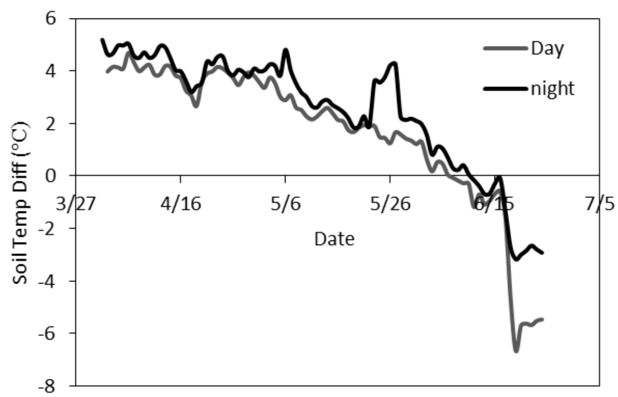

Figure 24. Soil temperature difference between inside and outside of high tunnel for the days and nights over the average of 2013 and 2015 spring seasons. Temperature differences were calculated as inside soil temperature minus outside soil temperature (bare ground).

Under the intense solar radiation after mid-June, this reduction of inside soil temperature could be beneficial for better root crop growth. In addition, canopy temperatures (measured 30 cm above the ground) inside the HTs were similar to the air temperatures (measured at 1.2 m above the ground) in *ES*. But in *LS*, diurnal temperatures at the canopy level were significantly greater (1-3°C) than that in the surrounding air (Figure 25). Compared with the large temperature fluctuation of inside air and canopy (±11°C), soil temperatures (measured 10 cm deep ground) varied just within ±3°C. The relatively warm and consistent soil temperatures in a HT can be considered as one of the critical variables to improve crop growth, particularly in a cold *ES* period.

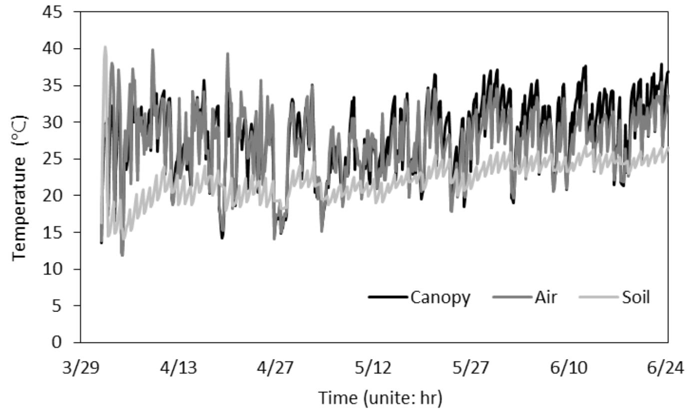

Figure 25. Comparison of canopy, air and soil temperatures inside the high tunnel during the daytimes in all two spring seasons of 2013 and 2015.

The HT structure decreased the wind speed significantly and alleviated adverse effects such as plant lodging. HTs used in this study are all oriented south to north, and prevailing winds at this site are typically from the south. Under this situation, leeward vented sides (northern) always had a warmer canopy temperature than the windward side (southern), due to the cooling effects of the incoming air-flux. Figure 26 shows that the outside wind speed was as high as 6-7 ms^{-1} and as low as 0.05 ms^{-1}; but, most measurements were distributed within 1-4 ms^{-1}. Inside wind speed was consistently reduced relative to the outside by an average of 80-90%; but, it increased when the side walls and end-doors were fully open in the *LS*. In addition, spring seasons are times when humidity related diseases usually peak in HTs. On a clear and sunny day, inside evapotranspiration rate from crop leaf and soil increases, while at nights, condensation can occur when the air cools down to the dew point and water can drip on the crops causing plant diseases. Results show that during the day, about 92 percent of total values of inside RH were lower than outdoor RH by 5-30% since air can hold more moisture as it warms (Figure 27a). However, inside RH were increased when the air was cooler at nights, resulting in just 70 percent of the total values of inside RH that were lower than the outdoor RH by 3-15% (Figure 27b).

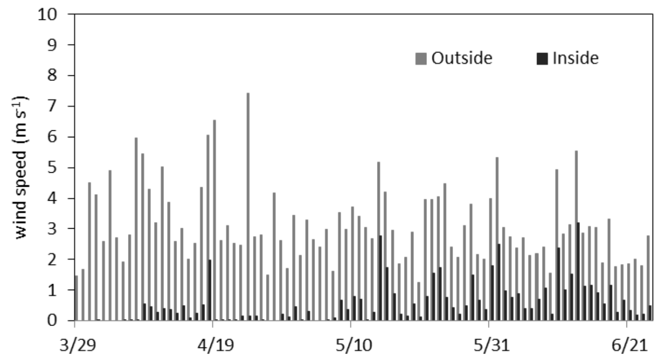

Figure 26. The comparison of wind speed inside and outside high tunnel during the day over the average of 2011, 2013 and 2015 spring seasons.

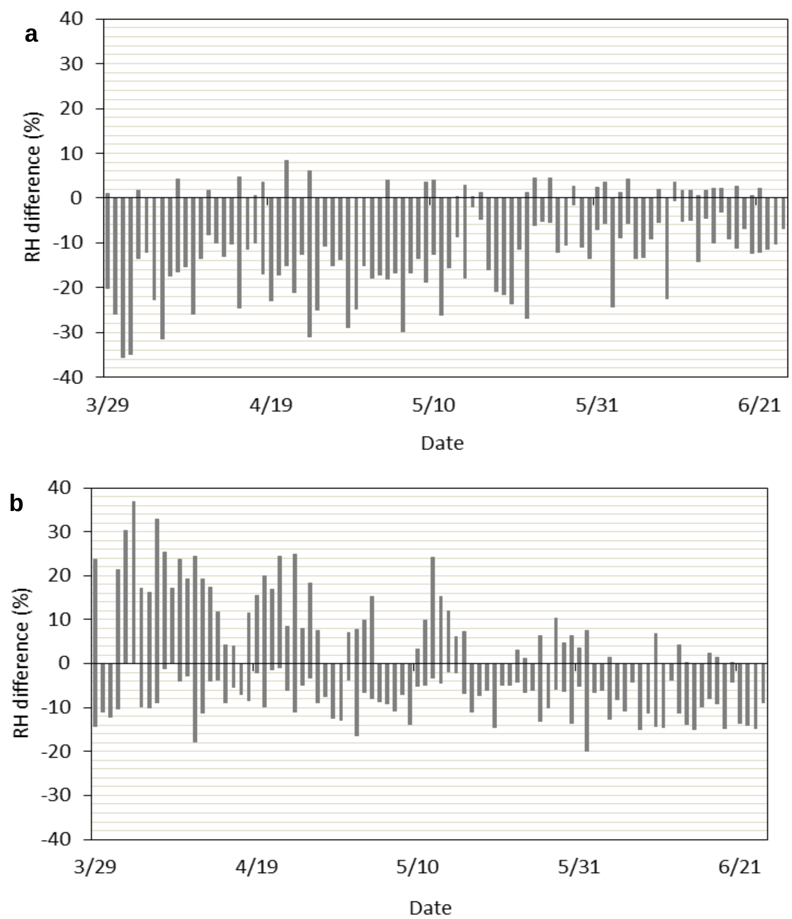

Figure 27. The comparison of inside and outside relative humidity (*RH*) during the days (a) and nights (b) over the average of 2011, 2013 and 2015 spring seasons. *RH* differences were calculated as inside minus outside.

Treatment impacts on pepper production

Behavours of surface mulches

Statistical analysis indicates that mulch treatments can be considered as the main contributing factor on total crop production ($p<0.001$) (Table 8). Figure 28 shows for each spring season, *black* mulch consistently produced yields higher than bare soil regarding both fruit weight and fruit number per plant. Compared with bare ground, *black* mulches increased the yield in g/plant by approximately 36% (2011), 126% (2013) and

81% (2015), and in fruit number per plant by 28% (2011), 95% (2013), and 90% (2015). However, as the years progress, yields achieved using *black* mulch decreased. In 2011, yields of 641.2 g/plant and 5.2 #/plant of peppers were achieved; but, the yield decreased to 434.3g/plant (32% reduction) and 2.1 fruits per plant (60% reduction) in 2013, and further to 360.8 g/plant (44% reduction) and 2.4 #/plant (54% reduction) in 2015. This observation occurred for the other mulches, which could be a result of short-rotation in vegetable production rather than the use of mulches (Karlen & Varvel, 1994). Many studies indicated that short rotation has been associated with a decrease in the diversity of the rhizosphere microbial community which is beneficial to the plant through the suppression of pathogens, and thus potentially resulting in decreased crop yields (Bennett et al., 2012; Schippers & Bakker, 1987). Many crops grown outdoors with continuous planting or short rotation have been reported to suffer yield reduction, such as maize, soybean, potato and sugarcane, compared to those grown in longer duration of two- or three-year rotation (Crookston et al., 1991; Kelley and Long, 2003; Larkin & Honeycutt, 2006; Pankhurst et al., 2005). In addition to the possibility of short rotation effects, auto-toxicity interaction may occur and cause phytotoxin production and build up in the soil with continuous culture over time, and further reducing overall yield of the subsequent crops. Tomato (*Solanum lycopersicum*) is considered to have this auto-toxicity impact and is in the same family as peppers, which may be the reason why spring pepper yield in 2013 decreased after the fall planting of 2012 spring tomatoes, and pepper production in 2015 continued to decrease after tomatoes were planted in 2014. Therefore, some researchers recommend not rotating pepper with tomato (Gleason & Edmunds, 2005). In comparison, the yield reduction rate in bare ground was much higher than in *black*. In 2011, there was 473 (g/plant) and 4.08 (fruits/plant) of peppers harvested from the bare ground, but the yields were reduced by 59% (g/plant) and 75% (fruits/plant) as an average of 2013 and 2015. There was also a notable reduction in clear yields from 2011 to 2013. Specifically, in 2011, *clear* plots produced the highest numerical yield; but there was no significant difference compared to that for *black* mulches. However, from 2011 to 2013, yield from plots using clear mulches was reduced by about 71% marketable fruit weight and 77% fruit numbers per plant. In addition to factors that may have impacted soil health degradation as discussed above, an excessive heat event occurred in 2013 when the HT doors were not opened in a timely manner. After this event more plant stress was observed in the clear treatments than in the other mulch treatments.

Table 8. Pepper yield and average soil temperatures at 10cm deep under different mulch treatments during the day and night in early and late spring of 2011, 2013 and 2015[a].

Year	Mulch	Yield		SoilTemp_day		SoilTemp_night	
		Weight	Count	ES†	LS†	ES†	LS†
		(g/plant)	(#/plant)	(°C)		(°C)	
2011	Black	641.15 a	5.22 ab	22.41 b	23.43 b	21.31 b	23.76 b
	Biobag	686.83 a	5.43 a	21.37 c	23.10 c	19.52 c	71.98 e
	Clear	708.83 a	5.48 a	24.94 a	23.94 a	23.21 a	75.76 a
	Spunbond	602.97 ab	4.80 ab	20.84 d	22.36 d	19.69 c	72.54 d
	Bare	473.08 bc	4.08 bc	21.36 c	22.58 d	18.82 d	73.60 c
	Veg	370.48 c	3.20 c	18.82 e	21.89 e	17.34 e	71.13 f
	Sig.level	*0.0039*	*0.0182*	*<0.0001*	*<0.0001*	*<0.0001*	*<0.0001*
2013	Black	434.31 a	2.05 a	20.16 c	22.66 d	18.93 b	23.02 d
	BlackCC	295.19 b	1.64 b	21.51 b	23.93 a	20.28 a	24.64 a
	Clear	208.67 c	1.22 c	21.93 a	23.03 c	20.17 a	23.48 c
	ClearCC	146.48 d	1.09 c	22.04 a	23.35 b	20.49 a	23.56 c
	Bare	192.10 cd	1.05 c	20.17 c	24.06 a	18.87 b	23.88 b
	Veg	1.83 e	0.0083 d	18.69 d	22.95 c	17.59 c	23.01 d
	Sig.level	*<0.0001*	*<0.0001*	*<0.0001*	*<0.0001*	*<0.0001*	*<0.0001*
2015	Black	360.84 a	2.43 a	21.62 a	25.42 c	19.63 a	26.10 b
	BlackCC	188.87 b	1.38 b	21.63 a	25.74 b	19.60 a	26.10 b
	Bare	199.06 b	1.28 b	20.72 b	26.47 a	18.69 b	26.52 a
	Sig.level	*<0.0001*	*0.0005*	*<0.0001*	*<0.0001*	*<0.0001*	*<0.0001*

[a] Mulch treatments: biodegradable black biobag (*Biobag*) and black spunbond (*spun*), black plastic with (*blackCC*) or without cover crops (*black*), clear plastic with (*clearCC*) or without cover crops (*clear*), vegetative mulch (*veg*) and bare ground (*bare*); *ES* and *LS*, referring to early and late spring, respectively, were characterized by diurnal soil temperature in specific early and late spring. Temperature values are daily means from 10:00 to 16:00 and nightly means from 9:00 to 8:00. Values followed by the same letter are not significantly different according to Fisher's LSD (P=0.1).

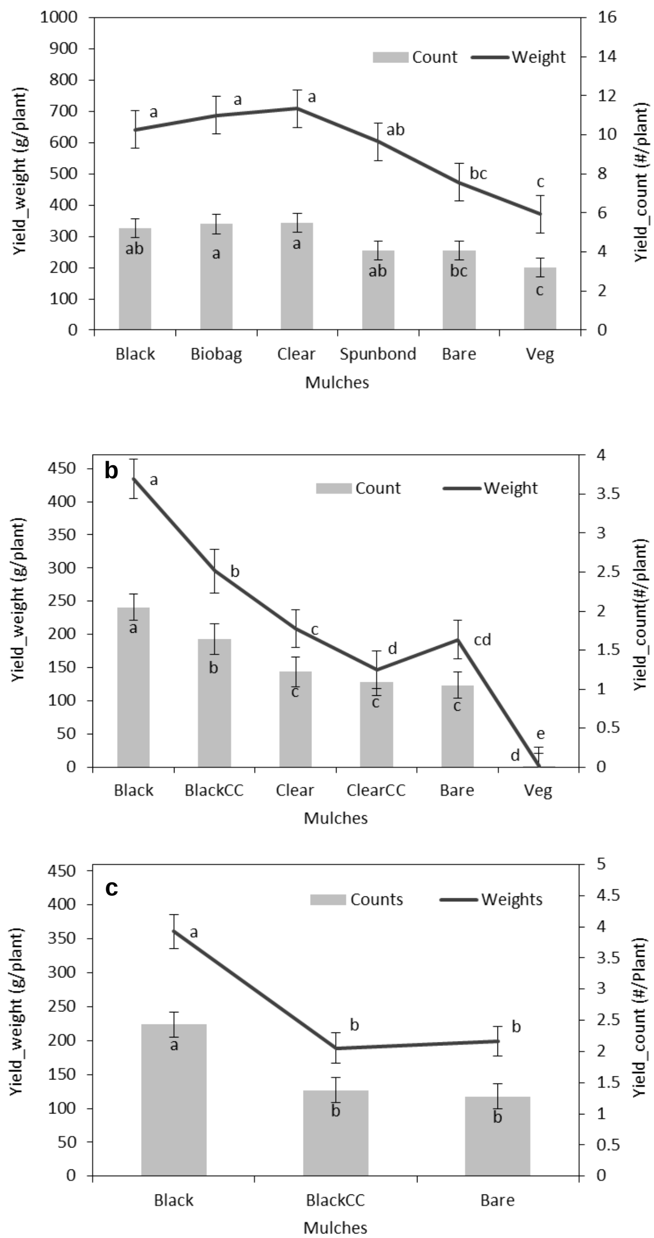

Figure 28. Marketable weight and count (mean ± SE) of pepper under the effects of different mulch [treatments (black plastic mulch (*black*), black plastic mulch with cover crops (*blackCC*), clear plastic mulch (*clear*), clear plastic mulch with cover crops (*blearCC*), bare ground (*bare*), Vegetative mulch (veg) over spring seasons of the year 2011 (a), 2013 (b) and 2015 (c) in high tunnels; Values followed by the same letter are not significant different according to Fisher's *LSD* (p=0.1)

Differences in pepper yield are related to many factors: cultivar, soil temperature, air temperature, soil moisture, nutrients and weed growth. But, our focus was on the impact of soil temperature to test our hypothesis that better utilization of solar energy in HTs would increase yield. Black polyethylene mulches had a significant effect on soil temperature, which is related to marketable production in most cases (Table 8). Compared with the *bare* ground treatment, the increased crop yield observed using *black* mulch was related to the latter's soil-warming ability. In 2011, soil temperatures under *black* mulch were consistently greater than that for *bare* ground (0.9-1.6°C) through the whole season, which promotes faster crop development. In 2013 and 2015, *black* mulch warmed the soil more in the *ES* compare to the bare ground; but, the opposite scenario occurred in *LS* showing that soil temperatures were significantly higher in bare ground by as much as 1.4°C. This was most likely due to weeding and a smaller crop canopy in the bare canopy allowing more solar radiation to be intercepted directly by the ground surface. The rapid increase of soil temperature on *bare* soil could have had an adverse effect on unprotected plant-roots and evapotranspiration rate reducing overall pepper development. Therefore, *black* mulch was considered to be more effective at utilizing solar radiation to create a more productive soil temperature environment. *Clear* mulch also has great soil-warming ability, even higher than *black* mulch. In 2011, *clear* mulch consistently provided the warmest soil temperatures among all mulch treatments and it significantly produced higher values (0.5-2.6°C) than that under *black*. Although *clear* retained a warmer microclimate underneath than *black*, the overall pepper yields did not improved significantly in 2011. This is probably due to poor weed control under *clear* mulch, resulting in competition for water and nutrients between the weeds and the crop. The rapid reduction of pepper yield under *clear* mulch from 2011 to 2013 was also related to the temperature. In May of 2013, cloud cover cleared unexpectedly creating extremely high temperature in the HTs for a couple of hours before the doors could be opened for ventilation. It was observed that the peppers grown with *clear* mulch were damaged more than the other surface mulches. Although there were many plants lost under *clear* mulch, it was observed that the surviving pepper plants were generally taller and reached flowering earlier than in bare ground with yield equaling that of bare in 2013. Except for the overheating accident described above, the positive effects of polyethylene mulches (*black* & *clear* varieties) on crop marketable yields were significantly higher when compared with the bare ground control. It is also consistent with the results of a study by Iqbal et al. (2009) which documented hot pepper productivity in poly/plastic tunnels. Therefore, *black* mulch is highly recommended because it can effectively warm the soil with less potential for overheating than clear, and it also prevents weed establishment reducing nutrient competition with the crop.

The use of the black biodegradable mulch, *biobag,* was not significantly different from *black* polyethylene mulch for pepper yield in 2011 (Figure 28a). Also, *spun* mulch had less marketable fruit weight by 6% and fruit numbers by 22% than *black mulch*, but not at a significant level (Table 8). Both of the biodegradable mulches produced significantly cooler soil temperatures than under *black*, by 0.5°C and 1.4°C for *biobag* and *spunbond*, respectively. The cooler temperatures may have been caused by slight biodegradation of these mulches, but also *biobag* is a very thin film and *spun,* being a fiber-based geotextile, allows more vapor to pass through it. In addition, weed pressure was also greater for *spun* than using the standard black mulch, due to the higher air permeability. As compared to bare ground, the biodegradable mulches performed well by improving the overall pepper production about 27% in fruit weight and 12% in fruit numbers probably due to the increased soil temperature around the crop root zones in the biodegradable mulch plots.

In addition, polyethylene mulch with cover crops significantly reduced both pepper marketable weight and numbers per plant, as compared with non-cover crop treatments in the springs of 2013 and 2015 (Figure 28b and Figure 28c). Although most studies show that cover crops like Hairy vetch exhibit desirable attributes including high nitrogen fixing ability and high biomass quality in vegetable production (Kumar & Abdul-Baki, 2005; Pullaro et al., 2006), the cover crop benefits were not realized in this study. Specifically, *blackCC* significantly reduced fruit weight per plant by 32-48% and number of fruit per plant by 20-43% compared to that under *black*; while, *clearCC* production was reduced by 30% in fruit weight per plant compared to *clear* without a *cover crop*, but there was no significant difference in fruit numbers per plant. This trend is probably related to the inability to establish a good cover crop stand over the winter months. Thus, the roots of the cover crops had little opportunity to fix nitrogen in soil. Also, cover crop residues that were imported and then incorporated into the soil had very little opportunity to breakdown and provide nutrients to the crop, but non-cover crop treatments had organic fertilizer applied that provided more easily available nutrients. A positive effect of incorporating cover crop residue under plastic mulch was increased soil temperature which could increase breakdown of organic matter into available nutrients. Average soil temperature under *blackCC* was around 1.4°C higher than that under *black* mulch, while the difference between *clearCC* and *clear* was only 0.2°C. Cover crops residue creates a larger amount of air space when mixed with soil as compared to the more compacted ground without cover crops, and after periodic irrigation, more water can be stored inside the pore spaces of the *clearCC* or *blackCC treatments*. Due to the higher heat capacity of water, the loose and wet soil with cover crops can conduct and store heat better than without cover crops; thus, *clearCC* or *blackCC* produced higher soil temperature than under *clear* or *black* mulch. Even though the cover crops had a positive effect of warming the soil, it appears that limited nutrient availability inhibited growth and yield when cover crops were incorporated without supplemental organic fertilizer.

The *veg* mulch treatment was expected to improve organic pepper production in HTs since it reduces diurnal temperature flux by reducing the solar energy reaching the soil surface during the *LS*, and by creating sub-optimum conditions for weed seed germination. However, according to the results, *veg* consistently produced the lowest pepper yield (Figure 28). The major concern with using *veg* mulch is that it cooled the soil to an extent where crop growth may have been detrimentally delayed, especially in the early stage of pepper growth. Results confirmed that under *veg* mulch, there was a significant reduction of soil temperature (1.5°C) with more weeds than that in bare ground during the whole season (Table 8). Therefore, *veg* mulch promoted making less efficient use of solar energy to extend the growing period beyond the normal growing season.

Interaction effects of row cover and mulch

For the *ES* period, row covers provided additional thermal protection for peppers. Table 9 shows that in 2015, row covers were the main contributing factor to improve the pepper marketable production ($p<0.01$). Yield weight and fruit numbers per plant using a row cover increased around 20% and 44%, respectively, as an average of all mulches in 2013 and 2015. Also, there were positive interaction between surface mulch and the row cover application on pepper yields for both years ($p<0.1$). In 2013, *black* mulch produced the highest yield when comparing the mulch treatments without row covers. With a row cover, the black mulch significantly increased fruit weight per plant by about 21% (2013) and 114% (2015) as compared with black mulch without a row cover, while it also increased the fruit number per plant about 21% (2013) and 81% (2015). Also, 86% more fruit was produced by using a row cover under *blackCC* in 2013 than that without using a row cover, but no significant increase was found in 2015. Both *clear* and *clearCC* mulch treatments using a row cover didn't provide an improvement to total crop production compared with not using a row cover in 2013. This may be a result of the accidental pepper loss described previously, thus causing a nonsignificant difference. Also, the use of a row cover in bare plots increased fruit weight per plant by 66% and number of fruit by 75% in 2013, while showing no significant improvement on pepper production in 2015. In addition, *veg* mulch without a row cover barely produced any peppers but the use of row covers saved a few more fruit. The increase in pepper yield from row covers was related to an increase in soil and canopy temperatures. Canopy and soil temperatures under a row cover were significantly increased from 0.7°C to 2.6°C in the canopy and from 0.5°C to 0.8°C in the soil at night. Moreover, soil temperature increases from row covers interacted differently with the mulch treatments. Figure 29 shows that during the night in early spring of 2013, significant increases in soil temperature were 0.5°C (*black*), 1.6°C (*blackCC*), 1.4°C (*clear*), 1.8°C (*clearCC*), 0.6°C (*bare*), and 1.1°C (*veg*) from using row covers. Also in the early morning hours before taking off the row covers, these differences under each mulch on soil temperatures showed larger variation compared to that at nights, with increases of 0.74°C (black), 1.64°C (*blackCC*), 1.87°C (clear), 1.8°C (*clearCC*), 1.7°C (bare), and 1.3°C (*veg*). *Black* mulch had the least soil temperature rise from row covers both during the day and night. The results indicate that *black* can act alone without a row cover to have a positive effect on the soil temperature and pepper yield but had a significant response to adding a row cover.

Table 9. Interactions of mulch and row cover on pepper yield and soil temperature inside high tunnel during the early springs of 2013 and 2015[a].

Year	Mulch	Row Cover	Yield		Soil Temperature (°C)	
			Weight	Count	Daytime	Nighttime
2013	Black	no	360.40 b	2.07 a	19.79 g	18.67 bcd
		yes	435.50 a	2.50 a	20.53 ef	19.19 bc
	BlackCC	no	260.00 cd	1.15 bcd	20.68 de	19.48 bc
		yes	330.40 bc	2.14 a	22.33 b	21.07 a
	Clear	no	235.40 d	1.38 b	20.26 f	19.45 bc
		yes	182.00 de	1.06 bcd	22.13 b	20.89 a
	ClearCC	no	165.10 e	1.19 bc	21.16 c	19.61 b
		yes	127.80 e	1.00 cd	22.92 a	21.37 a
	Bare	no	144.20 e	0.76 d	19.29 h	18.56 cd
		yes	240.00 d	1.33 bc	21.04 cd	19.19 bc
	Veg	no	0.01 f	0.00 e	18.08 i	17.06 e
		yes	3.67 f	0.02 e	19.31 h	18.13 d
	Mulch		<0.0001	<0.0001	<0.0001	<0.0001
	Row Cover		0.5279	0.1024	<0.0001	<0.0001
	Mulch x Row Cover		0.0048	0.0113	0.013	0.4987
2015	Black	no	229.90 b	1.73 b	21.46 c	19.64 b
		yes	491.80 a	3.13 a	21.77 b	19.61 b
	BlackCC	no	179.40 b	1.26 b	21.16 d	19.16 c
		yes	198.33 b	1.50 b	22.10 a	20.03 a
	Bare	no	189.79 b	1.18 b	20.15 e	18.29 d
		yes	208.33 b	1.38 b	21.29 cd	19.09 c
	Mulch		<0.0001	0.0005	<0.0001	<0.0001
	Row Cover		0.0014	0.0112	<0.0001	<0.0001
	Mulch x Row Cover		0.0022	0.0619	<0.0001	0.0013

[a] Values within mulch, row cover followed by the same letter are not significantly different according to Fisher's LSD (P=0.1).

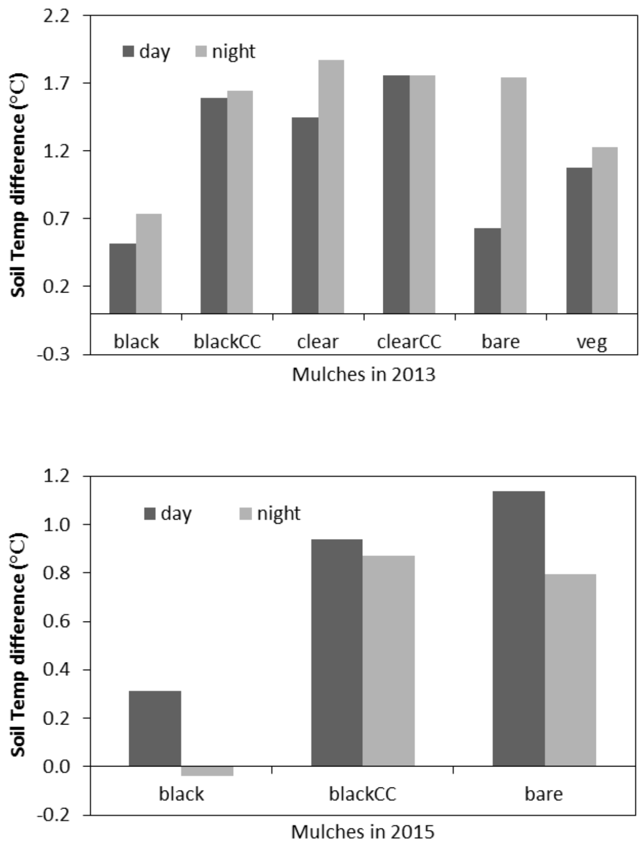

Figure 29. The effects of various mulches on soil temperature differences between each mulch type with and without a row cover in 2013 and 2015.

Interaction effects of irrigated water and mulch

Significant improvement of pepper yield was expected by using rainwater applied with drip irrigation, and results confirmed that the rainwater had the potential to increase the overall pepper production (Table 10). Compared with city water, rainwater significantly increased the total pepper weight (20%) and peppers numbers (19%) per plant in 2011 and 2013, respectively ($p<0.1$). Also, the interaction effects in 2013 show that the *clear* mulch and bare ground significantly improved pepper weights approximately 61% and 49%, respectively, by using rainwater irrigation compared to city water ($p<0.1$). However, results in 2015 didn't show any positive effects on pepper production by using rainwater irrigation compared to the city water, and the opposite result occurred with the total pepper weight in bare ground irrigated with city being 41% higher than those plots under rainwater irrigation.

Table 10. Interactions of mulch and water on pepper yield and soil temperature inside high tunnel during all three spring seasons of year 2011, 2013 and 2015[a].

Year	Mulch	Water	Yield		Soil Temp_day		Soil Temp_night	
			Weight	Count	ES†	LS†	ES†	LS†
			(g/plant)	(#/plant)	(°C)		(°C)	
2011	Black	City	589.40 abc	5.03 abc	21.98 cd	23.06 d	20.61 d	23.48 c
		Rain	692.90 ab	5.40 ab	22.84 b	23.81 b	21.99 c	24.03 b
	Biobag	City	593.97 abc	5.10 abc	21.06 e	22.54 e	19.66 ef	21.36 g
		Rain	779.70 a	5.77 a	21.68 d	23.66 b	19.38 f	23.06 d
	Clear	City	672.07 ab	5.20 abc	24.80 a	23.50 bc	22.67 b	23.97 b
		Rain	745.60 a	5.77 a	25.09 a	24.39 a	23.74 a	24.65 a
	Spunbond	City	518.33 bc	4.43 abc	20.74 ef	22.36 e	19.62 e	22.46 e
		Rain	687.60 ab	5.17 abc	20.94 ef	22.36 e	19.77 e	22.58 e
	Bare	City	513.23 bc	4.53 abc	20.67 f	21.91 f	19.59 e	22.52 e
		Rain	432.93 cd	3.63 cd	22.03 c	23.26 cd	18.04 f	23.72 bc
	Veg	City	285.63 d	2.60 d	19.06 g	22.00 f	17.02 g	21.53 g
		Rain	455.33 cd	3.80 bcd	18.58 h	21.78 f	17.66 f	21.95 f
	Mulch		0.0039	0.0182	<0.0001	<0.0001	<0.0001	<0.0001
	Water		0.0466	0.278	<0.0001	<0.0001	0.0183	<0.0001
	Mulch x Water		0.6344	0.7424	<0.0001	<0.0001	<0.0001	<0.0001
2013	Black	City	444.94 a	2.04 a	20.24 d	22.47 f	18.87 d	22.76 g
		Rain	423.67 a	2.06 a	20.08 d	22.86 e	18.91 d	23.28 e
	BlackCC	City	336.34 b	1.62 abc	21.16 c	23.68 b	20.21 bc	24.37 b
		Rain	254.04 bc	1.67 ab	21.86 b	24.18 a	20.68 ab	24.91 a
	Clear	City	159.97 d	0.92 d	21.26 c	23.22 cd	20.26 bc	23.63 d
		Rain	257.36 bc	1.52 bc	21.14 c	22.86 e	20.11 c	23.32 e
	ClearCC	City	128.79 d	1.01 d	21.75 b	23.34 c	20.12 c	23.32 e
		Rain	164.17 d	1.18 cd	22.33 a	23.36 c	21.13 a	23.32 e
	Bare	City	154.39 d	0.86 d	20.19 d	24.17 a	18.60 d	23.78 cd
		Rain	229.81 c	1.24 c	20.14 d	23.95 a	18.77 d	23.99 c
	Veg	City	3.67 e	0.02 e	18.93 e	23.00 de	17.40 e	22.95 fg
		Rain	0.02 e	0.01 e	18.46 f	22.91 e	17.52 e	23.07 ef
	Mulch		<0.0001	<0.0001	<0.0001	<0.0001	<0.0001	<0.0001
	Water		0.3362	0.0576	0.4223	0.536	0.0465	0.0005
	Mulch x Water		0.0718	0.4984	0.0068	0.0005	0.1936	0.0058
2015	Black	City	355.07 a	2.44 a	21.47 c	25.27 c	19.42 b	26.19 cd
		Rain	366.62 a	2.61 a	21.76 b	25.56 d	19.83 a	26.01 d
	BlackCC	City	188.30 b	1.35 b	21.19 d	25.39 d	19.33 b	26.34 bc
		Rain	189.44 b	1.40 b	22.07 a	26.09 a	19.86 a	26.69 a
	Bare	City	233.12 b	1.40 b	20.58 f	25.76 b	18.42 d	26.42 b
		Rain	165.00 c	1.16 b	20.86 e	26.09 a	18.36 c	26.81 a
	Mulch		<0.0001	0.0005	<0.0001	<0.0001	<0.0001	<0.0001
	Water		0.4989	0.7832	<0.0001	<0.0001	<0.0001	0.024
	Mulch x Water		0.4255	0.5528	0.0013	<0.0001	0.8614	0.0093

[a] Values within mulch, water followed by the same letter are not significantly different according to Fisher's LSD (P=0.1). †ES and LS were characterized by diurnal soil temperature in specific early and late spring.

Yield differences for the two water types are likely attributable to water temperature effects on soil temperature. Average temperature for all water types in 2011, 2013 and 2015 are given in Figure 30. During the *ES* period, the average temperature of the city water was significantly higher than rainwater stored in the solar tank (1.4°C in 2011, 3.7°C in 2013 and 1.7°C in 2015), but similar to that in gravity tank within 0.6°C. While in *LS*, the average temperature of rainwater from the gravity tanks was still consistently higher than that in solar tank by 1.1°C, while the temperature of city water was significantly lower than the water in the solar tank by 2.5°C in 2011 and 1.9°C in 2013. Due to some erroneous readings of thermistors placed into both city water and rainwater, water temperature datasets of 2015 *LS* datasets were not included in this discussion. The solar pump tanks were on the south side of the HTs and were exposed to more solar radiation than the gravity tanks which were located on the east and west side of the HTs. This could have been a factor causing warmer rainwater temperatures in the solar tanks; but, results show that rainwater stored in the solar tanks was always lower than that in the gravity tanks. The most likely reason was that the solar pump tanks had contact with soil surface causing conductive heat loss from the storage tank to the ground surface; whereas the gravity tanks were elevated off the ground in order to develop gravity pressure for irrigation. The city water was delivered several feet underground where soil temperatures are fairly stable (18.3°C in *ES* and 21°C in *LS*). The ground surface is colder in winter and warmer in summer than deeper in the soil where the city line is located therefore city water was warmer than stored rainwater toward winter and colder toward summer. To summarize the temperature of city water was higher than rainwater stored in either solar or gravity tanks in *ES*; while in *LS* during warmer weather, the rainwater temperatures in tanks increased quickly achieving a significant higher values rather than city water.

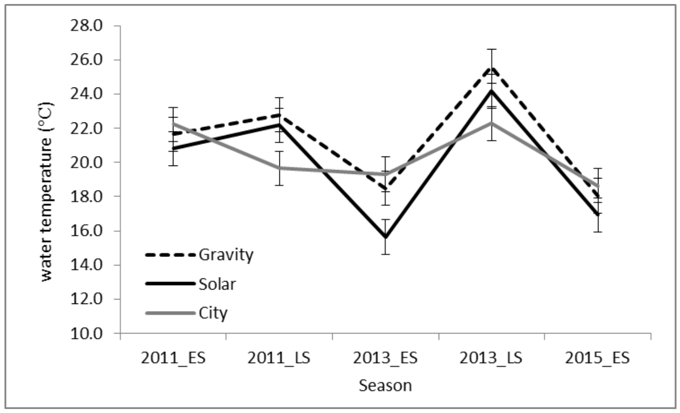

Figure 30. Fluctuations in average water temperature for three spring seasons of year 2011, 2013 and 2015. *Gravity* and *Solar* represent the rainwater inside the gravity and solar tanks, respectively, and *City* represents the municipal water from the underground pipes. *ES* means early spring and *LS* means late spring.

Just as water temperatures were different between the *ES* and *LS* seasons, soil temperatures responded in a similar manner since water was delivered directly to the ground surface through drip irrigation. Table 10 shows that rainwater generally produced warmer soil temperatures than city water during the entire spring season with several exceptions during the daytime for *veg* (*ES* 2011) and *clear* (*LS* 2013) mulch treatments; yet, rainwater treatment increased the fruit yield (by 64% for *clear* and 60% for *veg*). Also, the *bare* using rainwater was always warmer than that using city water, except the nighttime of *ES* 2011 when soil temperature in bare ground with city water was increased 1.5°C higher than that with rainwater leading to the slight yield improvement (17%) in the city water plots. In 2015, the pepper weight per plant in *bare* was about 41% higher by using the city resource, although the soil temperature was still higher (0.3°C) in rainwater plots. Also, biodegradable mulches *biobag* and *spun* usually had the similar performance to increase about 30% pepper weight in rainwater irrigated plots compared to that in city water plots, also likely due to the increased soil temperature by using rainwater stored in plots. Over the three years, *black* and *blackCC* mulches showed no significant difference for yield production using either rainwater or city water. In summary, rainwater was generally warmer than city water except in the cold *ES* seasons, and in general raised the soil temperatures by 0.3-0.8°C compared to the plots irrigated using city water. The response of different mulches to water is not that strong, but with several exceptions, results show that overall pepper yield was still increased by using rainwater as compared with city water.

Conclusions

HTs combined with the use of surface mulches and the row cover are relatively low-cost practices for enhancing crop growth, extending growth season, and assisting producers in maximizing profits with intensive production systems. The demand and adoption of HTs is high not only in the United States, but worldwide, due to the considerable benefits of environmental protection these structures provided during cool growing seasons. The three years of experiments demonstrated that HTs have the potential ability to accelerate pepper growth and improve overall crop production caused by the positive modification, such as, increased warming of inside air, canopy and soil temperature during the day and night compared to the outdoor temperature. HTs can also alleviate adverse effects of wind on crop growth. However, the level of inner microclimatic modification can vary depending on cloud cover, outside wind conditions, and how far the tunnel doors were opened.

Surface mulch had an effect on soil temperature, which influenced the crop growth performance and overall production. The extent of increase in soil temperature greatly depended on the color of plastic mulch: black and clear mulch tended to have the highest pepper yield– likely due to the increased soil temperature which was dependent on the amount of light energy the plastic mulch absorbed and/or transmitted to the soil. Clear plastics can produce the warmest soil conditions; thus, they are commonly employed in cooler climatic regions of the United States. The use of clear mulch is not recommended without precaution because plants located near holes inserted in the mulches can be exposed to an extremely high temperature when ventilation is inadequate.

In addition, clear mulch allows light onto the soil surfaces that promote weed growth under the mulch, which can compete with the crop. It is safer to use the black plastic mulch which has less potential ability to overheat the plants as the soil warms under the mulch. The black biodegradable *Biobag* and *Spunbond* mulches did not warm the soil to the same extent as the black polyethylene mulch; but, the marketable pepper yield was not statistically different between the biodegradable and standard black polyethylene. Although standard plastic mulches incur removal and disposal costs, this labor cost of standard plastic mulches can be offset by the initial higher investment of bio-biodegradable mulches. Therefore, black standard plastic mulch is highly recommended to be used in HTs.

The cover crops incorporated into the soil under *black* or *clear* mulch significantly reduced the overall pepper marketable yield in the springs of 2013 and 2015 as compared with the non-cover crop treatments. Although, a positive effect of incorporating cover crop residue under plastic mulch was increased soil temperatures, which can accelerate the breakdown of organic matter into available nutrients. It is speculated that the process of breaking down this residue tied up soil nutrients early in the crop development. In comparison, vegetative mulch generated the coolest soil temperatures and competed with crops for nutrients and water resources. Although the vegetative mulch was cut down periodically, they still grew and competed with the crop like weeds and always produced the significantly lowest yield while the cooler soil temperature potentially inhibited nutrient release and root development. Thus, vegetative mulch can be a disadvantage when the soil must be warmed quickly during a relatively cool early spring period.

Row covers added protection from freezing during cold nights plus produced higher pepper yield than that without row covers. But black plastics with a row cover always had the least effect on soil temperature and yield compared to that without a row cover. This result indicates that black mulches can act alone without a row cover to have a positive effect on the soil temperature and crop development. Finally, irrigation water type under different mulches had mixed effects on pepper yield values. Rainwater was warmer than city water except in the cold early spring period, but it generally increased the soil temperature around 0.3-0.8°C. Although there were several exceptions when soil temperatures were higher using city water than rainwater, overall pepper yield was still increased by using rainwater as compared with city water. Therefore, rainwater irrigation is not just about saving water but about storing up a reserve of high quality water to warm the soil for increased crop production.

The practices tested in this study will improve the utility of high tunnels at producing high value crops in an extended growing season. Even though soil temperature and pepper yield were increased by black plastic mulch, row covers and rain water, it was observed that the growing season still could not be extended much further because night time air temperature was only a few degrees warmer inside the high tunnel as compared with outside. The addition of row covers only added about 1-3°C of additional protection from freezing events above that provided by the high tunnels. Greater thermal protection is needed to further extend the growing season of high tunnels if a costly source of external heat is to be avoided. Additional thermal mass to store excess day-time heat and additional insulation to retain that heat are a means to meet this goal. Both the thermal mass and the insulation will need to be inexpensive with low labor requirements to be successfully used in small to medium organic vegetable operations. Cover crops were added to this experiment as a means to improve soil health and reduce the impact of intense cropping in high tunnels. However, cover crop effect on soil properties that allow greater heat transfer to the soil is all that was pertinent to this study. Cover crops did increase soil temperature when incorporated but yield was reduced. Establishing the cover crops was difficult especially in the winter months and incorporation just prior to planting the crop seemed to reduce nutrient availability for the peppers. Intercropping could provide better timing for establishing the cover crop and a good rotation scheme could allow better break down of residue before the vegetable crop is planted. Improved or equal yield with incorporated cover crops could provide better heat transfer into the soil thus improving season extension for high tunnels.

Part 2. Fall lettuce of 2011, 2013 and 2014

Material and Methods

This same type of experimental HT and climatic instrumentation used in this study were all described in Part 1. Romaine Lettuce (‘*coastal star*’) was grown during the fall seasons of 2011, 2013 and 2014. Specifically, in fall 2011 there were six different surface mulches and two sources of irrigation water. The twelve treatments were replicated and randomized in all three HTs following a split-plot design. Figure 31 (a) shows that there were five surface mulches compared with a bare soil control: 1) biodegradable white spunbond film (*spun*), 2) vegetative mulch from a cover crop (*veg*), 3) black polyethylene (*black*), 4) biodegradable brown paper (*paper*), 5) biodegradable black biobag film (*biobag*). There were six beds in each HT and these six different mulches were randomly arranged in different beds. Each bed was 12.19 m long by 0.91 m wide with double rows planted. Lettuce transplants were spaced 0.46 m apart within each planting row and the double planting rows were spaced 0.3 cm apart. Each row was divided into four plots with 12 plants in each plot totaling 48 plants per row. Lettuces were transplanted on Sep 30, 2011 in half of each house (snapdragon flower were added in another half HT), and then harvested on Dec 7, 2011. Moreover, in fall 2013, Figure 31 (b) shows that there were a total of 24 treatments including two water resources, five surface mulches (*black*, *veg*, *blackCC*, *clearCC*, *clear*) and a bare ground control, with or without a row cover. All the treatments were replicated and randomized in three HTs following a split-split plot design. Row covers were typically used at nights when the inside minimum temperature dropped below the optimum growth temperature of the lettuce (7°C). Lettuces were transplanted in each HT on Oct 2, 2013, and harvested on Dec 4, 2013. Additionally, in fall 2014, Figure 31 (c) shows that there were a total of 12 treatments including two water resources (rainwater & city water), two surface mulches (*black* & *blackCC*) and a bare ground control, with or without a row cover. Rainwater was harvested using a system designed to direct water off the roofs, and then gutters direct the water into black polyethylene tanks that are sized to store 55 cm of water per square meter of HT surface area. Also, rainwater was applied to the vegetable crops by two methods: gravity pressure and solar power which was detailed described in Part 1. Depending on the time of year, if enough rain had not fallen to adequately replenish the tanks, city water was added to the tanks in measured amounts. All the treatments were replicated and randomized in three HTs following a split-split plot design, but soil temperatures were only measured where water from the solar tanks was applied (the middle HT). Lettuces and snapdragon flowers were transplanted in each half of the HT on Sep 29, 2014 and harvested on Dec 5, 2014. Therefore, a summary of the treatment changes over three falls include the black biodegradable mulches *biobag* and *spun* as well as a white biodegradable mulch *paper* being applied just one time as a part of 2011 pilot project. Vegetative mulch (*veg*) being used twice in 2011 and 2013, but removed from 2014 due to the continuously low crop production. Clear polyethylene (*clear*) and clear polyethylene with cover crops (*clearCC*) being applied once in 2013, but not applied in 2014. Black polyethylene with cover crops (*blackCC*) being applied twice in 2013 and 2014, while the black polyethylene mulch (*black*) with bare ground control (*bare*) all repeated three times in 2011, 2013 and 2014.

The experiments in this study was also a randomized complete block design (RCBD) to determine statistical differences, based on a split-split-plot sub-design for lettuce marketable production and temperature changes. Lettuce yield was determined regarding plant weight per plant (g/plant) and plant number per plot (#/plot). Climatic analysis was divided into two periods including the early fall (*EF*) and late fall (*LF*), and analyses of yield values and temperatures were performed by SAS statistical software to determine differences between various treatments, as well as their interaction (SAS Institute Inc., Cary, NC).

Figure 31. The lettuce production of HTs in 2011, 2013 and 2014 followed by a split-split-plot design. In fall 2011, mulch treatment laid out through row 1 to row 6, including (1) black biodegradable spunbond (*spun*), (2) vegetative mulch from a cover crop (*veg*), (3) bare ground (*bare*), (4) black polyethylene film (*black*), (5) biodegradable brown paper (*paper*), and (6) black biodegradable biobag (*biobag*). In fall 2014, the mulch distribution followed by (1) black polyethylene film (*black*), (2) vegetative mulch from a cover crop (*veg*), (3) bare ground (*bare*), (4) black polyethylene film with a cover crop (*blackCC*), (5) clear polyethylene film with a cover crop (*clearCC*), and (6) clear polyethylene film (*clear*). In fall 2014, anothor crop snapdragon flower was added. Thus, the mulch treatments for lettuce were just laid out in three rows, incldluing (1) black polyethylene film (*black*), (2) bare ground (*bare*), and (3) black polyethylene film with a cover crop (*blackCC*). Also, two different water types for HT irrgation (rainwater and city water) were randomly arranged among the surface mulches through all three fall seasons of 2011, 2013 and 2014. In addition, over the fall 2013 and 2014, a floating row cover was put on half of each high tunnel covering half a length of the mulch rows at nights as an extra protection. All the treatments regarding water and surface mulch with or without a row cover were also arranged randomly in two other HTs at the UT site.

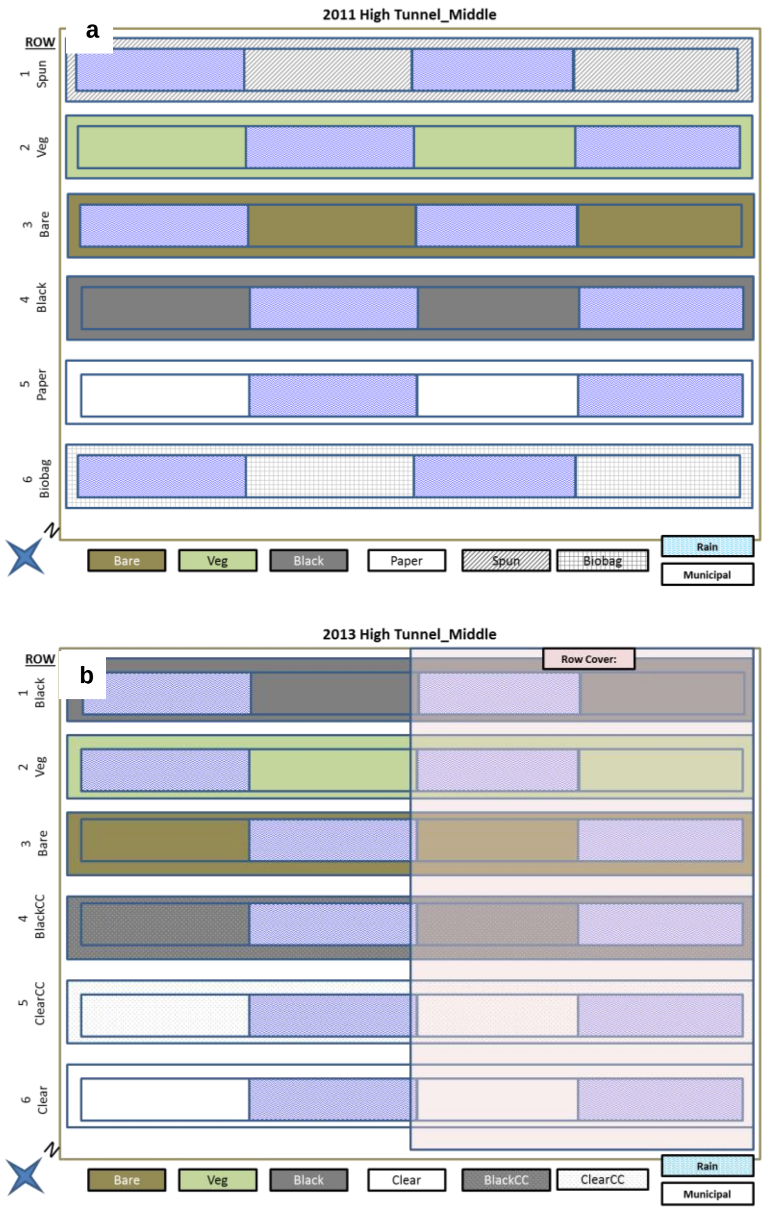

Figure 31 continued.

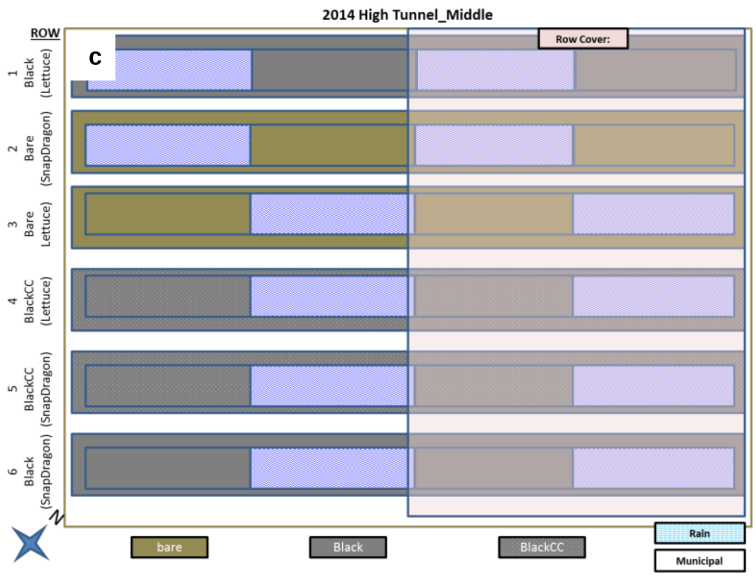

Figure 31 continued.

Results and Discussion

The protected HT affected inside microclimate in terms of solar radiation, air and soil temperature as well as wind speed and relative humidity. A total of 1380 solar radiation observations were measured over the span of three falls of 2011, 2013 and 2014. Generally, 9% of total solar radiation was reflected by the HT's polyethylene covering (dataset in 2011 was disregarded due to sensor failure). During the *EF* with the end-doors and side-curtains fully opened, inside air temperatures were consistently higher by 0.5-6.0°C as compared to outside; while in *LF* with the side curtains rolled down, daily maximum air temperature inside was raised from 1 to 11°C as compared with the outdoor conditions, depending on cloud cover, ambient wind conditions, and how far the tunnel sliding doors were opened. In addition, the comparison of shielded outside and shielded inside thermistor readings shows that HT night time air temperatures were 0.6-2.0°C higher than outdoor temperatures, and the average soil temperature inside the HTs at night was 1-3°C higher than field temperatures of bare ground over the span of the three falls.

Statistically, mulch treatments were the main contributing factor to the lettuce productivity in the falls of 2011, 2013 and 2014 ($p<0.001$) (Figure 32). In 2013 and 2014, *black* consistently produced higher yield than bare soil with an increase of 71% (2013) and 37% (2014) in g/plant. But there was no significant difference on lettuce production between using *black* and *bare* plots in 2011. *Clear* mulch also produced the highest yield in g/plant in 2013 but with no significant difference compared to that in *black*. Colored polyethylene mulches had a positive effect on soil temperature, which is related to marketable production in most cases (Table 11). Compared with *bare*, the increased crop yield using *black* was related to its soil-warming ability. Although some temperature values were missing due to sensor failures in *LF* 2011, average soil temperatures under *black* were consistently greater than that in *bare* by 0.8-1.3°C (2011), 0.6-0.9°C (2013) and 0.9-1.3°C (2014). The temperature raises under black mulch can promote faster lettuce growth and development, although the lettuce survival (#/plot) with *black* was reduced approximately 20% than *bare* in 2013. *Clear* also has great soil-warming ability, even higher than that under *black* by as much as 1.0°C. Although *clear* retained a warmer microclimate underneath than *black*, the overall lettuce yield did not improved significantly in spring 2013. This is probably due to poor weed control under *clear* resulting in competition for water and nutrients between the weeds and the crop. Also, when first transplanted to HTs in *EF*, warmer soil temperatures were produced by 1.4°C (day) and 2.1°C (night) for *clear* and 0.6°C and 0.9°C for *black* when compare to the bare ground. This thermal stress might not be beneficial on lettuce survival since the plants numbers per plot were significantly reduced in *clear* (10%) and *black* (20%) plots as compared with bare ground.

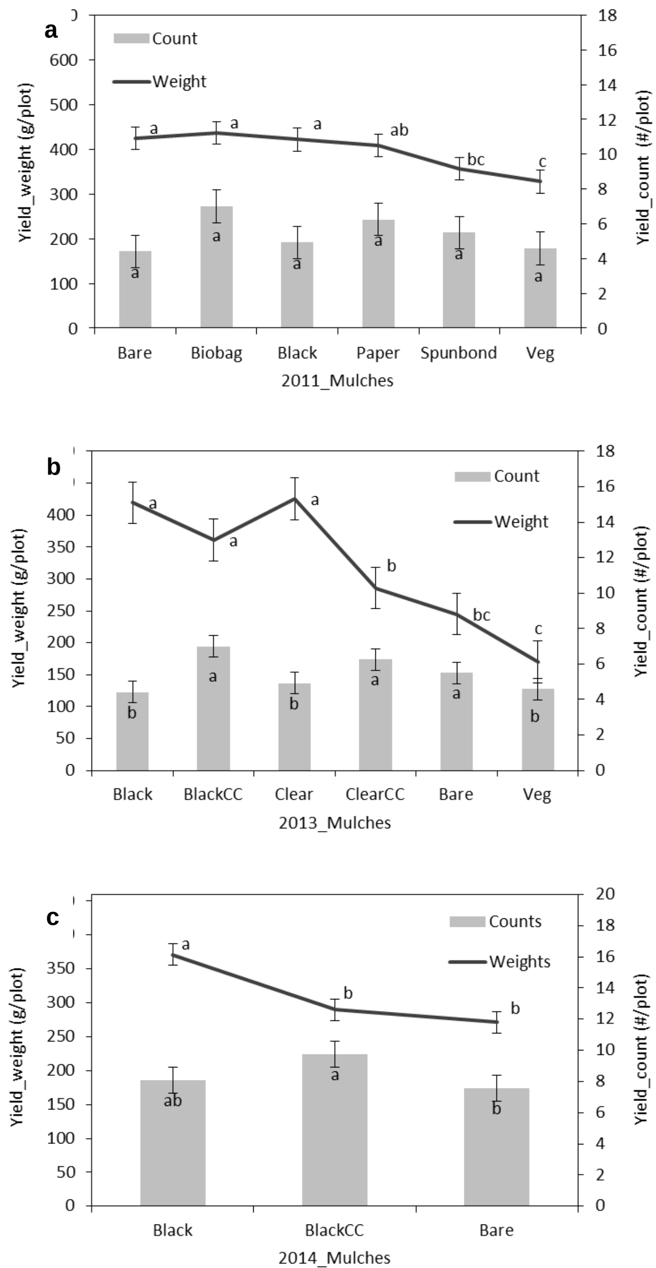

Figure 32. Marketable lettuce weight per plant and lettuce numbers per plot under the effects of different mulch over fall seasons of the year 2011 (a), 2013 (b) and 2014 (c) in high tunnels. Treatments include black biodegradable spunbond (*spun*), vegetative mulch from a cover crop (*veg*), bare ground (*bare*), black polyethylene film (*black*), clear polyethylene film (*clear*), black biodegradable biobag (*biobag*), black plastic mulch (*black*), black plastic mulch with cover crops (*blackCC*), clear plastic mulch with cover crops (*clearCC*) and brown biodegradable paper (*paper*). Values followed by the same letter are not significant different according to Fisher's *LSD* (p=0.1).

Table 11. Marketable lettuce weight per plant and lettuce numbers per plot as well as average soil temperatures at 10cm deep under different mulch treatments during the day and night in early and late fall of 2011, 2013 and 2014. Mulch systems include biodegradable black biobag (*biobag*), biodegradable black spunbond (*spun*), biodegradable brown paper (*paper*), black plastic with (*blackCC*) or without cover crops (*black*), clear plastic with (*clearCC*) or without cover crops (*clear*), vegetative mulch (*veg*) and bare ground (*bare*); *EF* and *LF* were characterized by diurnal soil temperature in specific early and late spring. Temperature values are daily means from 10:00 am to 16:00 pm and nightly means from 21:00pm to 8:00am. Values followed by the same letter are not significantly different according to Fisher's LSD (P=0.1).

Year	Mulch	Lettuce Yield		SoilTemp_day		SoilTemp_night	
		Weight	Count	EF†	LF†	EF†	LF†
		(g/plant)	(#/plot)	(°C)		(°C)	
2011	Black	421.6 a	7.7 a	18.22 a	-	14.42 a	15.39 a
	Biobag	436.9 a	8.3 a	17.12 b	-	13.26 c	14.17 c
	paper	409.1 ab	8.7 a	16.68 bc	-	-	-
	Spunbond	355.7 bc	9.3 a	16.21 c	-	13.01 d	13.99 d
	Bare	424.2 a	9.2 a	17.06 b	-	13.59 b	14.13 cd
	Veg	327.5 c	9.2 a	17.06 b	-	12.96 d	13.52 d
	Sig.level	*0.0311*	*0.73*	*0.0115*	-	*<0.0001*	*<0.0001*
2013	Black	419.4 a	4.4 b	19.97 c	14.12 b	19.74 c	14.31 e
	BlackCC	361.4 a	7.0 a	20.08 c	14.18 b	20.52 b	14.66 b
	Clear	425.8 a	4.9 b	20.80 b	14.20 b	20.86 b	14.66 b
	ClearCC	285.6 b	6.3 a	21.47 a	14.69 a	21.81 a	15.02 a
	Bare	244.9 bc	5.5 a	19.41 d	13.26 d	18.82 d	13.43 e
	Veg	170.4 c	4.6 b	19.22 e	13.01 d	18.36 d	13.28 e
	Sig.level	*<0.0001*	*<0.0001*	*<0.0001*	*<0.0001*	*<0.0001*	*<0.0001*
2014	Black	371.1 a	8.1 ab	18.38 a	13.07 a	19.48 a	13.86 a
	BlackCC	290.0 b	9.8 a	18.24 b	12.97 a	19.32 a	13.76 a
	Bare	271.2 b	7.6 b	17.30 c	12.12 b	18.16 b	12.86 b
	Sig.level	*<0.0001*	*0.1765*	*<0.0001*	*<0.0001*	*<0.0001*	*<0.0001*

Moreover, the use of the black biodegradable mulch *biobag* and brown biodegradable mulch *paper,* were not significantly different when compared to *black* for lettuce yield in 2011. However, white *spunbond* produced less marketable lettuce weight per plant by 13% than *paper*, but the difference in #/plot was not at a significant level. All of the degradable mulch plots produced significantly cooler soil temperatures than *black* by 1-1.2°C (*biobag*), 1.4-2.0°C (*spunbond),* and approximately 1.6°C (*paper*). The greater reduction of soil temperatures produced by *spunbond* (1.4-2.0°C) compared to that of *biobag* and *paper* mulch may be the reason for significantly decreased lettuce production under *spunbond* when compared to *black*.

Moreover, polyethylene mulch with cover crops (*blackCC* & *clearCC*) had the potential to save more lettuce heads in each plots by 21%-60% (#/plot). Probably because more air can penetrate through the cover crop residual, and thus the thermal stress from the plastic mulch surface would be mitigated when the film edges contacting to the lettuce transplants in the warm *EF* period. But these plastic mulch with cover crops can significantly reduce marketable lettuce weight per plant (18% in *blackCC* and 33% in *clearCC*), as compared with non-cover crop treatments as an average of 2013 and 2014. A positive effect of incorporating cover crop residue under plastic mulch was higher soil temperature which could increase breakdown of organic matter into available nutrients (except the *blackCC* in 2014). Specifically, average soil temperature under *blackCC* in *EF* and *LF* of 2013 was around 0.3-0.8°C higher than that under *black* at night*,* while the difference between *clearCC* and *clear* was 0.5-0.7°C and 0.3-0.9°C during the day and night, respectively. Thus, although the cover crops had a higher soil-warming ability to save more lettuce in each plot, it appears that limited nutrient availability provided by cover crop residues inhibited the growth of each lettuce head when cover crops were incorporated without supplemental organic fertilizer. In comparison, the *veg* mulch treatment always significantly produced the lowest lettuce yield. The major concern with using the vegetative mulch is that it cooled the soil to a point where crop growth may have been detrimentally delayed. Results confirmed that in the *veg* mulch, there was a significant reduction of soil temperature (0.6°C in 2011 and 0.3°C in 2013) than that in bare ground. Although the vegetative mulch was cut down periodically, they still grew and competed with the crop and always significantly produced the lowest yield while the cooler soil temperature potentially inhibited nutrient release and root development. Therefore, *veg* mulch with the coolest soil temperature was working against a goal of making better use of solar energy to extend the growing period beyond the normal growing season.

For the late fall period, row covers provided additional thermal protection for lettuce (Figure 33). Result shows that row covers were the important contributing factor to improve the overall marketable production (only in g/plant) of 2014 ($p<0.0001$): lettuce weight per plant using a row cover increased approximately 36% as an average of all treatments (*black*, *blackCC* and *bare*) compared to that without a row cover. Also in fall 2013, there were positive interactions between surface mulch and the row cover application on lettuce production ($p<0.1$): *black* mulch produced the highest yield when comparing the mulch treatments without row covers. With a row cover, the *black* mulch significantly increased lettuce weight per plant by 28% as compared with that without a row cover, and approximately 45% and 73% more lettuce weight per plant were significantly produced by using a row cover under *bare and veg*, respectively than that without using a row cover. Moreover, *blackCC*, *clear* and *clearCC* using a row cover had the potential to improve the total crop production compared with not using a row cover in spring 2013, but the improvement was not at a significant level. All the increases of lettuce yield from row covers were probably related to an increase in soil and canopy temperatures. Canopy and soil temperatures under a row cover were significantly increased from 0.8 to 2.3°C in the canopy and from 0.1 to 0.9°C in the soil at night. Although soil temperature increases from row covers interacted differently with the mulch treatments: 0.4°C in *black*, 0.6°C in *blackCC*, 0.1°C in *clear*, 0.8°C in *clearCC*, 0.7°C in *bare* and 0.2°C in *veg*, row covers had a positive effect on lettuce production in all plots with row covers.

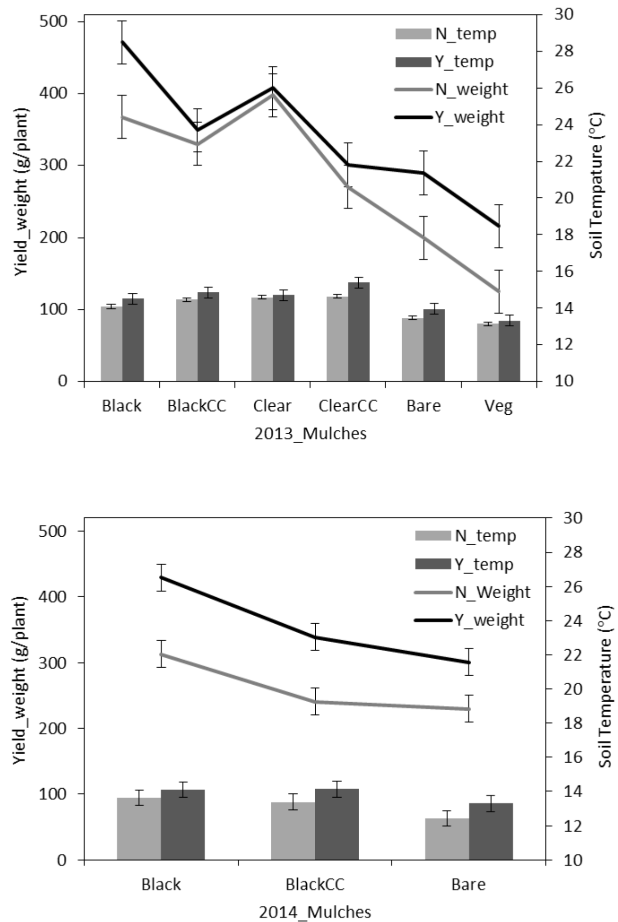

Figure 33. Interactions of mulch and row cover on lettuce yield (weight/plant) and soil temperature (°C) inside high tunnel during the late fall of 2013 and 2014. '*Y*' represents the mulch with row cover and '*N*' means the mulch without row cover.

Finally, lettuce yield was improved by using city water as compared to rainwater applied with drip irrigation (Figure 34). As an average of all mulches, city water increased the total lettuce weight per plant by 16% in 2011, 12% in 2013 and 8% in 2014, and also significantly increased total lettuce numbers per plot by 13% in 2013 (Table 12). Although the numeric values of lettuce number per plot were potentially higher by using city water than rainwater, but the differences is not on a significant level. Moreover, in 2011, the *biobag* mulch and *bare* ground irrigated using city water significantly improved lettuce weights by 23% and 36%, respectively compared to rain water ($p<0.0001$), although in subsequent years, city water did not significantly increase yield in bare soil treatment. In 2013, *black* and *veg* mulch yield was significantly increased when city water was used for irrigation by 36% and 20% in lettuce weight per plant, respectively; and while in 2014, black mulch with city water also significantly improved the lettuce production approximately by 17% (g/plant) over rainwater. Yield differences for the two water types were assumed to be explained by water temperature effects on soil temperature. Figure 34 shows that the average temperature of rainwater from the gravity tanks was consistently higher than that in solar tank. Also, in the early fall of 2011, 2013 and 2014, the average temperature of city water was significantly lower than the water in the solar tank by 2.4°C. But during the *LF* periods, the average temperature of the city water was significantly higher than rainwater stored in the solar tank (2.2°C in 2011, 1.3°C in 2013 and 0.8°C in 2014). Although water temperatures changed differentially between the early and late fall seasons, soil temperatures responded in a similar manner over different mulches. Table 12 shows that city water can generally produce warmer soil temperature than rainwater during the entire fall seasons with several exceptions in 2011 (*biobag*, *spunbond* and *bare* ground), but all these variations cannot change the fact of greater lettuce production in city water plots (23% for *biobag*, 13% for *spunbond* and 35% for *bare*). In summary, city water was warmer than rain water except in the early fall, and in general city water can raise the soil temperatures by 0.2-0.8°C. The response of different mulches to water shows that overall lettuce yield can be increased by using city water as compared with rain water. Another reason for increased lettuce production using city water may be related to water quality. The pH of city water was consistently around 6.4, while the rain water changed over time, but mainly was around at 6.7 to 7. Also city water generally provided more nutrients than rain water, around 11 to 16 times higher levels of K, Mg, and Ca which may promote lettuce growth and development.

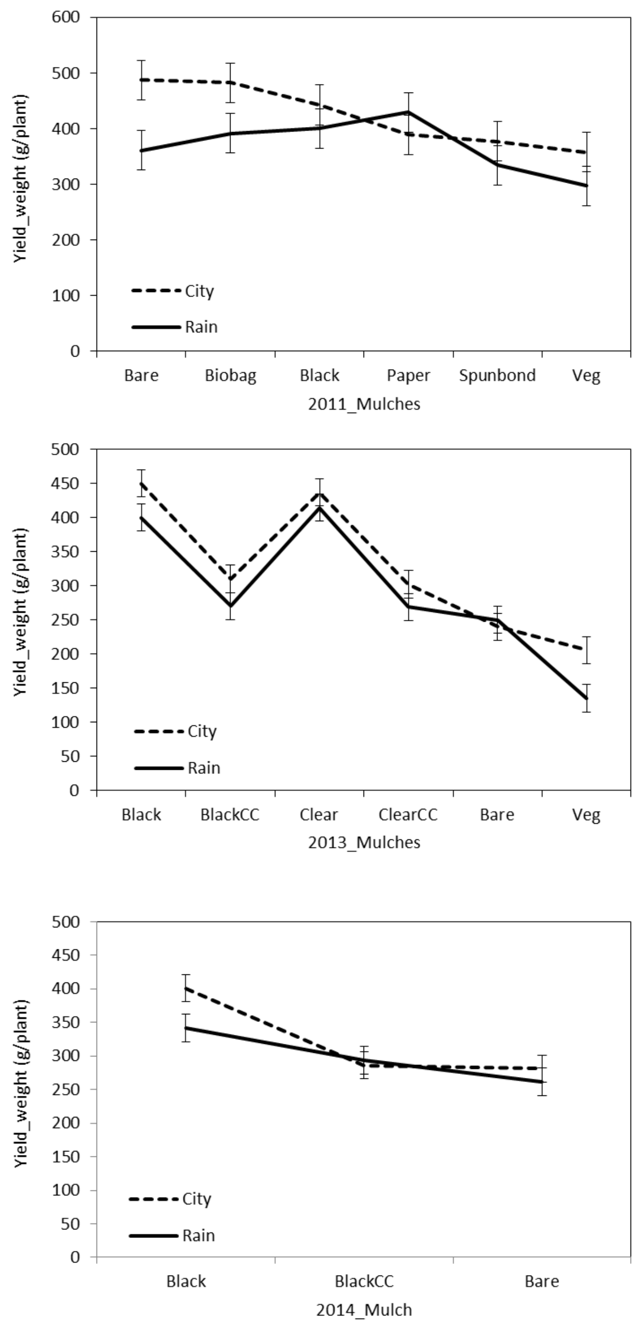

Figure 34. Marketable weight of lettuce (mean ± SE) under the effects of different irrigation water (rain & city) over fall seasons of the year 2011(a), 2013(b) and 2014 (c) in high tunnels. Treatments include biodegradable black biobag (*biobag*), biodegradable black spunbond (*spun*), biodegradable brown paper (*paper*), black plastic with (*blackCC*) or without cover crops (*black*), clear plastic with (*clearCC*) or without cover crops (*clear*), vegetative mulch (*veg*) and bare ground (*bare*);

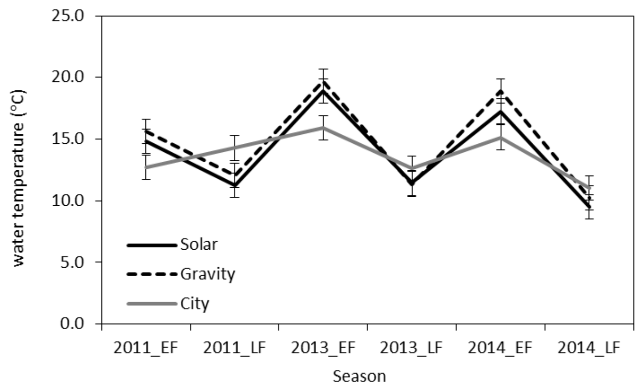

Figure 35. Fluctuations in average water temperature (mean ± SE) for three falls of year 2011, 2013 and 2014. *Gravity* and *Solar* represent the rainwater inside the gravity and solar tanks, respectively, and *City* represents the municipal water from the underground pipes. *EF* means early fall and *LF* means late fall.

Table 12. Interactions of mulch and water on the lettuce yield and soil temperature inside high tunnel during all three falls of year 2011, 2013 and 2014.

Year	Mulch		Water	Lettuce Yield		Soil Temp_day		Soil Temp_night	
				Weight	Count	EF†	LF†	EF†	LF†
				(g/plant)	(#/plot)	(°C)		(°C)	
2011	Black		City	442.67 abc	10.00 a	18.37 a	-	14.44 a	15.45 a
			Rain	400.58 bcd	7.33 ab	18.07 ab	-	14.40 a	15.34 a
	Biobag		City	482.52 ab	8.67 ab	16.94 bcd	-	13.10 fg	13.83 e
			Rain	391.33 cd	8.00 ab	17.30 abc	-	13.42 def	14.52 bc
	Paper		City	388.67 cd	9.67 ab	16.80 bcd	-	13.48 cde	14.53 bc
			Rain	429.50 abc	9.00 ab	16.56 c	-	-	-
	Spunbond		City	377.33 cde	8.33 ab	15.90 d	-	12.87 g	13.77 e
			Rain	334.00 de	10.00 a	16.53 c	-	13.15 efg	14.21 d
	Bare		City	487.33 a	8.33 ab	17.11 bc	-	13.19 efg	13.79 e
			Rain	361.04 cde	7.0 b	17.01 bc	-	13.99 b	14.48 c
	Veg		City	357.69 cde	9.00 ab	17.34 abc	-	13.61 cd	14.72 b
			Rain	297.33 e	9.00 ab	16.78 bcd	-	13.78 bc	14.55 bc
		Mulch		*0.0311*	*0.73*	*0.0115*	-	*<0.0001*	*<0.0001*
		Water		*0.0158*	*0.38*	*0.8917*	-	*0.0018*	*<0.0001*
		Mulch x Water		*0.3177*	*0.59*	*0.5621*	-	*0.0678*	*<0.0001*
2013	Black		City	450.0 a	5.17 bcd	20.15 c	14.28 c	20.04 cd	14.57 d
			Rain	400.0 a	3.67 d	19.79 d	13.97 d	19.43 ef	14.04 e
	BlackCC		City	310.3 abc	8.00 a	20.09 c	14.16 c	20.48 c	14.64 cd
			Rain	270.0 ab	6.00 cd	20.07 c	14.20 c	20.57 c	14.68 cd
	Clear		City	437.0 a	5.00 bcd	20.83 b	14.24 c	21.23 b	14.74 c
			Rain	414.7 a	4.8 bc	20.77 b	14.16 c	20.49 c	14.57 d
	ClearCC		City	302.2 bcd	6.17 bc	21.54 a	14.80 a	21.78 ab	15.10 a
			Rain	269.0 cd	6.33 bc	21.40 a	14.59 b	21.83 a	14.93 b
	Bare		City	239.7 de	6.50 ab	19.46 ef	13.48 e	18.97 fg	13.57 g
			Rain	250.1 cd	6.50 ab	19.35 f	13.03 g	18.68 g	13.29 h
	Veg		City	205.6 de	4.83 cd	19.63 de	13.86 d	19.62 de	13.88 f
			Rain	135.0 e	4.33 d	18.81 g	13.28 f	19.33 ef	13.80 f
		Mulch		*<0.0001*	*<0.0001*	*<0.0001*	*<0.0001*	*<0.0001*	*<0.0001*
		Water		*0.3362*	*0.0576*	*0.0002*	*<0.0001*	*0.1511*	*<0.0001*
		Mulch x Water		*0.0718*	*0.4984*	*0.005*	*<0.0001*	*0.2181*	*0.0023*
2014	Black		City	400.9 a	8.83 ab	18.51 a	13.17 a	19.62 a	13.98 a
			Rain	341.3 b	7.33 ab	18.26 b	12.96 b	19.34 b	13.74 b
	BlackCC		City	286.2 c	10.17 a	18.24 b	12.97 b	19.36 b	13.78 b
			Rain	293.8 c	9.33 ab	18.24 b	12.98 b	19.27 b	13.74 b
	Bare		City	281.0 c	6.00 b	17.49 c	12.25 c	18.18 c	12.89 c
			Rain	261.4 c	5.6 ab	17.11 d	11.98 d	18.13 c	12.82 c
		Mulch		*<0.0001*	*0.1765*	*<0.0001*	*<0.0001*	*<0.0001*	*<0.0001*
		Water		*0.12*	*0.9542*	*0.0021*	*0.0072*	*0.0954*	*0.0192*
		Mulch x Water		*0.1956*	*0.2697*	*0.0587*	*0.0893*	*0.4201*	*0.217*

Values within mulch, water followed by the same letter are not significantly different according to Fisher's LSD (P=0.1). EF† and LF† were characterized by nighttime soil temperature in specific early and late fall.

Conclusions

The three-year experiments demonstrated that HTs combined with the use of surface mulches and the row cover as well as different irrigation water can be expected to have significant effects on soil temperature, which influenced lettuce growth and development. The mulches had significant effects on soil temperature, which was related to marketable lettuce production over the fall of 2011, 2013 and 2014. *Clear* and *black* plastics all have good soil-warming ability, thus produced the most lettuce weights. But, the thermal stress with higher soil temperature produced in *clear* and *black* plastics may cause significant lettuce reduction on plant numbers per plot when compare to the bare ground. The biodegradable *biobag*, *spunbond* and *paper* mulches did not heat the soil as much as the *clear* or *black* mulch, but the marketable lettuce yields produced by *biobag* and *paper* mulches were not statistically different than the standard *black* polyethylene. Only *spunbond* reduced the overall yield by 20% in g/plant compared to *black* mulch. In addition, the cover crops incorporated into the soil under *black* or *clear* mulch had the potential to save more lettuces plants in each plots, but overall lettuce weight per head was reduced significantly as compared with the non-cover crop treatments, even though a positive effect of incorporating cover crop residue under plastic mulch was increased soil temperature. Moreover, vegetative mulch generated the coolest soil temperatures, and consistently produced the lower lettuce yield which is not recommended to be applied in HTs. Additionally, row covers added protection during cold nights in late fall (0.8 to 2.3°C in the canopy and 0.1 to 0.9°C in the soil), and thus produced higher lettuce yield than that without row covers. Finally, city water was warmer than rain water except in the early fall period, and it generally increased the soil temperature around 0.2-0.8°C compared to the rainwater plots. Although there were several exceptions when soil temperatures were higher using rainwater than city water, overall lettuce yield was still increased by using city water. Also, city water generally provided more nutrients than rainwater in terms of K, Mg, and Ca which may promote lettuce growth and development. Therefore, city water irrigation may not just be about warming the soil but also provides more nutrients for increased lettuce production.

Chapter 5
Conclusions and Future Work

This study developed an energy balance method to simulate the heat exchange mechanisms between the inside and outside of a HT in order to estimate the ventilation rate. The simulated ventilation rate was then compared to measured air velocity multiplied by the cross-sectional area to determine the incoming air-flux using both a 2D sonic anemometer and a hot-wire anemometer. Result shows that the ventilation rate calculated by energy balance model was as high as 12 m^3s^{-1}, and there was a good agreement between the ventilation rate estimated by the energy balance model and the air-flux calculations based on air velocity measurements. In addition, an EBn model was derived to estimate either the ventilation rate (air flux) or the inside temperature from outside weather data by using the simplified relationships between inside and outside conditions. Although the result only concerns one specific experimental case, other HTs with similar size and ventilation system may also be successfully modeled. Also, advanced artificial neural networks can discover the best structure of the prediction models, like the number of hidden layer and neurons, and the significances of input parameters. Results show that the average air temperature (Air_ave) from an array of 15 thermistors inside the HT was predicted more accurately by ANN than using the prediction of single inside temperature at the center of HT. Moreover, ANN input sensitivity was conducted revealing that relative humidity and wind direction had the least significant impact on the prediction of inside air temperature. The other four inputs were found to be sufficient for the ANN modeling with the ranked importance as follows: outside air temperature, vent opening level, solar radiation and wind speed. The performance of ANN was compared with a theoretical model on ventilation prediction, and results suggest that the ANN model was more accurate than the mathematical model. Further work is needed to address more training datasets to increase the model stability and accuracy with better architecture selection. Therefore, the ability to better estimate ventilation adjustments can improve the crop growth environment and save the cost of making additional ventilation adjustments throughout the day whether or not a human operator has the ability to adjust to all pertinent factors without quantifying them. The energy balance model needs to be applied to several different sizes and configuration of HTs in order to validate it as a useful prediction tool. Also, automation of the door opening with an inside temperature sensor powered by solar energy can be used in future research, to gather more training datasets for ANN models in a step ahead prediction of vent-opening. Thus, the potential of using this ANN model can play an important role in the ventilation design or at least provide an operational guide to producers on how to adjust their vents in advance to obtain an optimum air temperature based on public weather forecasts for 1 or 2hr time scale.

A three-year experiment demonstrated that the HT truly has the potential to accelerate pepper growth and improve overall crop production caused by positive modification, such as, increased warming of inside air, canopy and soil temperature compared to the outdoor temperature during the day and night. In addition to ventilation management, this study showed that HTs combined with the use of surface mulches, row cover, and irrigation water source can be expected to have a significant effect on soil temperature, which can influence the yield of different crops. Results show that black polyethylene mulch is highly recommended for pepper and lettuce production in high tunnels.

Unfortunately, the benefit of cover crop to improve soil healthy was not found in this study, although there was a positive soil temperature rise surrounding plant root-zones caused by cover crops. Furthermore, row covers continuously added protection from freezing during the cold nights resulting in a higher crop production. Stored rainwater was warmer than the city water except in the cold period of early spring or late fall, and rainwater irrigation is tended to increase the overall production of pepper but lettuce yielded better by using city water.

Even though soil temperature and pepper yield were increased by using different practices in an extended growing season, it was observed that the growing season still could not be extended much further because night time air temperature was only a few degrees warmer inside the high tunnel as compared with outside. The addition of row covers added about 2°C of additional protection in canopy temperature from freezing events above that provided by the high tunnels. Greater thermal protection is needed to further extend the growing season of high tunnels if a costly source of external heat is to be avoided. Additional thermal mass to store excess day-time heat and additional insulation to retain that heat are a means to meet this goal. Both the thermal mass and the insulation will need to be inexpensive with low labor requirements to be successfully used in small to medium organic vegetable operations. Cover crops were added to this experiment as a means to improve soil health and reduce the impact of intense cropping in high tunnels. However, cover crop effect on soil properties that allow greater heat transfer to the soil is all that was pertinent to this study. Cover crops did increase soil temperature when incorporated but yield was reduced. Establishing the cover crops was difficult especially in the winter months and incorporation just prior to planting the crop seemed to reduce nutrient availability for crops. Intercropping could provide better timing for establishing the cover crop and a good rotation scheme could allow better break down of residue before the vegetable crop is planted.

References

Abdel-Ghany, Ahmed M. (2011). Solar energy conversions in the greenhouses. Sustainable Cities and Society, 1(4), 219-226. doi: http://dx.doi.org/10.1016/j.scs.2011.08.002

Abdel-Ghany, AM, & Al-Helal, IM. (2011). Solar energy utilization by a greenhouse: General relations. Renewable Energy, 36(1), 189-196.

Arin, Levent, & Ankara, Sozer. (2001). Effect of low-tunnel, mulch and pruning on the yield and earliness of tomato in unheated glasshouse. J. Appl. Hort, 3(1), 23-27.

Baptista, FJ, Bailey, BJ, Randall, JM, & Meneses, JF (1999). Greenhouse Ventilation Rate: Theory and Measurement with Tracer Gas Techniques. Journal of Agricultural Engineering Research, 72(4), 363-374. doi: http://dx.doi.org/10.1006/jaer.1998.0381

Baxevanou, Catherine, Fidaros, Dimitris, Bartzanas, Thomas, & Kittas, Constantinos. (2010). Numerical simulation of solar radiation, air flow and temperature distribution in a naturally ventilated tunnel greenhouse. Agricultural Engineering International: CIGR Journal, 12(3-4), 48-67.

Baytorum,(1986). Bestimmung des Luftwechsels bei gelüfteten Gewächshäusern, Gartenbautechnische Informationen Heft 27, Institut für Technik in Gartenbau und Landwirtschaft, Universität Hannover 155pp.

Baytorun, N, Abak, K, Tokgöz, H, & Altuntas, Ö. (1993). Effect of different greenhouse covering materials on inside climate and on the development of tomato plants. Paper presented at the II Symposium on Protected Cultivation of Solanacea in Mild Winter Climates 366.

Bennett, A. J., Bending, G. D., Chandler, D., Hilton, S., & Mills, P. (2012). Meeting the demand for crop production: the challenge of yield decline in crops grown in short rotations. Biological Reviews, 87(1), 52-71.

Blomgren, Ted Alan, & Frisch, Tracy. (2007). *High Tunnels: Using Low Cost Technology to Increase Yields, Improve Quality, and Extend the Growing Season*: University of Vermont Center for Sustainable Agriculture.

Boulard, T, & Baille, A. (1995). Modelling of air exchange rate in a greenhouse equipped with continuous roof vents. Journal of Agricultural Engineering Research, 61(1), 37-48.

Boulard, T, Haxaire, R, Lamrani, MA, Roy, JC, & Jaffrin, A. (1999). Characterization and modelling of the air fluxes induced by natural ventilation in a greenhouse. Journal of Agricultural Engineering Research, 74(2), 135-144.

Boulard, T., Kittas, C., Papadakis, G., & Mermier, M. (1998). Pressure Field and Airflow at the Opening of a Naturally Ventilated Greenhouse. Journal of Agricultural Engineering Research, 71(1), 93-102. doi: http://dx.doi.org/10.1006/jaer.1998.0302

Boulard, T., Wang, S., & Haxaire, R. (2000). Mean and turbulent air flows and microclimatic patterns in an empty greenhouse tunnel. Agricultural and Forest Meteorology, 100(2–3), 169-181. doi: http://dx.doi.org/10.1016/S0168-1923(99)00136-7

Bot, Gerardus PA. (1983). Greenhouse climate: from physical processes to a dynamic model. Landbouwhogeschool te Wageningen.

Businger, JA. (1963). The glasshouse climate physics of plant environment. Ed. Van Wijk, North Publ. Co., Amsterdam, 270-318.

Campen, JB, & Bot, GPA. (2003). Determination of greenhouse-specific aspects of ventilation using three-dimensional computational fluid dynamics. Biosystems Engineering, 84(1), 69-77.

Chalabi, ZS, & Bailey, BJ. (1989). Simulation of the energy balance in a greenhouse. Divisional Note, AFRC Institute of Engineering Research (UK).

Conner, David S, Montri, Adam D, Montri, Dru N, & Hamm, Michael W. (2009). Consumer demand for local produce at extended season farmers' markets: guiding farmer marketing strategies. Renewable Agriculture and Food Systems, 24(04), 251-259.

Coombes, Peter J, & Barry, Michael E. (2007). The effect of selection of time steps and average assumptions on the continuous simulation of rainwater harvesting strategies. Water science and technology, 55(4), 125-133.

Crookston, RK, Kurle, JE, Copeland, PJ, Ford, JH, & Lueschen, WE. (1991). Rotational cropping sequence affects yield of corn and soybean. Agronomy Journal, 83(1), 108-113.

Dayan, Joshua, Dayan, E, Strassberg, Y, & Presnov, E. (2004). Simulation and control of ventilation rates in greenhouses. Mathematics and computers in simulation, 65(1), 3-17.

Demchak, Kathleen. (2009). Small fruit production in high tunnels. HortTechnology, 19(1), 44-49.

Demrati, H., Boulard, T., Bekkaoui, A., & Bouirden, L. (2001a). SE—Structures and Environment. Journal of Agricultural Engineering Research, 80(3), 261-271. doi: http://dx.doi.org/10.1006/jaer.2001.0740

Demrati, H., Boulard, T., Bekkaoui, A., & Bouirden, L. (2001b). SE—Structures and Environment: Natural Ventilation and Microclimatic Performance of a Large-scale Banana Greenhouse. Journal of Agricultural Engineering Research, 80(3), 261-271. doi: http://dx.doi.org/10.1006/jaer.2001.0740

Emmert, EM. (1956). Plastic row covering. Kentucky Farm and Home Science. Spring, 2(2), 6-7.

Fernandez, JE, & Bailey, BJ. (1992). Measurement and prediction of greenhouse ventilation rates. Agricultural and Forest Meteorology, 58(3), 229-245.

Ferreira, PM, Faria, EA, & Ruano, AE. (2002). Neural network models in greenhouse air temperature prediction. Neurocomputing, 43(1), 51-75.

Gleason, Mark Lawrence, & Edmunds, Brooke Aurora. (2005). Tomato diseases and disorders: Iowa State University, University Extension.

Gullino, M Lodovica, Albajes, Ramon, & van Lenteren, Joop C. (1999). Setting the stage: characteristics of protected cultivation and tools for sustainable crop protection Integrated Pest and Disease Management in Greenhouse Crops (pp. 1-15): Springer.

Gupta, Ajaya Kumar, & Moss, Peter James. (1993). Guidelines for design of low-rise buildings subjected to lateral forces: CRC Press.

Greer, Lane, & Dole, John M. (2003). Aluminum foil, aluminium-painted, plastic, and degradable mulches increase yields and decrease insectvectored viral diseases of vegetables. HortTechnology, 13(2), 276-284.

Ham, Jay M, Kluitenberg, GJ, & Lamont, WJ. (1993). Optical properties of plastic mulches affect the field temperature regime. Journal of the American Society for Horticultural Science, 118(2), 188-193.

Haykin, Simon, & Lippmann, Richard. (1994). Neural Networks, A Comprehensive Foundation. International Journal of Neural Systems, 5(4), 363-364.

Hinrichs, C Clare. (2003). The practice and politics of food system localization. *Journal of rural studies, 19*(1), 33-45.

Huff, Pete. (2015). Extending the Growing Season. Institute for Agriculture and Trade Policy.

Ibarra-Jiménez, L, Quezada-Martin, MR, & de la Rosa-Ibarra, M. (2004). The effect of plastic mulch and row covers on the growth and physiology of cucumber. Animal Production Science, 44(1), 91-94.

Iqbal, Qumer, Amjad, Muhammad, Asi, Muhammad Rafique, Ali, Muhammad Asif, & Ahmad, Riaz. (2009). Vegetative and reproductive evaluation of hot peppers under different plastic mulches in poly/plastic tunnel. Pak. J. Agri. Sci, 46(2), 113-118.

Jain, Dilip, & Tiwari, Gopal Nath. (2002). Modeling and optimal design of evaporative cooling system in controlled environment greenhouse. Energy Conversion and Management, 43(16), 2235-2250.

Jamaludin, Diyana, Ahmad, Desa, Kamaruddin, Rezuwan, & Jaafar, Hawa ZE. (2014). Microclimate inside a tropical greenhouse equipped with evaporative cooling pads. Pertanika Journal of Science & Technology, 22(1), 255-272.

Jensen, Merle H, & Malter, Alan J. (1995). *Protected agriculture: a global review* (Vol. 253): World Bank Publications.

Kacira, Murat, Sase, Sadanori, & Okushima, Limi. (2004). Effects of side vents and span numbers on wind-induced natural ventilation of a gothic multi-span greenhouse. Japan Agricultural Research Quarterly: JARQ, 38(4), 227-233.

Kadir, Sorkel, Carey, Edward, & Ennahli, Said. (2006). Influence of high tunnel and field conditions on strawberry growth and development. HortScience, 41(2), 329-335.

Kalogirou, Soteris A, & Bojic, Milorad. (2000). Artificial neural networks for the prediction of the energy consumption of a passive solar building. Energy, 25(5), 479-491.

Kalogirou, Soteris A. (2001). Artificial neural networks in renewable energy systems applications: a review. Renewable and sustainable energy reviews, 5(4), 373-401.

Kalogirou, S., Eftekhari, M., & Pinnock, D. (1999). Prediction of air flow in a single-sided naturally ventilated test room using artificial neural networks. Proceedings of Indoor Air, 99, 975-980.

Kapanen, Anu, Schettini, Evelia, Vox, Giuliano, & Itävaara, Merja. (2008). Performance and environmental impact of biodegradable films in agriculture: a field study on protected cultivation. Journal of Polymers and the Environment, 16(2), 109-122.

Karlen, D. L., Varvel, G. E., Bullock, D. G., & Cruse, R. M. (1994). Crop Rotations for the 21st Century. Advances in Agronomy, 53(C), 1-45. DOI: 10.1016/S0065-2113(08)60611-2

Kasirajan, Subrahmaniyan, & Ngouajio, Mathieu. (2012). Polyethylene and biodegradable mulches for agricultural applications: a review. Agronomy for Sustainable Development, 32(2), 501-529.

Katan, J. (1981). Solar heating (solarization) of soil for control of soilborne pests. Annual Review of Phytopathology, 19(1), 211-236.

Kelley, KW, Long, JH, & Todd, TC. (2003). Long-term crop rotations affect soybean yield, seed weight, and soil chemical properties. Field Crops Research, 83(1), 41-50.

Kendirli, Berna. (2006). Structural analysis of greenhouses: A case study in Turkey. Building and environment, 41(7), 864-871.

Khaoua, SA Ould, Bournet, PE, Migeon, C, Boulard, T, & Chassériaux, G. (2006). Analysis of greenhouse ventilation efficiency based on computational fluid dynamics. Biosystems Engineering, 95(1), 83-98.

Kindangen, Jefrey Ignatius. (1996). Artificial neural networks and naturally ventilated buildings: a method of predicting window size and location with subsequent effect on interior air motion using neural networks. Building research and information, 24(4), 203-208.

Kindelan, M. (1980). Dynamic modeling of greenhouse environment. Transactions of the ASAE, 23(5), 1232-1239.

Kirschbaum, M. U. (1995). The temperature dependence of soil organic matter decomposition, and the effect of global warming on soil organic C storage. Soil Biology and biochemistry, 27(6), 753-760

Kittas, C., & Bartzanas, T. (2007). Greenhouse microclimate and dehumidification effectiveness under different ventilator configurations. Building and Environment, 42(10), 3774-3784. doi: http://dx.doi.org/10.1016/j.buildenv.2006.06.020

Kittas, C, Draoui, B, & Boulard, T. (1995). Quantification of the ventilation of a greenhouse with a roof opening. Agricultural and Forest Meteorology (Netherlands).

Kittas, C, Katsoulas, N, & Baille, A. (2001). Influence of greenhouse ventilation regime on the microclimate and energy partitioning of a rose canopy during summer conditions. Journal of Agricultural Engineering Research, 79(3), 349-360.

Kittas, C., Karamanis, M., & Katsoulas, N. (2005). Air temperature regime in a forced ventilated greenhouse with rose crop. Energy and Buildings, 37(8), 807-812. doi: http://dx.doi.org/10.1016/j.enbuild.2004.10.009

Körner, Oliver, & Van Straten, G. (2008). Decision support for dynamic greenhouse climate control strategies. Computers and Electronics in Agriculture, 60(1), 18-30.

Kumar, V., Abdul-Baki, A., Anderson, J. D., & Mattoo, A. K. (2005). Cover crop residues enhance growth, improve yield, and delay leaf senescence in greenhouse-grown tomatoes. HortScience, 40(5), 1307-1311.

Lamont, William James. (2005). Plastics: Modifying the microclimate for the production of vegetable crops. HortTechnology, 15(3), 477-481.

Larkin, Robert P, & Honeycutt, C Wayne. (2006). Effects of different 3-year cropping systems on soil microbial communities and Rhizoctonia diseases of potato. Phytopathology, 96(1), 68-79.

Liakatas, A, Clark, JA, & Monteith, JL. (1986). Measurements of the heat balance under plastic mulches. Part I. Radiation balance and soil heat flux. Agricultural and forest meteorology, 36(3), 227-239.

Liebman, M, & Davis, AS. (2000). Integration of soil, crop and weed management in low-external-input farming systems. WEED RESEARCH-OXFORD-, 40(1), 27-48.

López, Alejandro, Valera, Diego Luis, & Molina-Aiz, Francisco. (2011). Sonic anemometry to measure natural ventilation in greenhouses. Sensors, 11(10), 9820-9838.

Lu, Tao, & Viljanen, Martti. (2009). Prediction of indoor temperature and relative humidity using neural network models: model comparison. Neural Computing and Applications, 18(4), 345-357.

Majdoubi, H, Boulard, Thierry, Fatnassi, Hicham, & Bouirden, L. (2009). Airflow and microclimate patterns in a one-hectare Canary type greenhouse: an experimental and CFD assisted study. Agricultural and Forest Meteorology, 149(6), 1050-1062.

Majdoubi, H, Boulard, Thierry, Fatnassi, Hicham, & Bouirden, L. (2009). Airflow and microclimate patterns in a one-hectare Canary type greenhouse: an experimental and CFD assisted study. Agricultural and Forest Meteorology, 149(6), 1050-1062.

Mendez, Carolina B, Klenzendorf, J Brandon, Afshar, Brigit R, Simmons, Mark T, Barrett, Michael E, Kinney, Kerry A, & Kirisits, Mary Jo. (2011). The effect of roofing material on the quality of harvested rainwater. water research, 45(5), 2049-2059.

Miles, Carol, Wallace, Russ, Wszelaki, Annette, Martin, Jeffrey, Cowan, Jeremy, Walters, Tom, & Inglis, Debra. (2012). Deterioration of potentially biodegradable alternatives to black plastic mulch in three tomato production regions. HortScience, 47(9), 1270-1277.

Montero, JI, Munoz, P, Anton, A, & Iglesias, N. (2005). Computational fluid dynamic modelling of night-time energy fluxes in unheated greenhouses. Acta Horticulturae, 691(1), 403.

Moreno, MM, & Moreno, A. (2008). Effect of different biodegradable and polyethylene mulches on soil properties and production in a tomato crop. Scientia Horticulturae, 116(3), 256-263.

Nääs, IA, Moura, DJ, Bucklin, RA, & Fialho, FB. (1998). An algorithm for determining opening effectiveness in natural ventilation by wind. Transactions of the ASAE, 41(3), 767-771.

Nederhoff, EM, Van de Vooren, J, & Udink ten Cate, AJ. (1983). A method to determine ventilation in greenhouses. Paper presented at the III International Symposium on Energy in Protected Cultivation 148.

Ngouajio, Mathieu, Auras, Rafael, Fernandez, R Thomas, Rubino, Maria, Counts, James W, & Kijchavengkul, Thitisilp. (2008). Field performance of aliphatic-aromatic copolyester biodegradable mulch films in a fresh market tomato production system. HortTechnology, 18(4), 605-610.

Nimah, MN. (2005). Cucumber yield under regular deficit irrigation and mulching treatments. Paper presented at the III International Symposium on Cucurbits 731.

Norton, Tomás, Sun, Da-Wen, Grant, Jim, Fallon, Richard, & Dodd, Vincent. (2007). Applications of computational fluid dynamics (CFD) in the modelling and design of ventilation systems in the agricultural industry: A review. Bioresource technology, 98(12), 2386-2414.

Olsen, JK, & Gounder, RK. (2001). Alternatives to polyethylene mulch film—a field assessment of transported materials in capsicum (Capsicum annuum L.). Animal Production Science, 41(1), 93-103.

Ozgener, Onder, & Hepbasli, Arif. (2006). An economical analysis on a solar greenhouse integrated solar assisted geothermal heat pump system. Journal of Energy Resources Technology, 128(1), 28-34.

Pankhurst, CE, Stirling, GR, Magarey, RC, Blair, BL, Holt, JA, Bell, MJ, & Garside, AL. (2005). Quantification of the effects of rotation breaks on soil biological properties and their impact on yield decline in sugarcane. Soil Biology and Biochemistry, 37(6), 1121-1130.

Papadakis, G, Briassoulis, D, Mugnozza, G Scarascia, Vox, G, Feuilloley, P, & Stoffers, JA. (2000). Review Paper (SE—Structures and Environment): Radiometric and thermal properties of, and testing methods for, greenhouse covering materials. Journal of Agricultural Engineering Research, 77(1), 7-38.

Papadakis, G, Frangoudakis, A, & Kyritsis, S. (1989). Theoretical and experimental investigation of thermal radiation transfer in polyethylene covered greenhouses. Journal of Agricultural Engineering Research, 44, 97-111.

Patil, S. L., Tantau, H. J., & Salokhe, V. M. (2008). Modelling of tropical greenhouse temperature by auto regressive and neural network models. Biosystems engineering, 99(3), 423-431.

Pérez-López, Antonio José, López-Nicolas, José Manuel, & Núñez-Delicado, Estrella. (2007). Effects of agricultural practices on color, carotenoids composition, and minerals contents of sweet peppers, cv. Almuden. Journal of agricultural and food chemistry, 55(20), 8158-8164.

Pimpini, F, Granguinto, G, Babbo, G, & Xodo, E. (1987). The Effect of Protective Structures and of Pinching on the Earliness of table Tomatoes in the Greenhouse. Protte, 16(8-9), 63-73.

Pullaro, T. C., Marino, P. C., Jackson, D. M., Harrison, H. F., & Keinath, A. P. (2006). Effects of killed cover crop mulch on weeds, weed seeds, and herbivores. Agriculture, ecosystems & environment, 115(1), 97-104.

Reid J, K. Klotzback, N. Hoover, and H. Hoover. 2010. Evaluation of Harris Seed Pepper Varieties in High Tunnels. Cornell University Cooperative Extension.

Rezaeian Zadeh, Mehdi, Amin, Seifollah, Khalili, Davar, & Singh, Vijay P. (2010). Daily outflow prediction by multi layer perceptron with logistic sigmoid and tangent sigmoid activation functions. Water resources management, 24(11), 2673-2688.

Ruano, AE, Crispim, EM, Conceicao, EZE, & Lucio, MMJR. (2006). Prediction of building's temperature using neural networks models. Energy and Buildings, 38(6), 682-694.

Sanders, Phillip. (2006). Evaluation of a High Tunnel Production System as a Means of Enhancing Market Opportunities for Alabama Growers.

Sarnacke, P, & Wildes, S. (2008). Disposable Bioplastics—A Market Opportunity Study. Omni Tech International, Ltd, Michigan, USA, 1-35.

Schales, FD, & Sheldrake, R. (1963). Mulch effects on soil conditions and tomato plant response. Paper presented at the Proceedings 4th National Agricultural Plastic Congress.

Schippers, B., Bakker, A. W., & Bakker, P. A. (1987). Interactions of deleterious and beneficial rhizosphere microorganisms and the effect of cropping practices. Annual review of phytopathology, 25(1), 339-358.

Siwek, Piotr, Kalisz, Andrzej, & Wojciechowska, Renata. (2007). Effect of mulching with film of different colours made from original and recycled polyethylene on the yield of butterhead lettuce and celery. Folia Hort. Supl, 19(1), 25-35.

Stanghellini, C, Kempkes, FLK, & Knies, P. (2003). *Enhancing environmental quality in agricultural systems.* Paper presented at the International Symposium on Managing Greenhouse Crops in Saline Environment 609.

Stevanović, Sanja. (2013). Optimization of passive solar design strategies: A review. Renewable and Sustainable Energy Reviews, 25, 177-196.

Teasdale, John R. (1996). Contribution of cover crops to weed management in sustainable agricultural systems. Journal of Production Agriculture, 9(4), 475-479.

Teasdale, John R, & Daughtry, Craig ST. (1993). Weed suppression by live and desiccated hairy vetch (Vicia villosa). Weed science, 207-212.

Teitel, Meir, & Tanny, Josef. (1999). Natural ventilation of greenhouses: experiments and model. Agricultural and Forest Meteorology, 96(1), 59-70.

Thomas, Bertil, & Soleimani-Mohseni, Mohsen. (2007). Artificial neural network models for indoor temperature prediction: investigations in two buildings. Neural Computing and Applications, 16(1), 81-89.

Tong, G, Christopher, DM, & Li, B. (2009). Numerical modelling of temperature variations in a Chinese solar greenhouse. Computers and Electronics in Agriculture, 68(1), 129-139.

Tong, G, & Li, B. (2006). Simulation and experiment of solar radiation on surfaces of solar greenhouses. J. China Agric. Univ, 11(1), 61-65.

Verlinde, W, Gabriëls, Donald, & Christiaens, JPA. (1998). Ventilation coefficient for wind-induced natural ventilation in cattle buildings: a scale model study in a wind tunnel. Transactions of the ASAE, 41(3), 783-788.

Vine, Edward. (2008). Breaking down the silos: the integration of energy efficiency, renewable energy, demand response and climate change. Energy Efficiency, 1(1), 49-63.

Wang, S, Boulard, T, & Haxaire, R. (1999). Air speed profiles in a naturally ventilated greenhouse with a tomato crop. Agricultural and forest Meteorology, 96(4), 181-188.

Wang, S, & Deltour, JM. (1996). Experimental ventilation function for large greenhouses based on a dynamic energy balance model. International Agricultural Engineering Journal, 5(3), 103-112.

Wang, S, Feng, G, Chen, D, Cao, Z, Qi, Y, & Liu, Y. (1999). Study on macro-management of protected horticulture development in China. Transaction of the Chinese Society of Agricultural Engineering, 15(1), 153-158.

Waterer, Doug. (2003). Yields and economics of high tunnels for production of warm-season vegetable crops. HortTechnology, 13(2), 339-343.

Waterer, Doug. (2010). Evaluation of biodegradable mulches for production of warm-season vegetable crops. Canadian Journal of Plant Science, 90(5), 737-743.

Wells, OS, & Loy, JB. (1985). Intensive vegetable production with row covers. HortScience (USA).

Wells, Otho S. (1998). Rowcovers and High Tunnels–Growth-enhancing Technology. Vegetable Production Using Plasticulture. Paper presented at the Proceeding of an American Facility for Horticulture Science at American Society for Plasticulture. Seminar Series. ASHS Press.

Wien, H Chris. (2009). Floral crop production in high tunnels. HortTechnology, 19(1), 56-60.

Wszelaki, A. L., C. Miles, R. Wallace, and E. Belasco. 2013. A Case Study on the Uses (and Abuses) of High Tunnels for Fruit and Vegetable Production. Proceedings of the 6th National Small Farm Conference, p. 43-46, Memphis, TN.

Yonaba, H, Anctil, F, & Fortin, V. (2010). Comparing sigmoid transfer functions for neural network multistep ahead streamflow forecasting. Journal of Hydrologic Engineering, 15(4), 275-283.

Zhang, Q, Wong, YW, Fok, SC, & Bong, TY. (2005). Neural-based air-handling unit for indoor relative humidity and temperature control. ASHRAE Transactions, 111(PART 1), 63-70.

Vita

Muzi Zheng was born in Shenyang, Liaoning province, China. She lived in Shenyang until she was 23 years old before coming to USA. She obtained her Bachelor's degree from Shenyang Agriculture University, China in Biological Engineering in the year of 2011. Immediately after getting her bachelor's degree, she moved to the United States and obtained her Master degree in Civil and Environmental Engineering, UTK in May, 2013. At the same year, she started her study in Dr. Brian Leib's group to pursue a Ph.D degree in the Biosystems Engineering Department at the University of Tennessee, focusing on ventilation model and production management in an experimental high tunnel. She completed her Ph.D degree in August 2017.